JPL PUBLICATION 80-6

Evaluation of High-Energy Lithium Thionyl Chloride Primary Cells

H. A. Frank

(NASA-CR-162791) EVALUATION OF HIGH-ENERGY LITHIUM THIONYL CHLORIDE PRIMARY CELLS (Jet Propulsion Lab.) 99 p HC A05/MF A01 CSCL 10A

N80-17552

Unclas G3/44 47259

February 1, 1980

National Aeronautics and Space Administration

Jet Propulsion Laboratory
California Institute of Technology
Pasadena, California

JPL PUBLICATION 80-6

Evaluation of High-Energy Lithium Thionyl Chloride Primary Cells

H. A. Frank

February 1, 1980

National Aeronautics and
Space Administration

Jet Propulsion Laboratory
California Institute of Technology
Pasadena, California

PREFACE

The work described in this report was performed by the Control and Energy Conversion Division of the Jet Propulsion Laboratory, California Institute of Technology, Pasadena, California and completes a portion of the work requirements under NASA RTOP 506-23-25, "Advanced Nickel-Cadmium and Probe Batteries."

ACKNOWLEDGEMENT

The author wishes to acknowledge the assistance of Mr. Larry Whitcanack in setting up for and carrying out all of the tests described within this report.

ABSTRACT

JPL is carrying out a program for NASA aimed at developing improved primary lithium batteries for aerospace applications. One element of this program is concerned with evaluating commercial primary lithium cells in order to establish baseline pèrformance data.

This report describes the results of an evaluation of what is believed to be one of the most advanced cells of this type. This is the Altus Model AL-250 Li-$SOCl_2$ type cell with nominal capacity of 6 Ah.

Maximum energy density of this cell at low rates (less than C/30, where "C" is the cell capacity in amp-hrs and 30 corresponds to a 30-hr discharge time) was found to be near 300 Wh/kg. An equation which predicts the operating voltage of this cell as a function of current and state of charge is presented herein. Heat generation rates of these cells were determined as a function of current in a calorimeter. It was found that heat rates could be theoretically predicted with some degree of accuracy at currents less than 1 amp or the C/6 rate. No explosions were observed in the cells during the condition of overdischarge or reversal nor during high rate discharge. It was found, however, that the cells can vent when overdischarge currents are greater than C/30 and when discharge rates are greater than 1.5C.

CONTENTS

Figures

Tables

SECTION I

INTRODUCTION

JPL is carrying out a program for NASA aimed at developing improved primary lithium batteries for aerospace applications. The need for such batteries in future NASA missions was described in a prior JPL publication (Ref. 1-1).

One aspect of this program is concerned with evaluating commercial primary lithium cells. Such an evaluation is essential because it provides the baseline cell performance data for comparison with the performance of advanced developed cells. Characteristics of interest are: (a) operating voltage as a function of current and state of charge; (b) energy density; (c) power density; (d) heat generation rates as a function of current; (e) performance during overdischarge or reversal; (f) performance during high-rate discharge; and (g) shelf-life capability.

This report documents the results of an experimental evaluation of what is believed to be one of the most advanced, commercially available types of primary lithium cells. This is the lithium-thionyl chloride-type cell ($Li-SOCl_2$). The reason for selecting this type of cell is that it is reported to deliver the highest energy density of all lithium cells (Ref. 1-1). Data is presented on all of the above-mentioned characteristics, except shelf life. The data was reduced and normalized where possible so that it could be used to predict the performance of other sizes and types of $Li-SOCl_2$ cells. The normalized data will serve as a guide for judging the merits of advanced $Li-SOCl_2$ cells.

SECTION II

TEST PROGRAM

The cells examined herein were designated as Altus Model AL-250. As shown in Fig. 2-1, the cells are disc shaped with a diameter of 6.35 cm and a thickness of 0.95 cm. The cells ranged in weight from 72 to 74 g and impedances ranged from 3 to 15 ohms. The cell case is made of stainless steel and serves as the positive terminal. The center pin, shown in Fig. 2-1, is the negative terminal and is insulated from the case by a ceramic-to-metal seal. The thickness of the ceramic is designated so that it will rupture at a specified internal pressure.

A. ELECTRICAL AND THERMAL TESTS

Eighteen cells were discharged over a range of currents and temperatures while installed inside a calorimeter. Test conditions are given in Table 2-1. The discharges were carried out at constant current using a power supply as a current regulator with a series dissipative load to ensure proper power supply voltage. Cell voltages and heat rates were recorded on tape on a Hewlett Packard Data Acquisition System. The calorimeter used for the heat rate measurements was borrowed from the NASA Goddard Space Flight Center. The unit was developed for NASA Goddard under a contract with Rocketdyne and had been previously used by NASA Goddard to measure heat rates in nickel-cadmium cells. Figure 2-2 is a photograph of the calorimeter assembly and Fig. 2-3 is a close-up view of a cell installed inside the unit. The unit is described and its operating principles are given in Ref. 2-1. No special safety precautions were taken in electrical and thermal tests since the cells were operated within their designated operating limits. In addition, the calorimeter provided adequate protection.

B. FORCED REVERSAL TESTS

Twenty cells were discharged completely over a range of currents and then forced into the condition of reversal. The total amount of discharge was 12 Ah or 200 percent of the nominal rated capacity of 6 Ah. Test conditions, including currents and times, are given in Table 2-2. The tests were repeated five times at each of the indicated current levels in order to obtain some indication of reproducibility. The discharges and reversals were carried out with a power supply, as described above. Cell voltages and external surface temperatures were recorded for each test. If a cell vented this was also recorded, along with weight loss. No attempt was made to analyze the vented products. Safety precautions were employed here since the test conditions were known to be out of limits for this type of cell. The precautions consisted of: (1) carrying out the tests in a concrete test pit with remote data acquisition, and (2) using a specially designed flak suit when removing the cells from the test pit, as shown in Fig. 2-4.

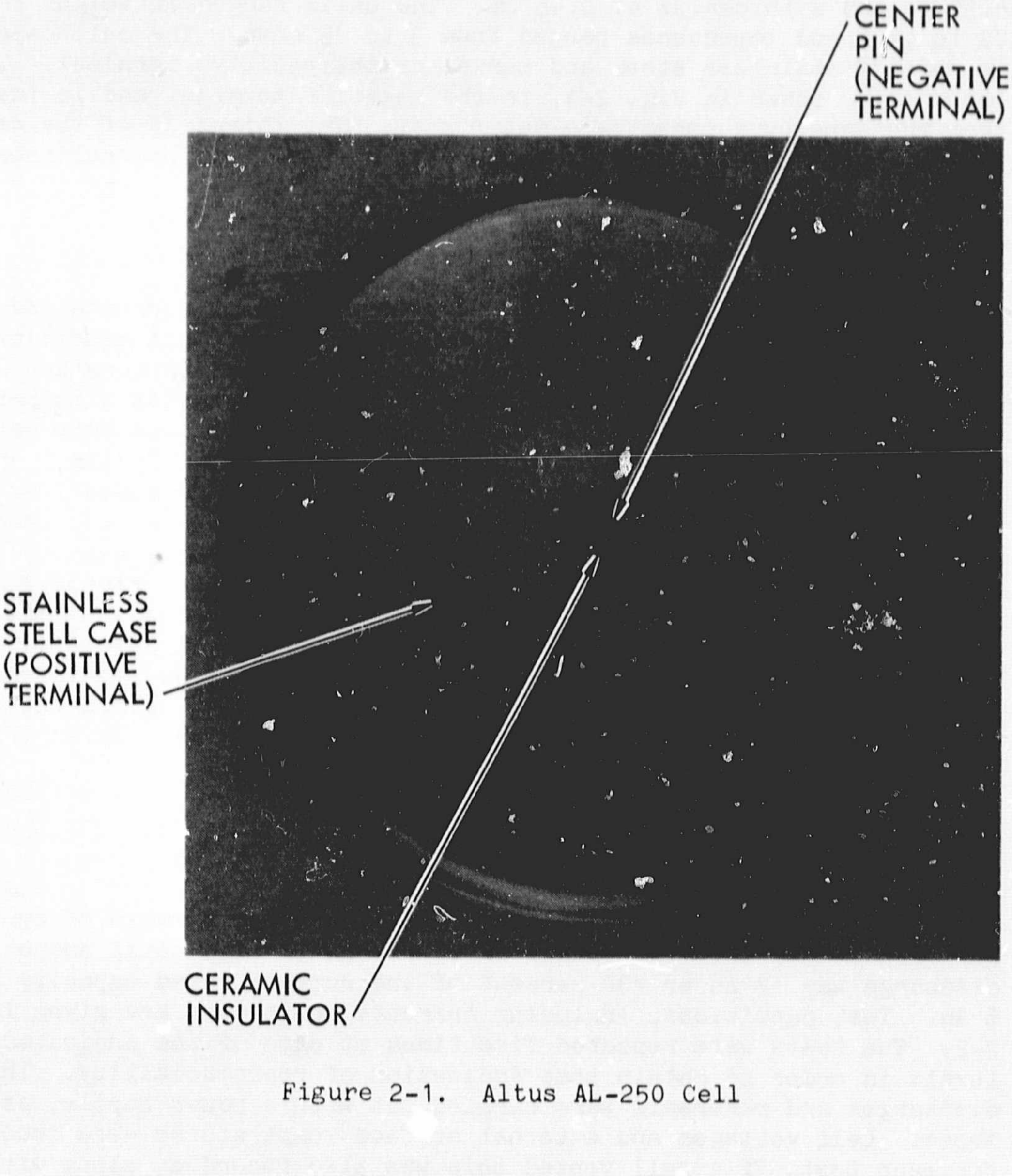

Figure 2-1. Altus AL-250 Cell

Table 2-1. Test Conditions for Electrical and Thermal Tests

Cell No.	Current (Amps)	Ambient Temperature (°C)
62	5.0	0
43	2.0	0
45	1.0	0
77	0.5	0
204	0.2	0
220	0.1	0
56	5.0	21
54	2.0	21
50	1.0	21
196	0.5	21
168	0.2	21
203	0.1	21
75	5.0	40
157	2.0	40
145	1.0	40
205	0.5	40
149	0.2	40
155	0.1	40

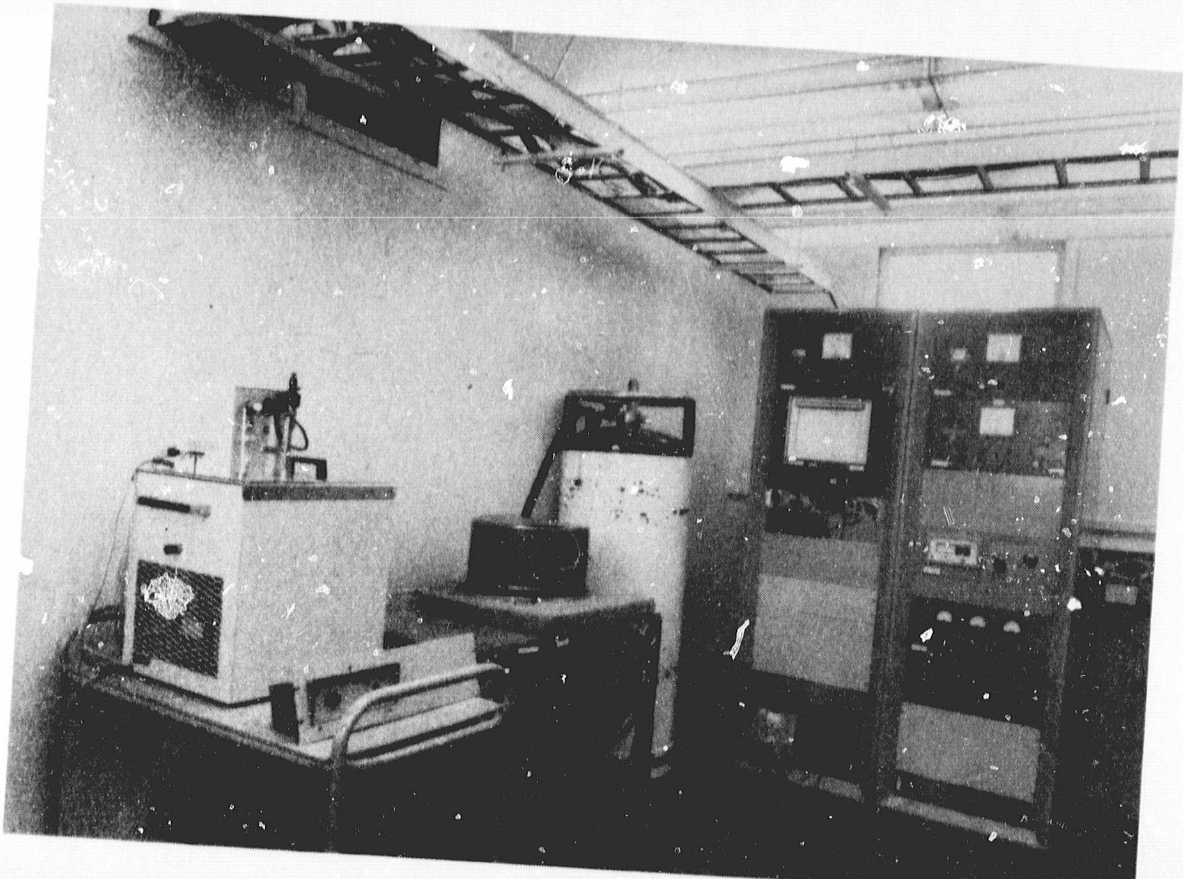

Figure 2-2. Calorimeter Assembly

ORIGINAL PAGE IS
OF POOR QUALITY

Figure 2-3. Altus AL-250 Cell Installed in the Calorimeter

Table 2-2. Test Conditions for Discharge and Reversal Tests

Cell No.	Current (Amps)	Time (Hours)
64	2.0	6
58	2.0	6
6	2.0	6
8	2.0	6
53	2.0	6
9	1.0	12
12	1.0	12
7	1.0	12
17	1.0	12
42	1.0	12
55	0.5	24
26	0.5	24
70	0.5	24
24	0.5	24
38	0.5	24
12	0.2	60
39	0.2	60
44	0.2	60
3	0.2	60
16	0.2	60

Figure 2-4. Removal of AL-250 Cells from Test Pit

ORIGINAL PAGE IS
OF POOR QUALITY

C. HIGH-RATE DISCHARGE TESTS

Twenty cells were discharged at high rates by placing them across low-resistance ohmic loads. Test conditions are given in Table 2-3. The tests were repeated five times at each of the indicated loads in order to obtain some indication of reproducibility. Cell voltages, currents, and external surface temperatures were recorded for each test. If a cell vented this was also recorded along with weight loss. No attempt was made to analyze the vented products. The same safety precautions were employed as in the forced reversal tests above since the test conditions were known to be out of limits for this type of cell.

Table 2-3. Test Conditions for High-Rate Discharge Tests

Cell No.	Load (Ohms)
71	0.4
50	0.4
32	0.4
74	0.4
18	0.4
27	0.3
3	0.3
9	0.3
17	0.3
35	0.3
5	0.2
11	0.2
23	0.2
25	0.2
15	0.2
11	0.1
4	0.1
17	0.1
8	0.1
19	0.1

SECTION III

RESULTS AND DISCUSSION

A. ELECTRICAL CHARACTERISTICS

A typical discharge curve for this type of cell is shown in Fig. 3-1, which gives the operating voltage as a function of time during the course of constant-current discharge at 1.0 amp at 21°C to a 1.0 V cutoff. The voltage remains above 3.0 V during most of the discharge, and then falls sharply after the voltage reaches 2.5 V. The capacity of this cell is 330 minutes at 1.0 amp or 5.5 Ah. Inspection of the additional constant-current discharge data in Appendix A reveals that capacity increases at lower currents and decreases at higher currents. This trend of diminished capacity with increased rate is similar to that observed in other types of cells (Ref. 3-1).

Given the experimentally determined discharge curves and known cell weights, it is possible to calculate and prepare a Ragone plot for these cells (Ref. 3-2). This plot gives the relation between energy density (Wh/kg) and power density (W/kg), and is useful for design purposes and for comparing performance with other types of cells. This plot is given in Fig. 3-2 at three different ambient temperatures, together with a Ragone plot for a conventional Le Clanche "D"-size dry cell. Inspection of this figure reveals several significant points. First, at low level power densities, the Li-$SOCl_2$ cells can deliver energy densities approaching 300 Wh/kg. Under these conditions, the energy density of the Li-$SOCl_2$ cells is about three times that of the conventional Le Clanche dry cells. Next, at higher power densities, the Li-$SOCl_2$ cells deliver markedly more energy density than the Le Clanche cells. Finally, ambient temperature has a definite effect on performance. As temperature increases in the range of 0°C to 40°C, Fig. 3-2 indicates that it is possible to obtain either a higher energy density at a given power density or a higher power density at a given energy density.

Another useful method for correlating this discharge data is to establish constants for the so-called "Shepherd equation" for the cells (Ref. 3-3). This equation is useful in design and modeling activities since it enables operating voltages to be predicted at any given time and at any given current during the course of discharge. The general form of the equation is as follows:

$$E = E_s - K\left(\frac{Q}{Q-it}\right) i - Ni$$

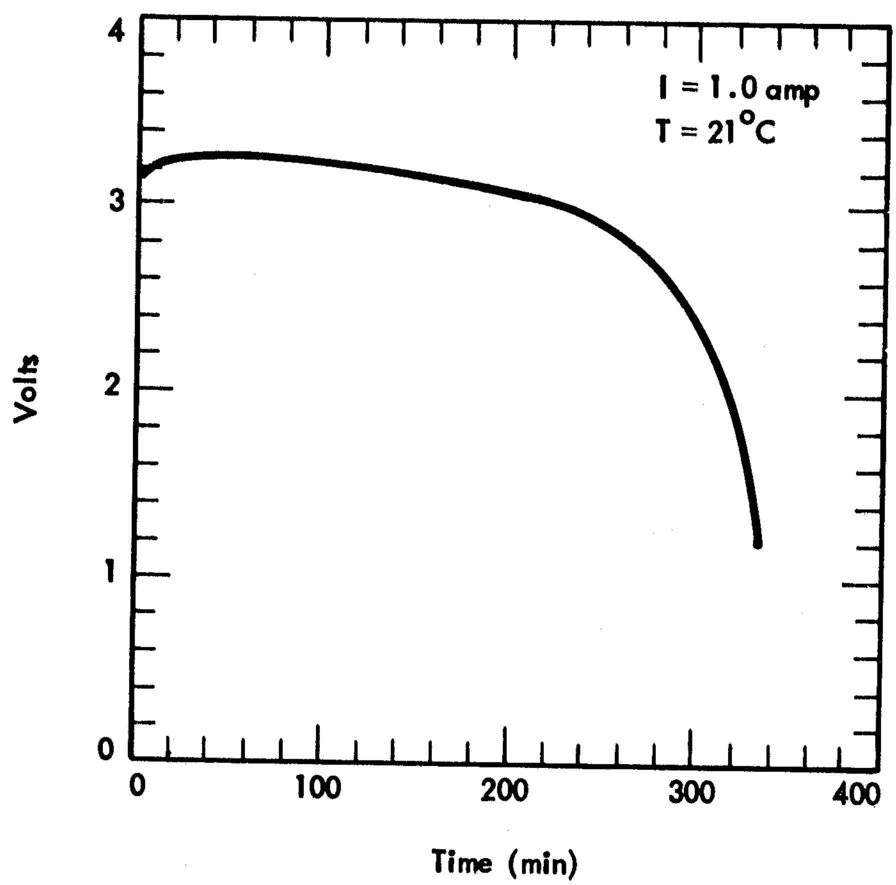

Figure 3-1. Typical Discharge Characteristics of AL-250 Cells

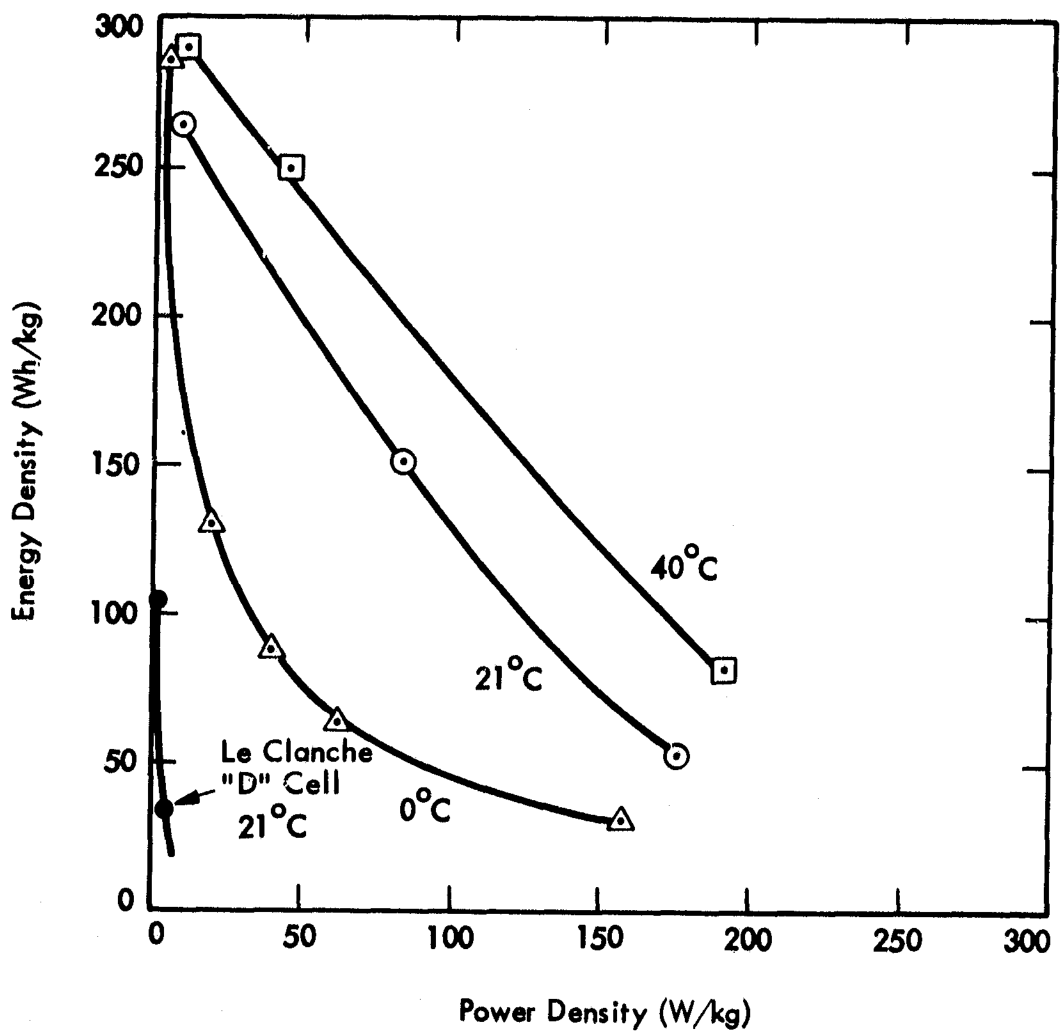

Figure 3-2. Ragone-Type Plot for AL-250 Cells

where E = operating cell voltage (V).

E_s = experimentally determined constant that corresponds to open circuit voltage

K = experimentally determined constant that corresponds to polarization resistance (ohms)

Q = experimentally determined constant that corresponds to cell capacity (amp-hours)

N = experimentally determined constant that corresponds to internal resistance (ohms)

i = cell current (amps)

t = time on discharge (hrs)

The constants E_s, K, Q, and N are determined from experimental discharge data, either by the original method given by Shepherd (Ref. 3-3) or by a modified, simpler, and reportedly more accurate method given by Taylor and Siwek (Ref. 3-4). In accordance with the latter method, the constants were determined as follows:

E_s = 3.5 V

K = 0.108 ohms

Q = 8.1 amp-hr

N = 0.032 ohms

The resultant Shepherd equation is:

$$E = 3.5 - 0.108 \frac{8.1}{8.1 - it} i - 0.032i$$

The equation was applied to the prediction of a few discharge curves, which it did with a fair degree of accuracy.

B. THERMAL CHARACTERISTICS

Typical data obtained in the calorimetric studies are given in Fig. 3-3, which shows operating voltage and heat rates during the course of constant current discharge to a cutoff voltage. In this particular case, the current was 1.0 amp, the ambient temperature was 21°C, and the cutoff voltage was 1.0 V. Appendix A gives a complete set of computer-drawn graphs of similar runs at currents of 5, 2, 1, 0, 0.5, 0.2, and 0.1 amps, and at temperatures of 0°C, 21°C, and 40°C.

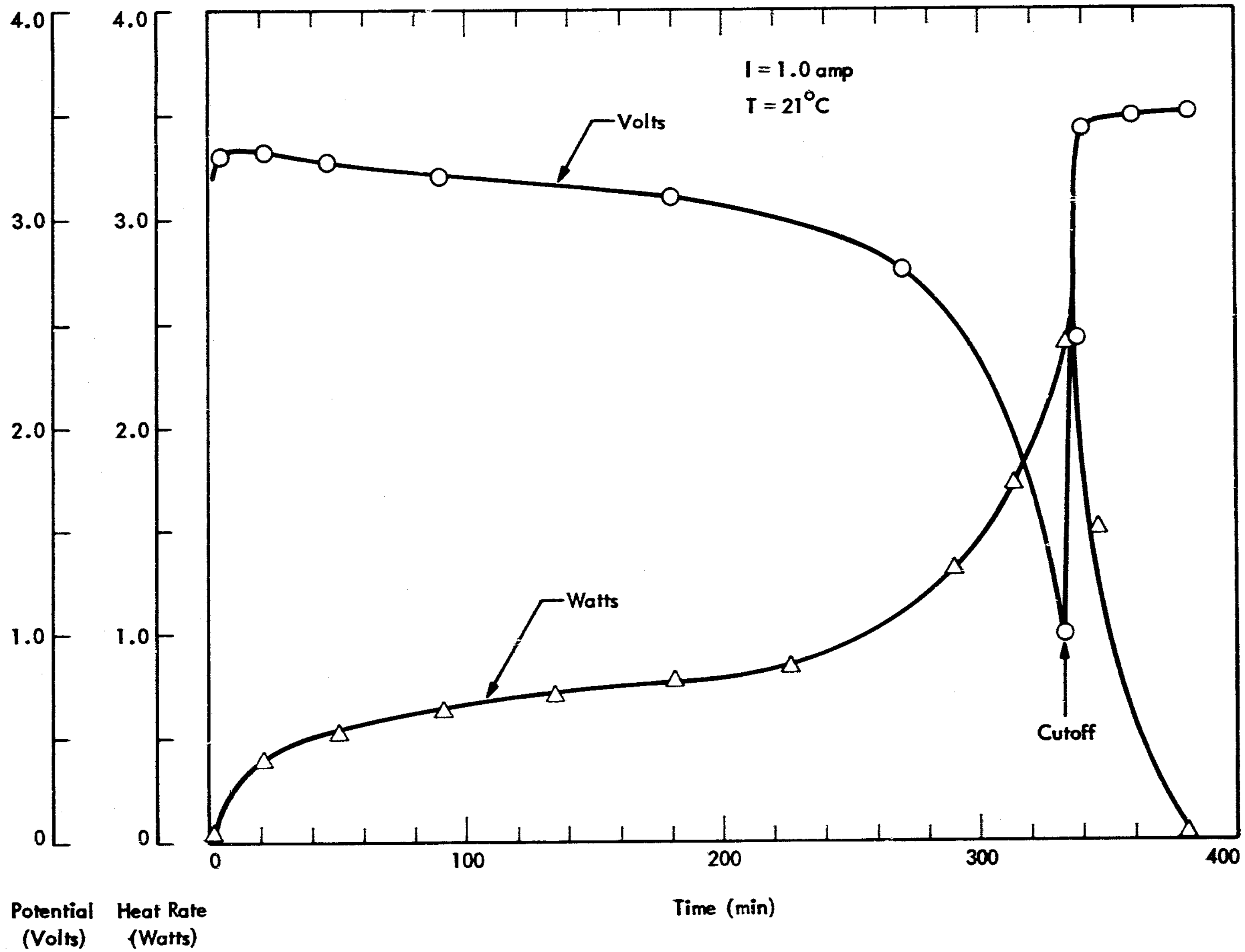

Figure 3-3. Typical Calorimetric Data for AL-250 Cells

Figure 3-3 also shows a gradual increase in heat rate in the first 265 minutes of discharge, during which the voltage declined gradually from 3.30 to 2.75 V. Thereafter, the heat rate increased sharply until the cutoff point, while the voltage declined sharply from 2.75 to 1.0 V. After the cutoff point the heat rate dropped rapidly to zero, while the voltage returned sharply to the open circuit condition near 3.5 V.

Figures 3-4 and 3-5 show the relationship between heat rate and current at the midpoint (when half of the capacity is depleted), and at the end of discharge, respectively. Also shown therein are the theoretically calculated heat rates based on a thermoneutral voltage of 3.34 V, as proposed by Schlaikjer (Ref. 3-5). These figures reveal several significant factors. First, heat rates increase in an essentially linear manner with current. Second, there is a fairly good correspondence between theoretical and actual heat rates at currents below 1.0 amp. At very low current, when the discharge voltage is above 3.34 V, theory predicts negative heat rates; i.e., cell reaction is endothermic, and the cell absorbs heat from its surroundings. This phenomenon was the case, as shown in Fig. 3-4. On this basis, the theoretical method of predicting heat rates based on a thermoneutral voltage of 3.34 V appears to be valid at low currents of approximately C/6 and below. Third, at currents above 1 amp, the theoretically predicted heat rates are lower than actual at the midpoint of discharge and higher than actual at the end of discharge. This phenomenon implies that there may be changes in the reaction mechanism and, perhaps, chemical reactions that occur at rates of about C/6 and above.

The effect of ambient temperature on heat rate is given in Fig. 3-6, which shows that the heat rate increases somewhat with temperature in the range of 0°C to 40°C. A brief calculation reveals an increase of about 1%/°C.

C. PERFORMANCE DURING THE CONDITION OF FORCED REVERSAL

Typical performance characteristics of these cells during the course of discharge and forced reversal are given in Fig. 3-7. In this particular case, the cell was discharged at a constant current of 2 amps for a period of 6 hours at 20°C. During the first 120 minutes, the cell was in its normal discharge mode, since cell voltage was positive. During the time span from 120 minutes to 360 minutes, the cell was in the condition of reversal, since its voltage was negative. Cell-surface temperature rose gradually during the initial portion of discharge and then more sharply near the end of discharge. Shortly after the onset of reversal, the cell began venting and its temperature began to decline sharply and eventually taper off. Voltage during reversal was peaked at -0.2 V and then stabilized at -0.1 V. Weight loss of the cell from venting was 2.1 g.

A photograph of the cell after venting is given in Fig. 3-8. The dark area on the surface was a brown deposit, which emerged from the cracked ceramic disc in the center of the cell. A small amount of this material was also found sprayed on one wall of the test chamber.

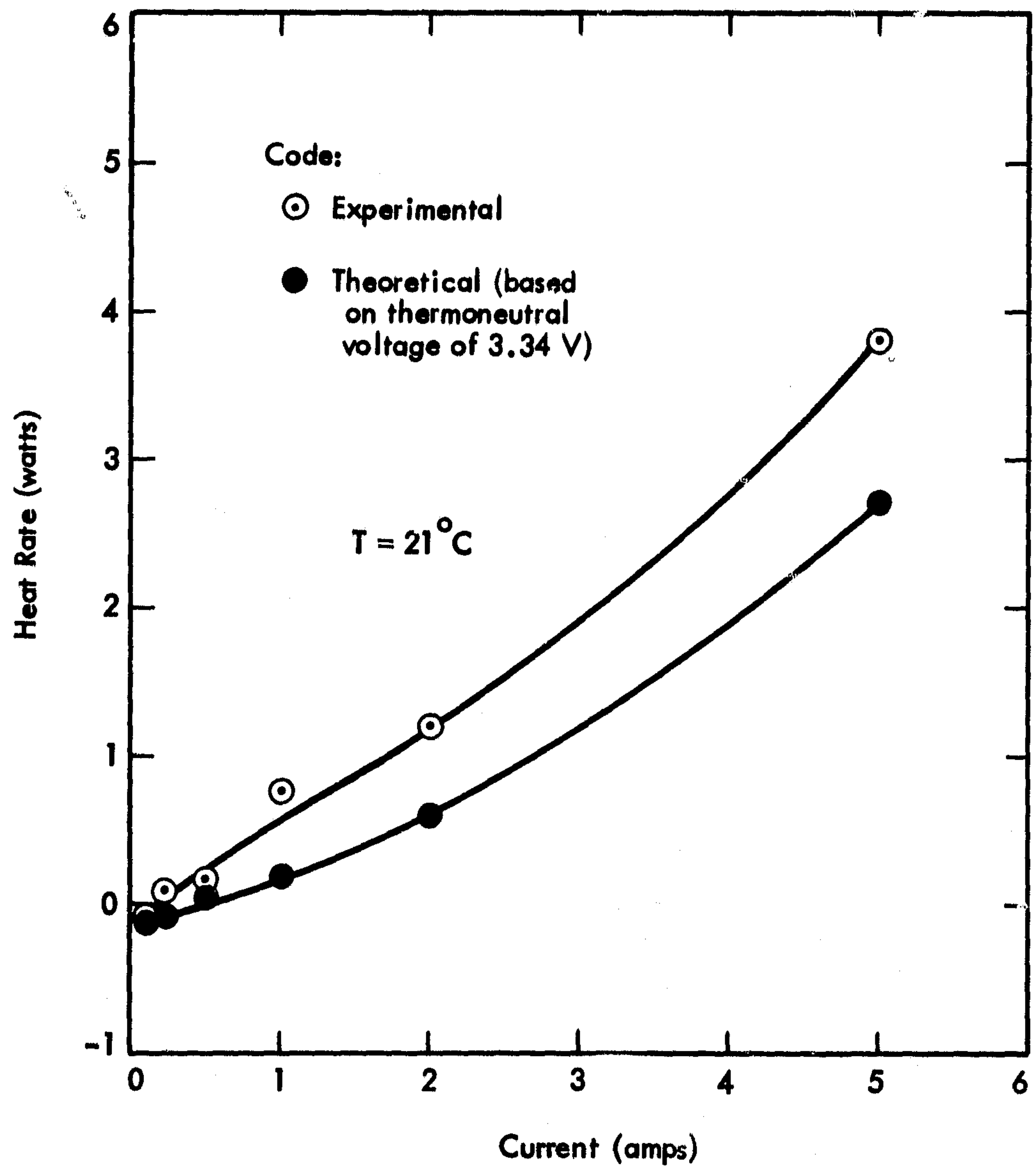

Figure 3-4. Heat Rates at Midpoint of Discharge of AL-250 Cells

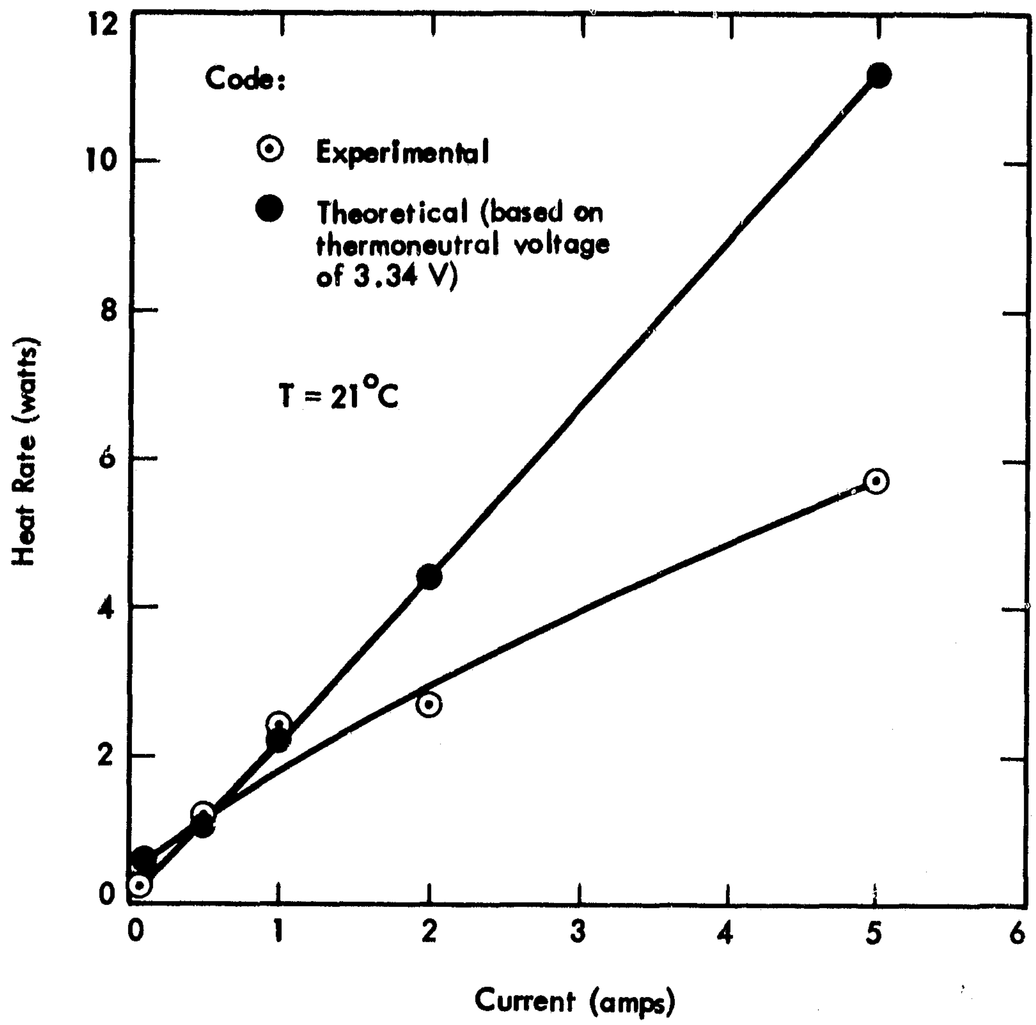

Figure 3-5. Heat Rates at the End of Discharge of AL-250 Cells

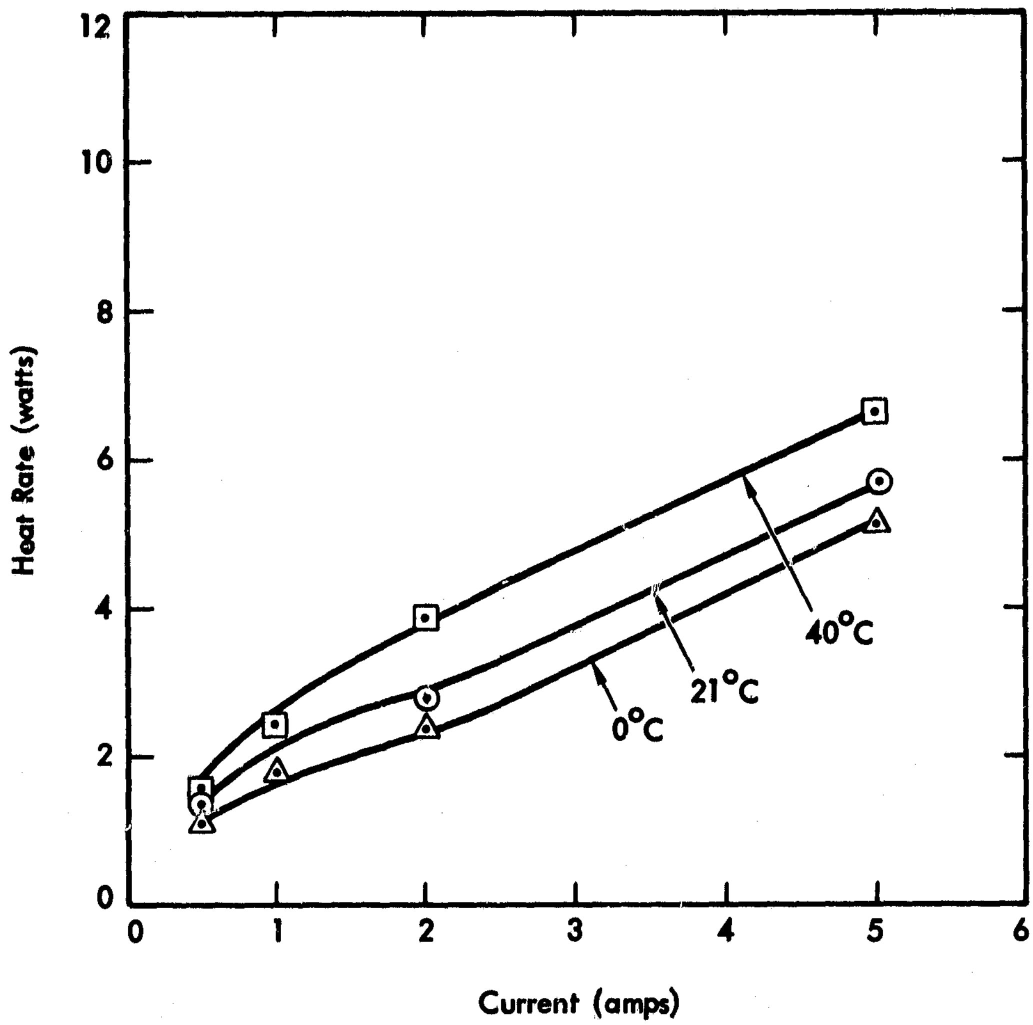

Figure 3-6. Effect of Ambient Temperature on Heat Rates of AL-250 Cells at the End of Discharge

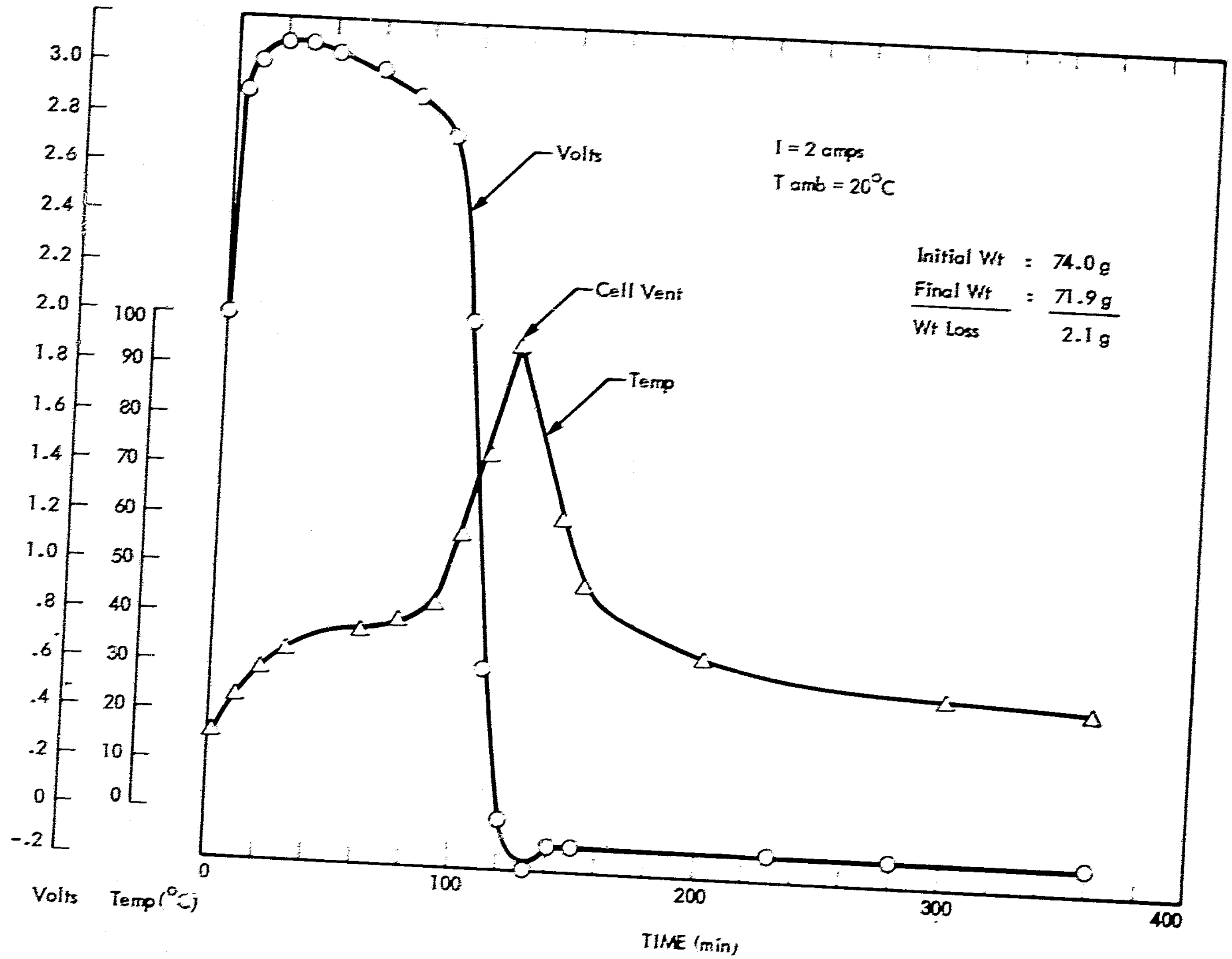

Figure 3-7. Typical Discharge and Reversal Characteristics AL-250 Cells

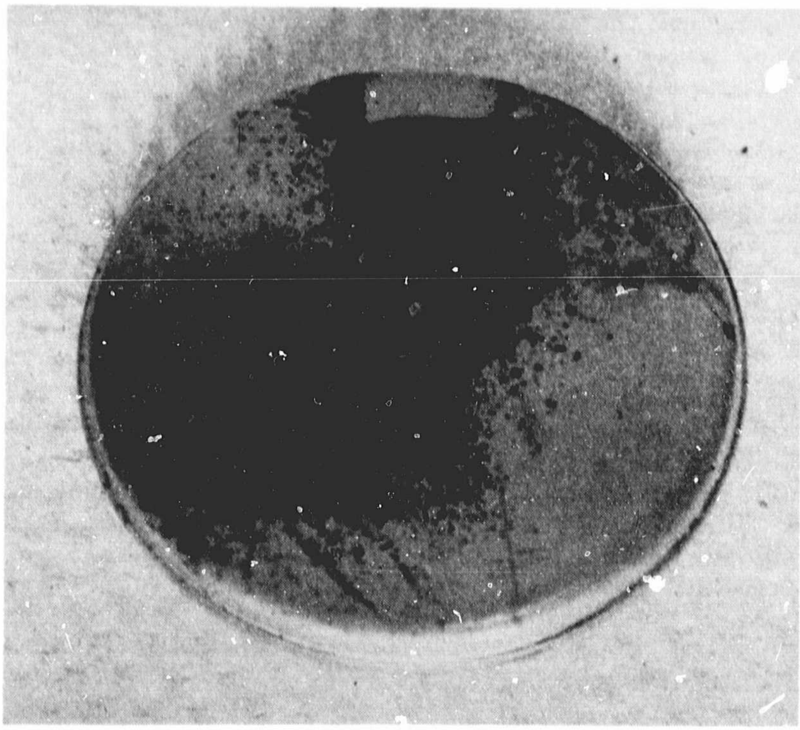

Figure 3-8. AL-250 Cell After Venting

Computer-drawn graphs of the complete set of discharge and reversal tests are given in Appendix B, and highlights of these tests are summarized in Table 3-1, which reveals the following:

(1) At 2 amps, 4 out of 5 cells vented; maximum temperature was 95.6°C, and the maximum reverse voltage was -1.0 V.

(2) At 1 amp, 3 out 5 cells vented; maximum temperature was 86.1°C, and the maximum reverse voltage was <-6.0 V. Erratic voltage behavior was noted in those cases where reverse voltages were < -6.0 V. In these cases, the cells appeared to exhibit brief periods of an "open" condition, i.e., as if the plates had separated temporarily and created a high internal resistance. During these periods, the voltages could not be measured because the voltage pen recorder reached the -6 V limit of the chart. In all likelihood, the voltages reached the lower limit set by the power supply.

(3) At 0.5 amps, 1 out of 5 cells vented, maximum temperature was 82.2°C, and the maximum reverse voltage was <-6.0 V (as explained above).

(4) At 0.2 amps, none of the cells vented; maximum temperature was 35.6°C, and the maximum reverse voltage was<-6.0 V (as explained above).

Although none of the cells exhibited catastrophic failures (i.e., explosions) in these reversal tests, a number of them vented. Venting appeared to occur at reversal currents of 0.5 amps (C/12) and above, with the probability of venting increasing with the magnitude of the current. At reversal currents of 0.2 amps (C/30) and below, the cells appeared to be immune to venting. Regardless of the current level, however, the cells occasionally exhibited short-term but large negative voltage excursions during reversal. These voltage excursions signified momentary "open" conditions within the cells and may cause severe voltage regulation problems in a battery of cells.

D. PERFORMANCE DURING THE CONDITION OF HIGH-RATE DISCHARGE

Originally, it was planned to observe performance of these cells during short-circuit conditions (conditions that could conceivably arise if the cells were mishandled). Discussions with the vendor revealed, however, that such short-circuit tests might not be appropriate since the cells were not designed to withstand these conditions. As an alternative, it was decided to subject the cells to high-rate discharges by placing them across low-resistance loads in the range of 0.4 to 0.1 ohms (as suggested by the vendor).

Table 3-1. Summary of Discharge and Reversal Tests

Cell No.	Current (amps)	Time (hours)	T max (^oC)	V min (volts)	Vented	Wt Loss (gm)
64	2	6	95.6	-0.2	yes	2.1
58	2	6	88.9	-0.2	no	--
6	2	6	94.4	-0.4	yes	1.1
8	2	6	93.9	-1.0	yes	2.1
53	2	6	84.4	-0.3	yes	1.8
9	1	12	78.3	<-6.0	no	--
12	1	12	83.9	<-6.0	yes	3.8
7	1	12	86.1	<-6.0	yes	3.9
7	1	12	85.0	<-6.0	yes	3.7
42	1	12	58.9	-0.4	no	--
55	0.5	24	50.0	-0.6	no	--
6	0.5	24	55.6	-0.8	no	--
70	0.5	24	82.2	<-6.0	no	--
24	0.5	24	60.0	<-6.0	yes	2.1
38	0.5	24	42.2	-0.1	no	--
12	0.2	60	35.6	<-6.0	no	--
39	0.2	60	29.4	-0.4	no	--
44	0.2	60	28.9	<-6.0	no	--
3	0.2	60	29.4	-0.4	no	--
16	0.2	60	28.3	-0.4	no	--

Typical performance characteristics of these cells during high-rate discharge are given in Fig. 3-9. In this particular case, the cell was placed on discharge across a 0.2 ohm load at 20°C. Recordings were then made of cell current, voltage, and temperature (see Fig. 3-9). Current reached a maximum during the first 2 minutes of nearly 11 amps and then dropped sharply to a level near 7-1/2 amps for an additional 5 minutes; it then fell rapidly once again during the next 2 minutes. The current finally tapered down to 0 amp after 40 minutes. The voltage profile was similar to the current profile; it reached a maximum near 1.6 V during the first two minutes, then dropped sharply to a level near 1.1 V for an additional five minutes. It then dropped sharply during the following two minutes, and finally tapered down to 0 volts after 40 minutes. Cell temperature reached a maximum of 120°C, at which point venting occurred. The indicated weight loss from venting was 2.39g.

Computer-drawn graphs of the complete set of high-rate discharge tests are given in Appendix C, and highlights of these tests are shown in Table 3-2. The table reveals the following:

(1) Across a 0.4-ohm load, 1 out of 5 cells vented and the maximum temperature attained was 110.0°C.

(2) Across a 0.3-ohm load, 1 out of 5 cells vented and the maximum temperature attained was 112.8°C.

(3) Across a 0.2-ohm load, 4 out of 5 cells vented and the maximum temperature was 123.3°C.

(4) Across a 0.1-ohm load, 5 out of 5 cells vented and maximum temperature was 121.1°C.

Although none of the cells exhibited catastrophic failures (i.e., explosions) in these high-rate discharge tests, a number of them did vent. The probability of venting is 100% when the cells are discharged across loads of less than 0.2 ohms. The probability of venting diminishes as the load is increased from 0.2 to 0.4 ohms. To ensure that no venting occurs, it appears that the load must be greater than 0.4 ohms, which corresponds approximately to the C/0.7 rate.

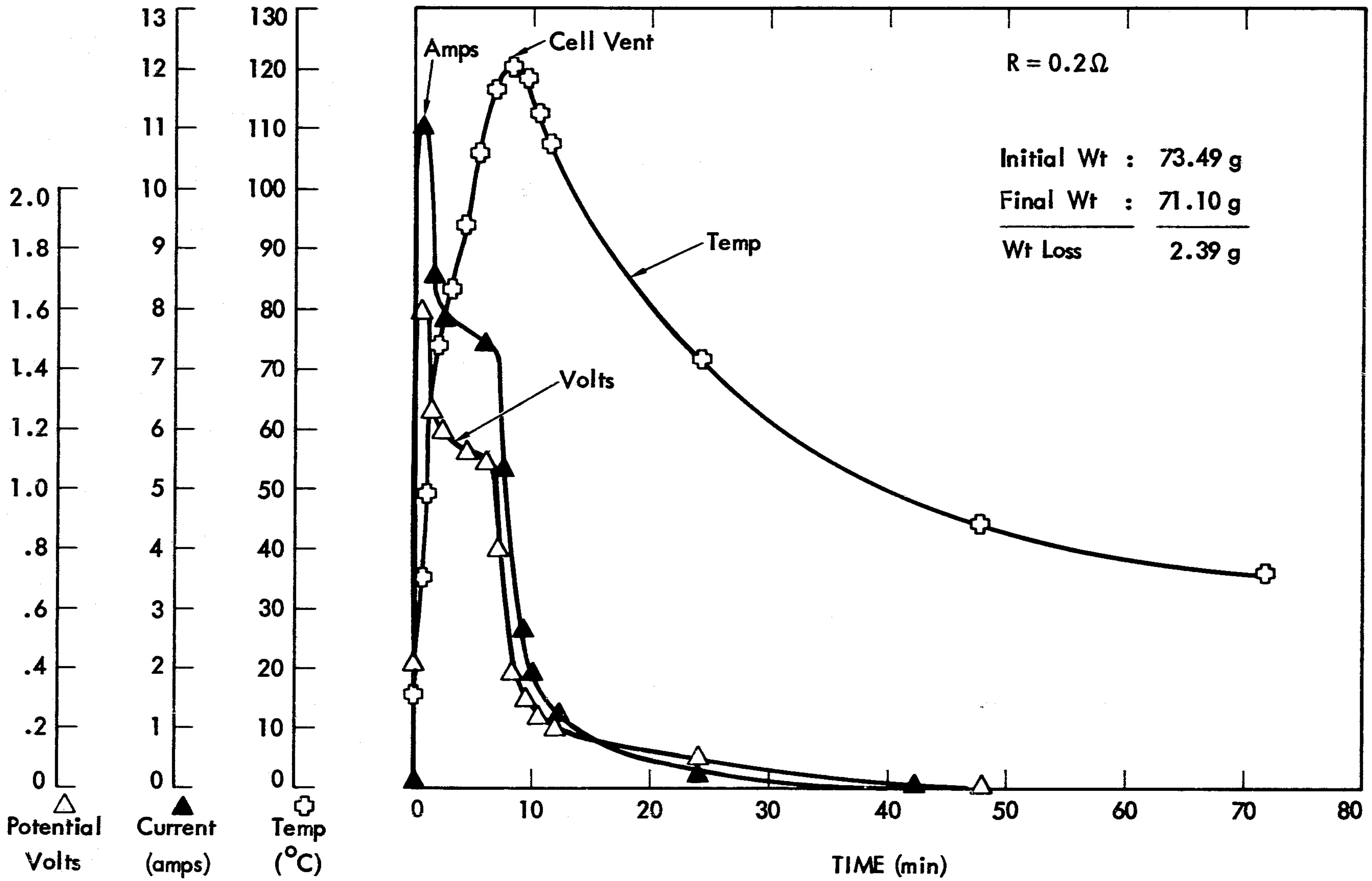

Figure 3-9. Typical High-Rate Discharge Characteristics of AL-250 Cells

Table 3-2. High Rate Discharge Tests

Cell No.	Load (ohms)	I max. (amps)	T max. (^{o}C)	Vented	Wt. Loss (grams)
71	0.4	9.0	90.6	No	-
50	0.4	8.4	87.2	No	-
32	0.4	6.8	91.7	No	-
74	0.4	9.2	110.0	Yes	2.6
18	0.4	7.0	93.9	No	-
27	0.3	10.5	112.8	Yes	<0.1
3	0.3	7.5	102.2	No	-
9	0.3	9.0	106.1	No	-
17	0.3	7.0	102.2	No	-
35	0.3	9.2	106.1	No	-
5	0.2	8.8	115.6	Yes	<0.1
11	0.2	11.0	120.0	Yes	2.4
23	0.2	8.4	97.8	Yes	0.1
25	0.2	12.5	123.3	No	
15	0.2	10.2	106.1	Yes	5.3
11	0.1	12.0	121.1	Yes	4.7
4	0.1	10.1	117.8	Yes	5.5
17	0.1	12.6	115.5	Yes	5.5
8	0.1	10.0	121.1	Yes	4.0
19	0.1	13.3	115.5	Yes	0.3

SECTION IV

CONCLUSIONS

Conclusions regarding the performance of the nominal 6-Ah $Li-SOCl_2$ cell are summarized below:

(1) Maximum deliverable energy density from the cell is near 300 Wh/kg. This energy density is attainable, however, only at low-power densities near 10 w/kg and corresponding low-discharge rates of C/30. The cells can deliver higher power densities, but only at reduced energy densities.

(2) The Shepherd equation for this cell has been established, enabling the operating voltage to be predicted as a function of current and state of charge.

(3) At currents below 1.0 amp (or C/6) the experimental heat generation rates compare quite favorably to those predicted from theory based on a thermoneutral voltage of 3.34 V. At higher currents, the experimental values do not agree with theory, and this is attributed to the onset of chemical side reactions and/or a change in the reaction mechanism.

(4) The cells do not explode under the condition of overdischarge or reversal, but they can, however, vent during overdischarge at currents greater than 0.2 amps or rates greater than C/30. The cells also sometimes exhibit brief "open" periods during overdischarge in which impedance temporarily increases and there is a large negative voltage excursion.

(5) The cells do not explode under the condition of high-rate discharge, but they can, however, vent when discharged across loads of less than 0.4 ohms and corresponding rates greater than 1.5C.

(6) It would have been desirable to conduct failure analyses on those cells that had vented in order to gain further insight into the failure mechanism. This was not possible, however, because of a prior agreement with the vendor that the cells were not to be opened.

REFERENCES

1-1. Frank, H. A., Primary Lithium Battery Technology and Its Application to NASA Missions, JPL Publication 79-6, Jet Propulsion Laboratory, California Institute of Technology Pasadena, California, February 15, 1979.

2-1. Johnston, W. V., "Development of Calorimeter for Spacecraft Batteries," Rocketdyne Final Report on Contract NAS 5-21514, Prepared for Goddard," Space Flight Center, Accession No. N721 24129, NASA CR No. 118029, April 1971.

3-1. Vinal, G. W., Storage Batteries, 4th Ed., pp. 216-218, John Wiley & Sons, Inc.. New York, 1954.

3-2. Ragone, D. V. "Review of Battery Systems for Electrically Powered Vehicles," Society of Automotive Engineers Paper No. 680453, Mid-year meeting, Detroit, Michigan, May 20-24, 1968.

3-3. Shepherd, C. M., "Design of Primary and Secondary Cells," Journal of the Electrochemical Society, Vol. 112, No. 7, pp. 657-664, July 1965.

3-4. Taylor, D. F., and Siwek, E. G., "The Dynamic Characterization of Lead-Acid Batteries for Vehicle Applications," Society of Automotive Engineers Paper No. 730252, International Automotive Engineering Congress, Detroit, Michigan, January 8-2, 1973.

3-5. Schlaikjer, C. R. et al., "Discharge Reaction Mechanisms in Li-$SOCl_2$ Cells," Journal of the Electrochemical Society, Vol. 126, No. 4, pp. 513-522, April 1979.

APPENDIX A

COMPUTER-DRAWN GRAPHS OF CONSTANT-CURRENT DISCHARGE TESTS IN CALORIMETER

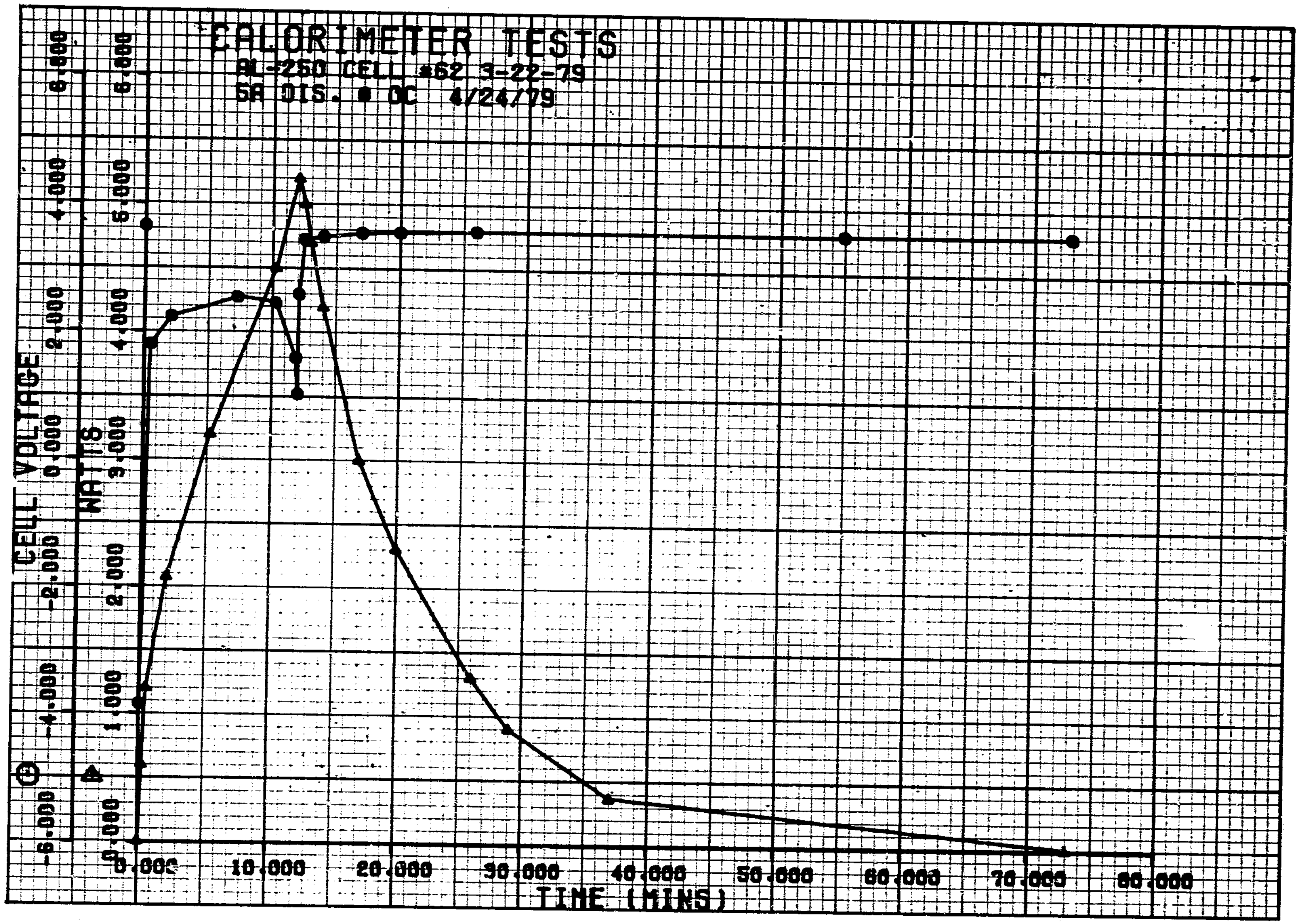

Figure A-1. Calorimeter Test at $0^{o}C$ and at 5 amps for Cell #62

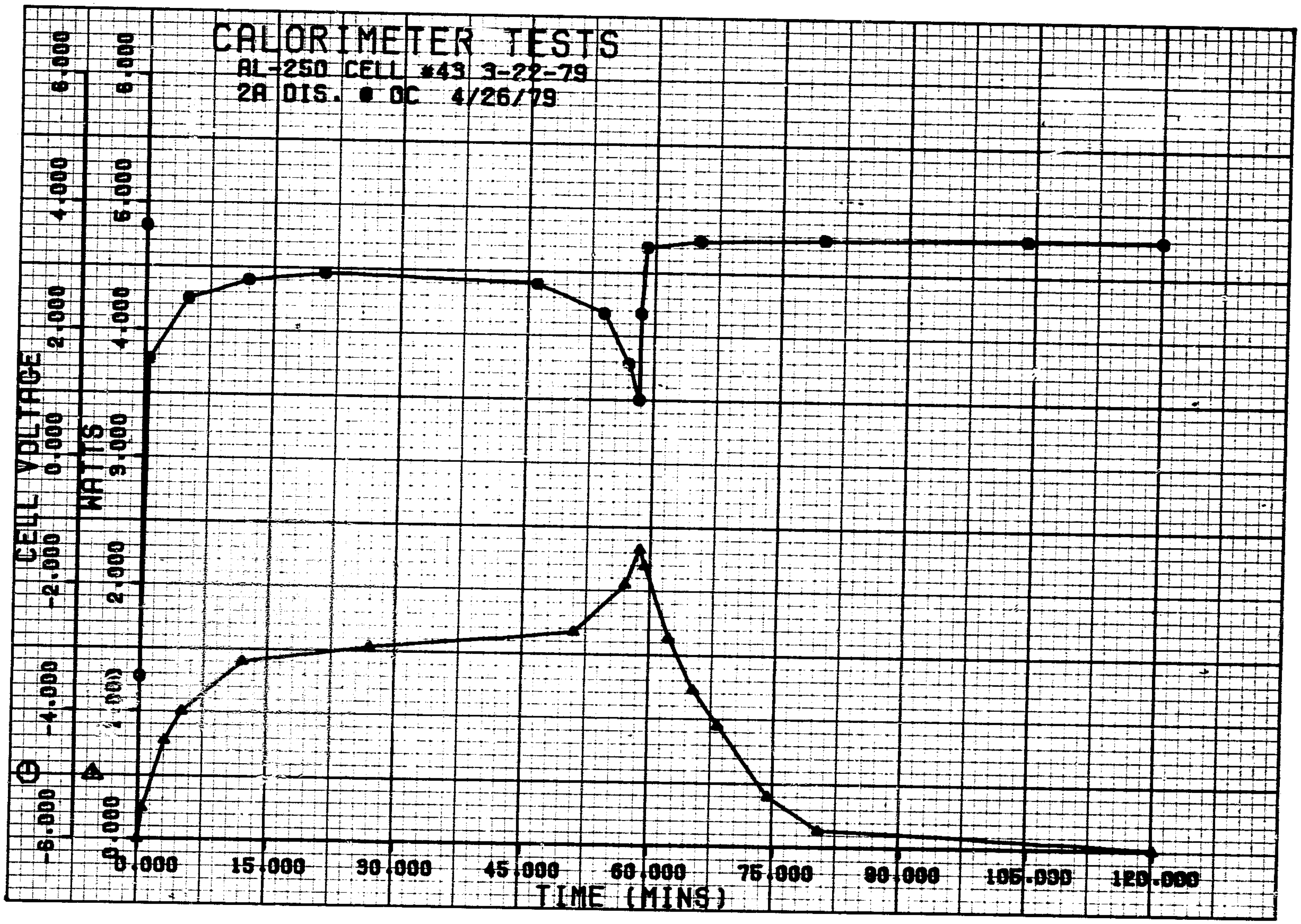

Figure A-2. Calorimeter Test at $0^{o}C$ and at 2 amps for Cell #43

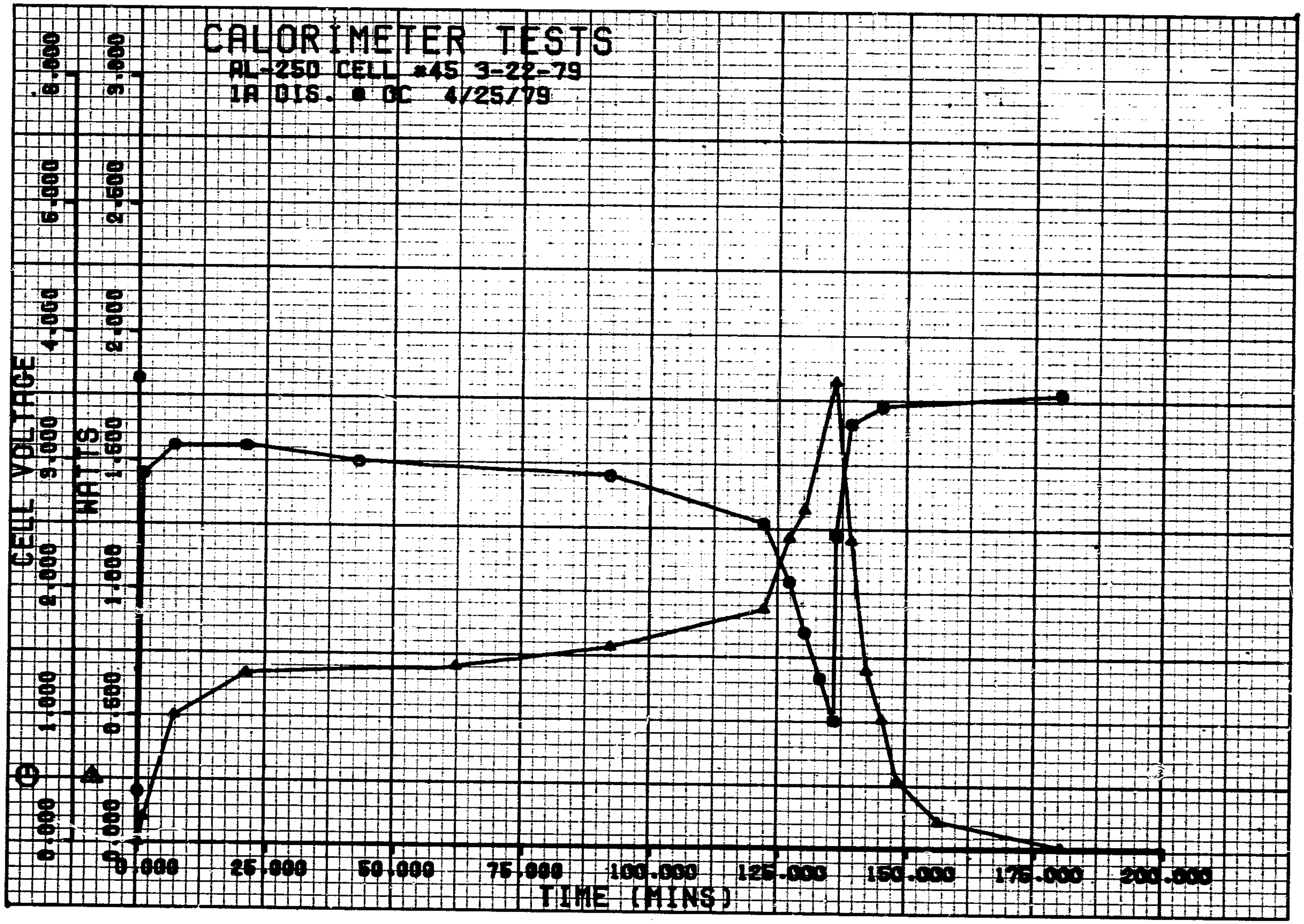

Figure A-3. Calorimeter Test at 0°C and at 1 amp for Cell #45

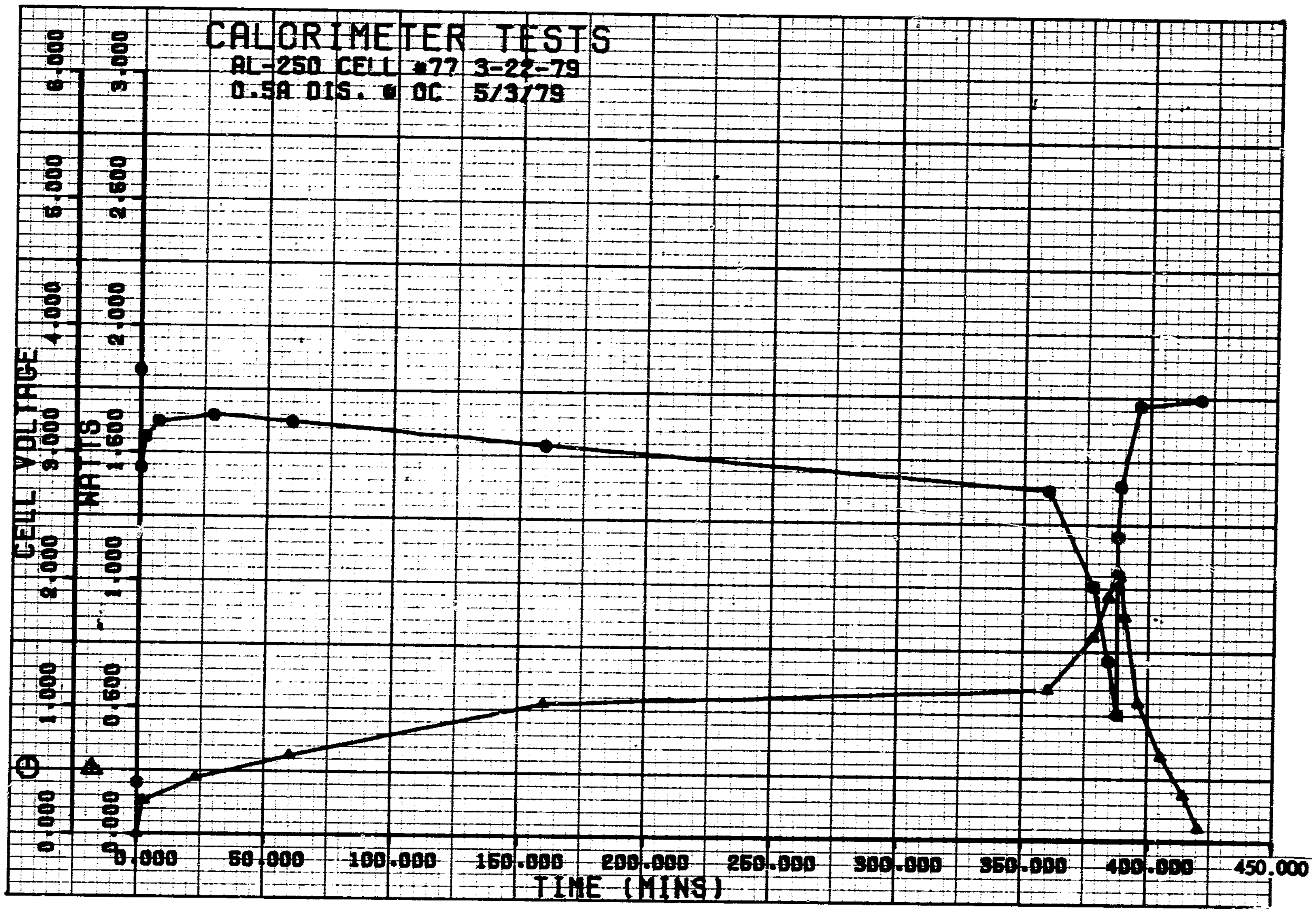

Figure A-4. Calorimeter Test at 0°C and at 0.5 amps for Cell #77

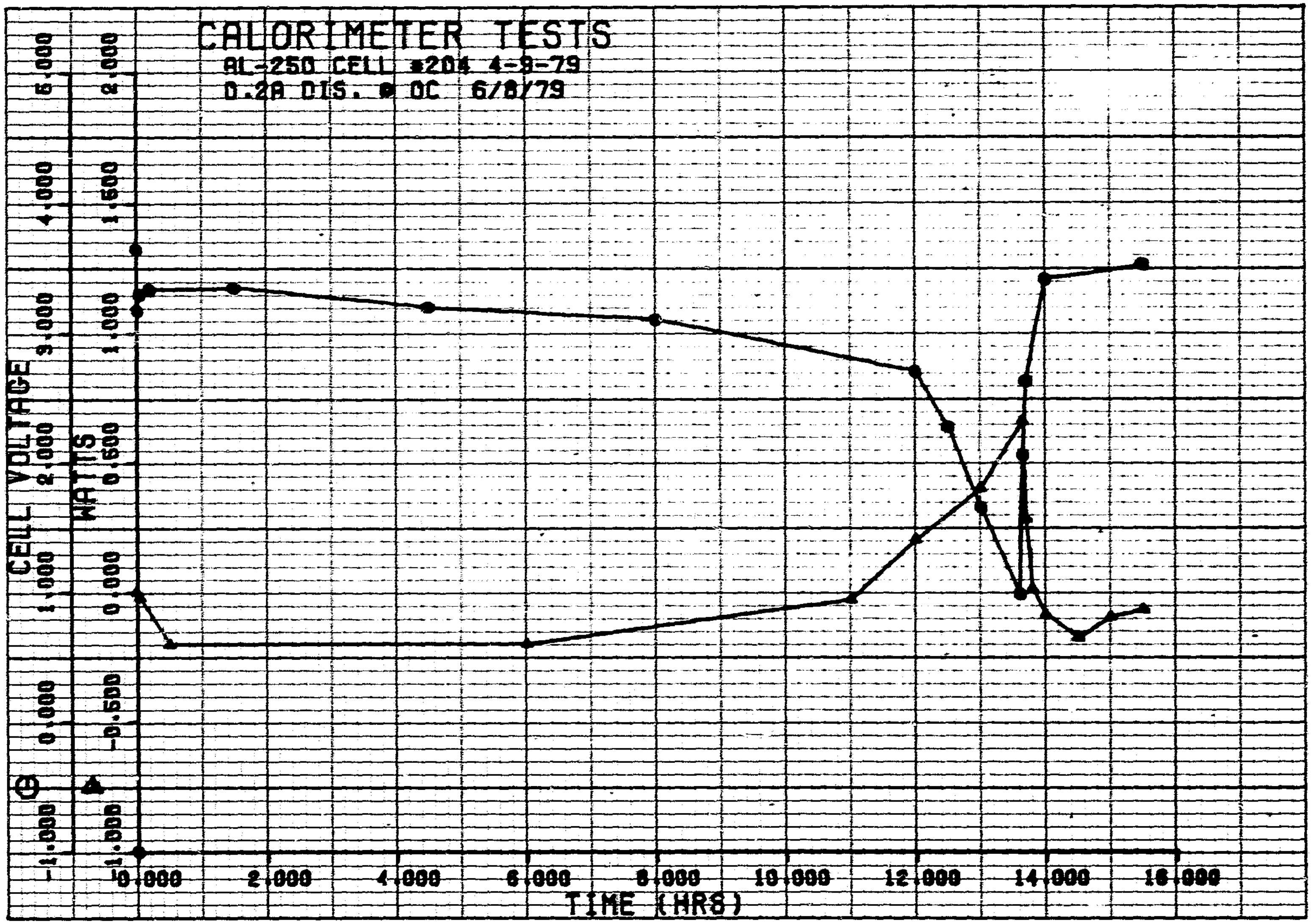

Figure A-5. Calorimeter Test at 0°C and at 0.2 amps for Cell #204

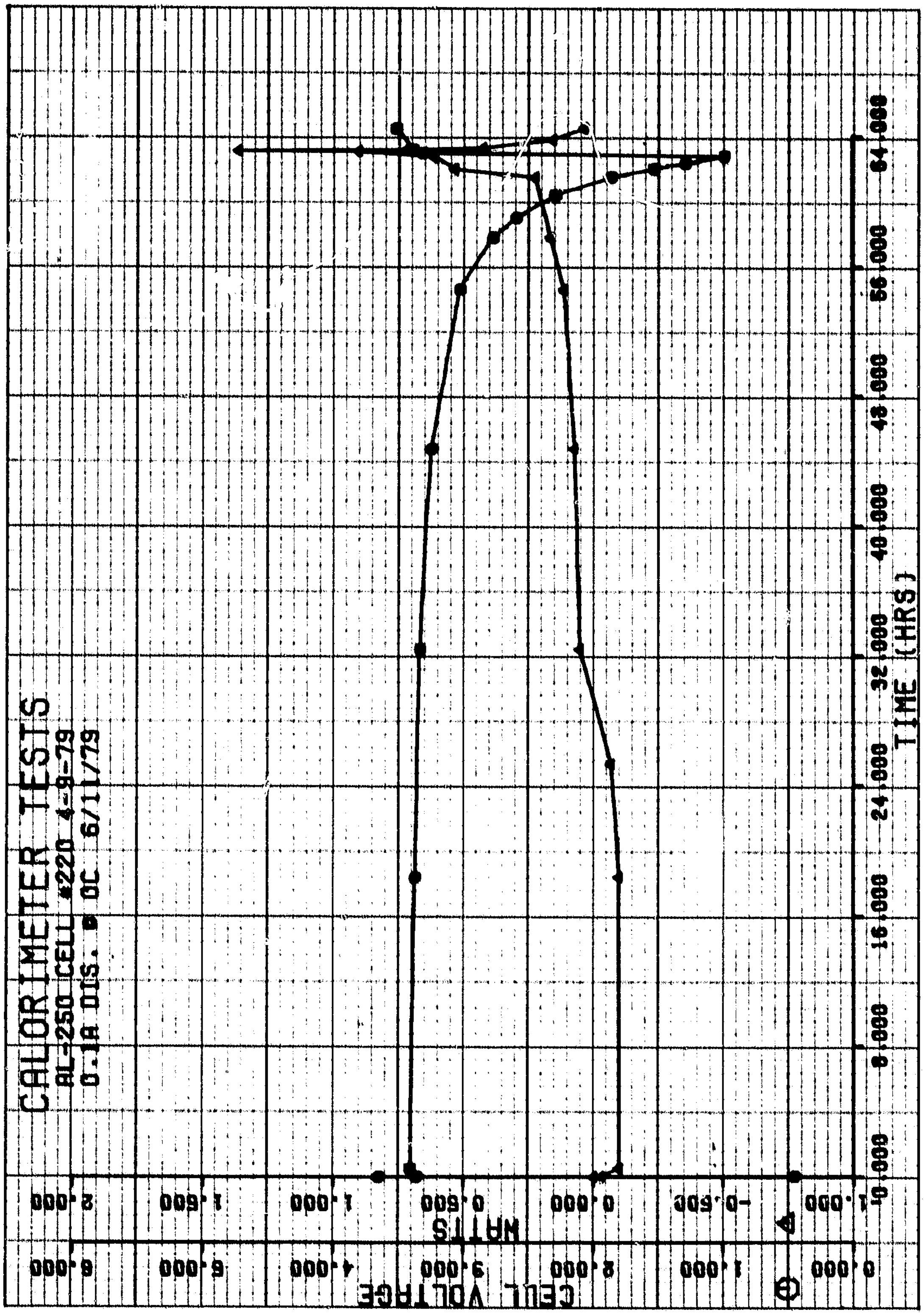

Figure A-6. Calorimeter Test at 0°C and at 0.1 amps for Cell #220

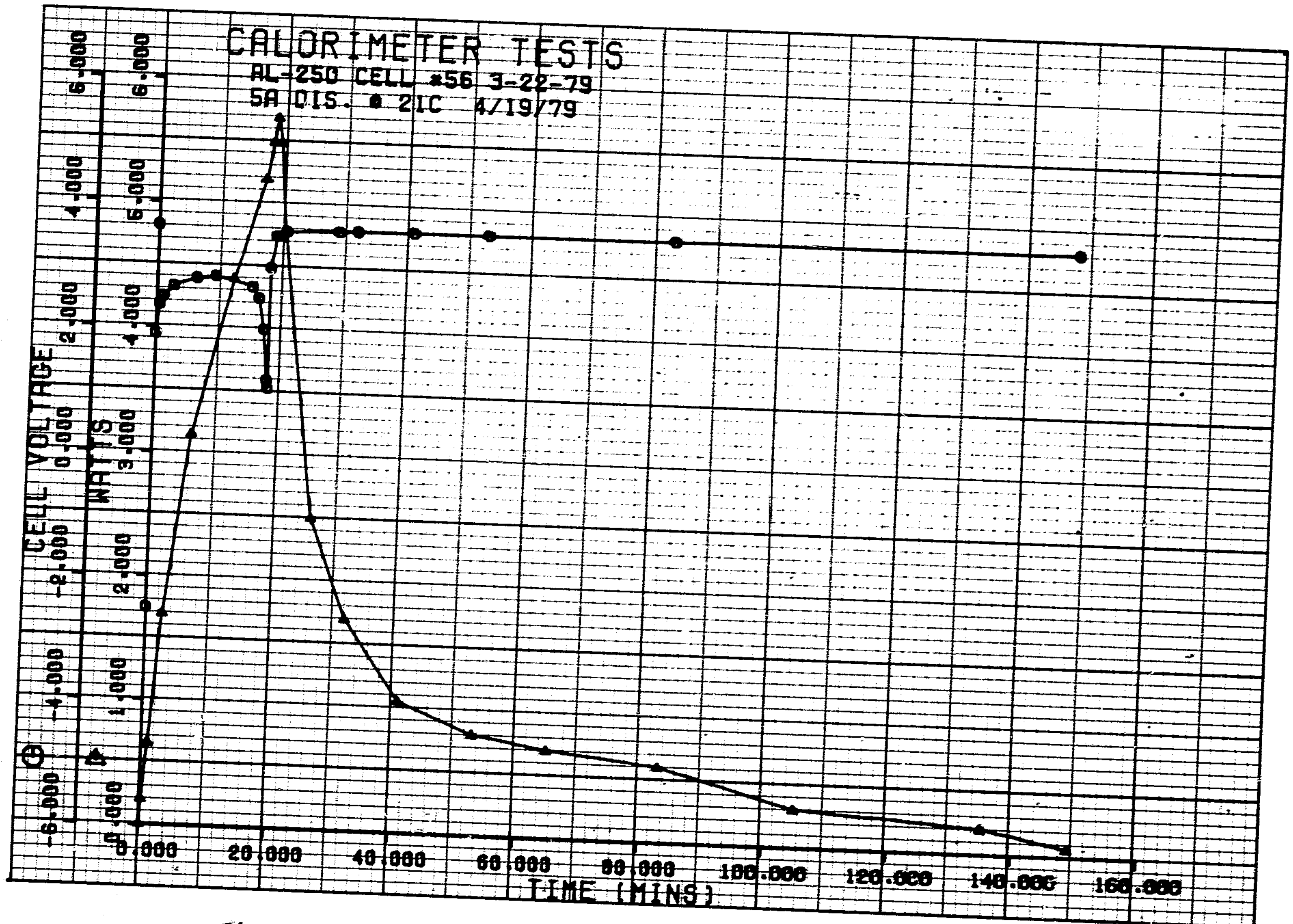

Figure A-7. Calorimeter Test at 21°C and at 5 amps for Cell #56

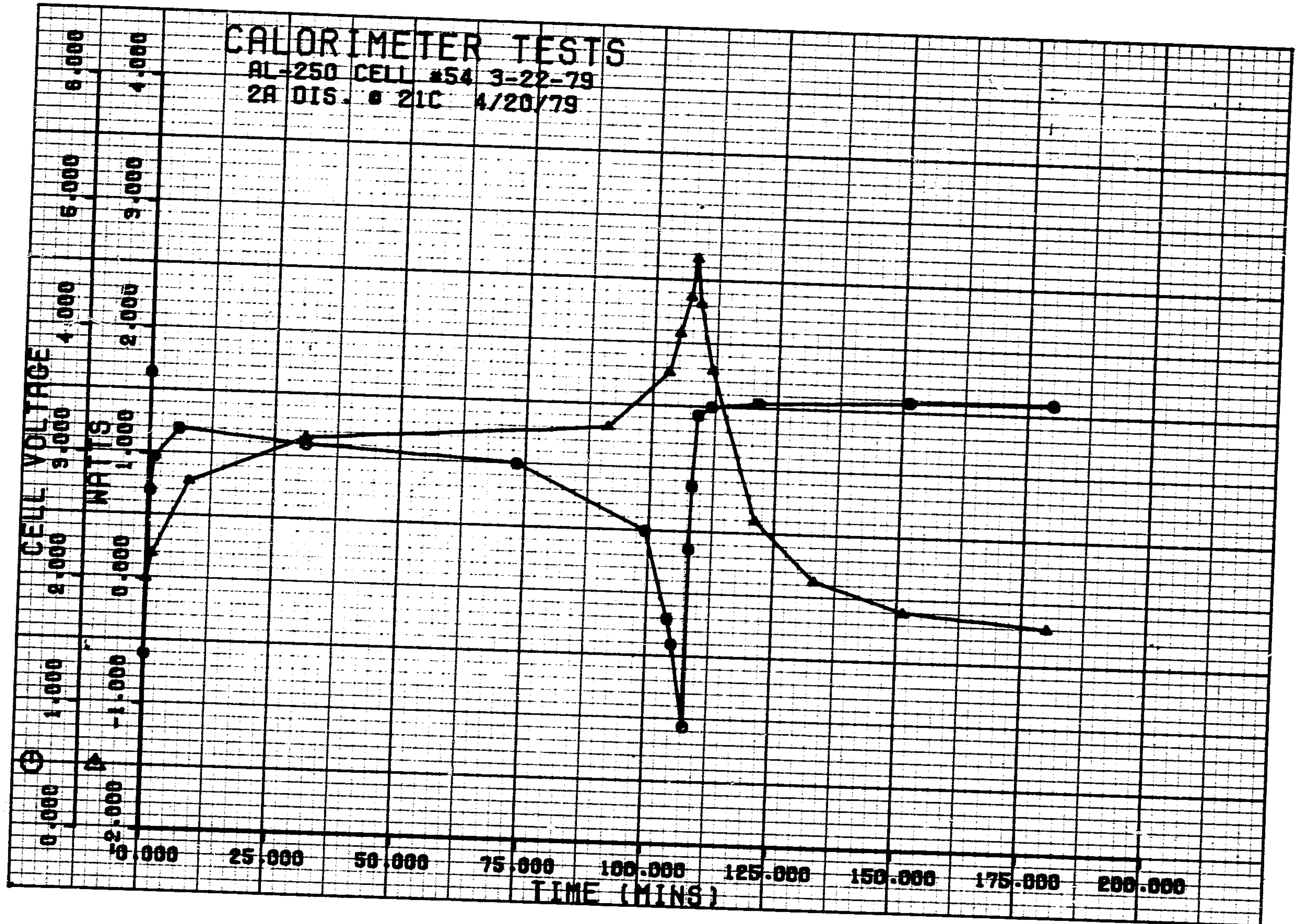

Figure A-8. Calorimeter Test at 21°C and at 2 amps for Cell #54

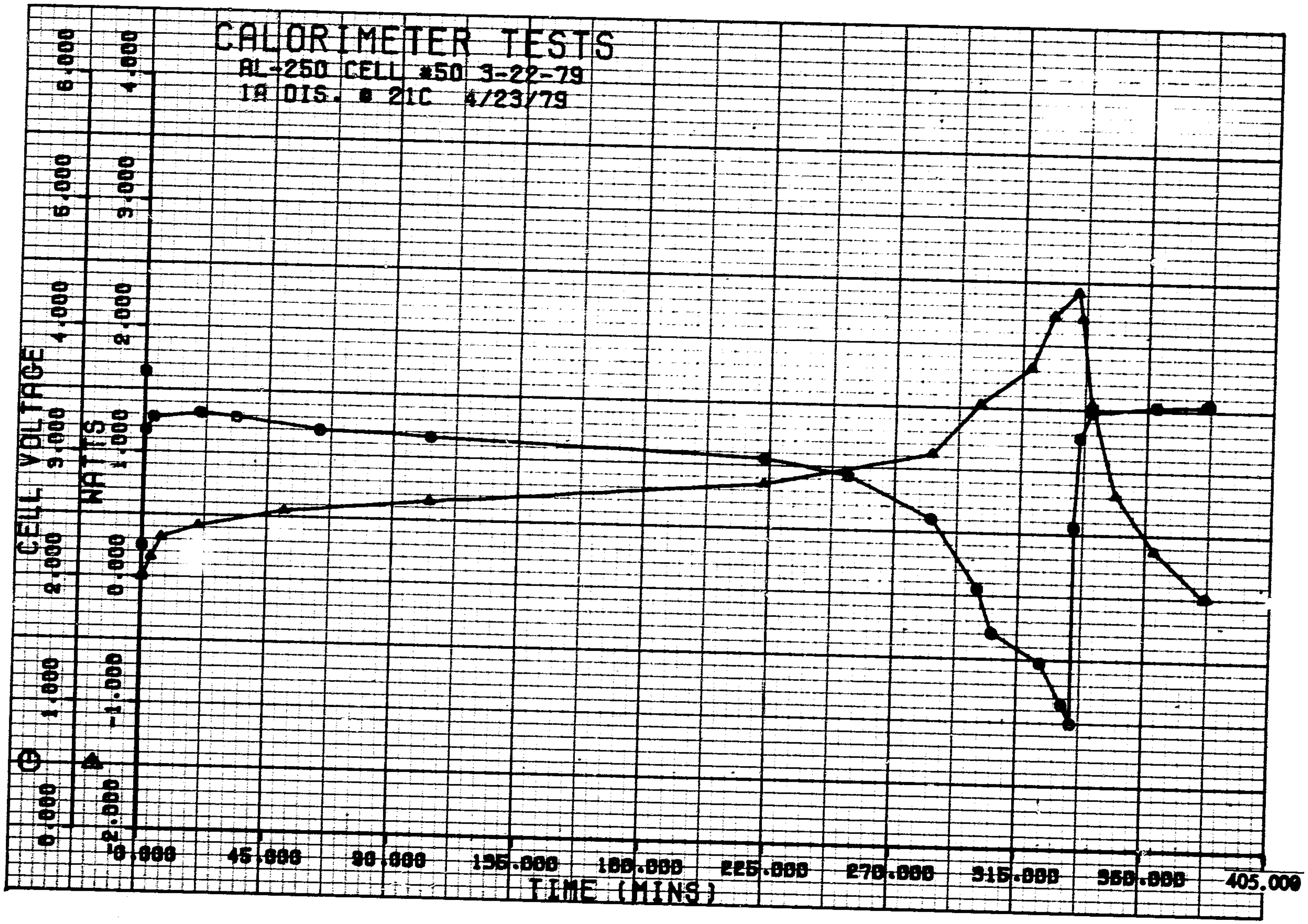

Figure A-9. Calorimeter Test at 21°C and at 1 amp for Cell #50

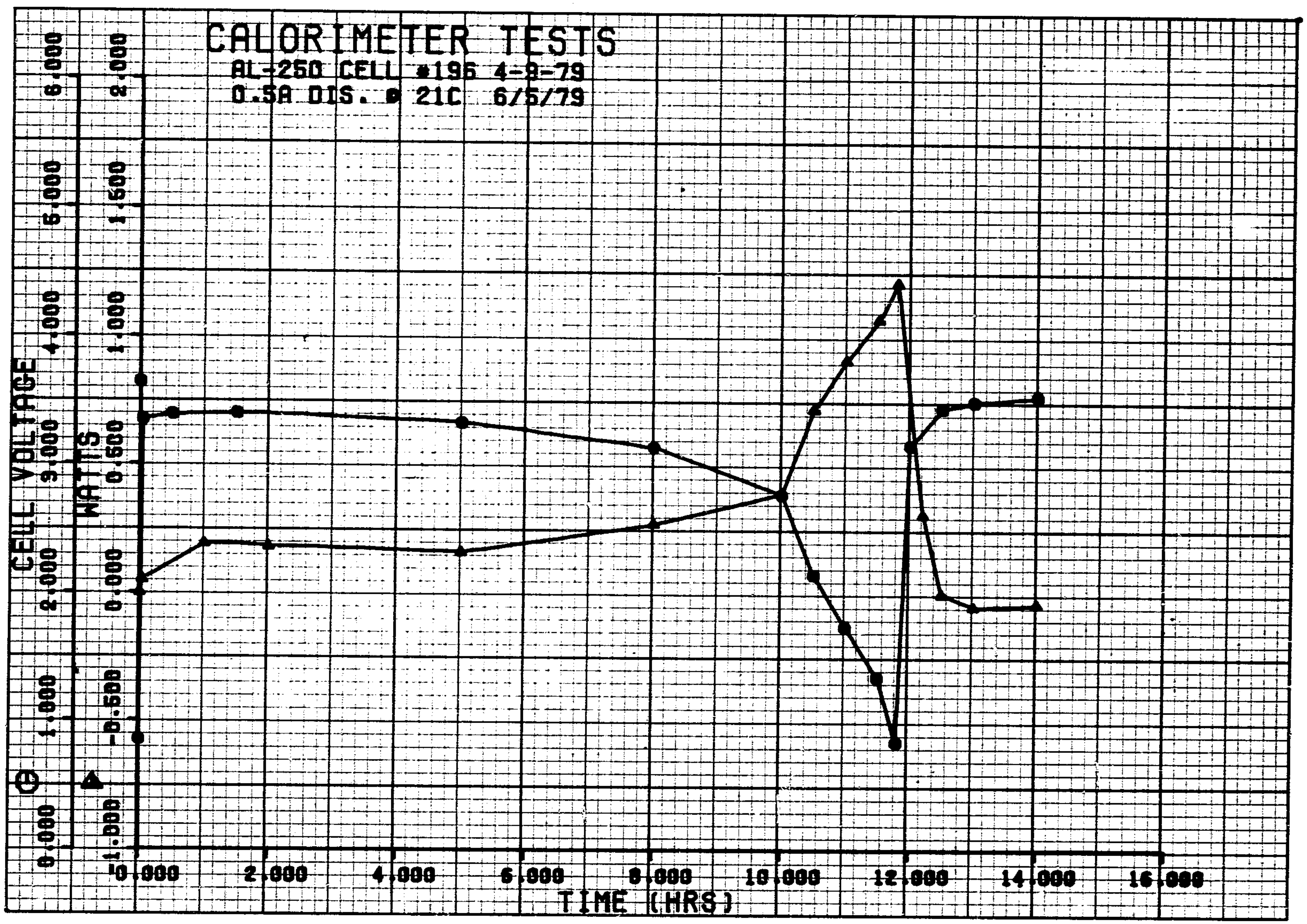

Figure A-10. Calorimeter Test at 21°C and at 0.5 amps for Cell #196

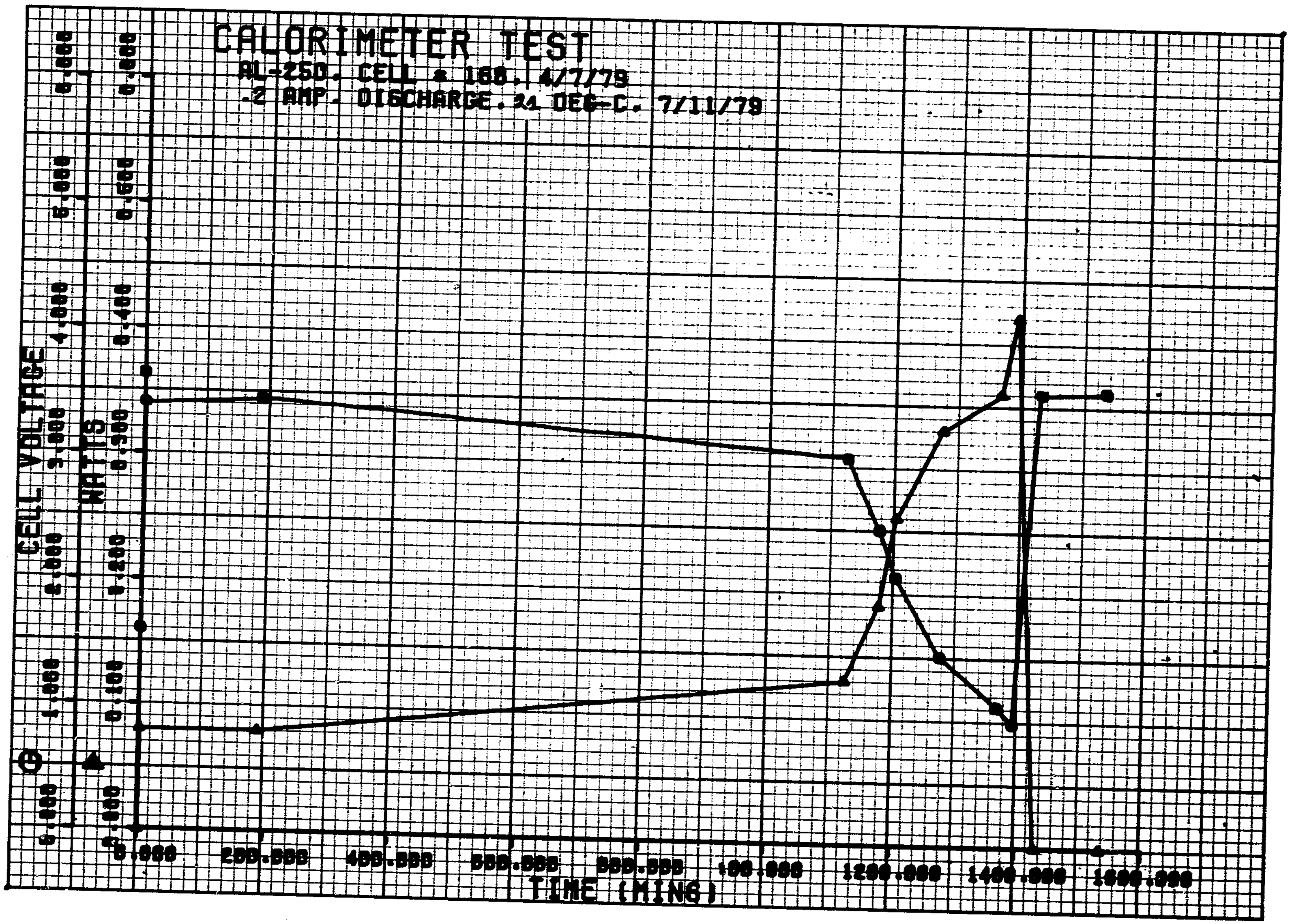

Figure A-11. Calorimeter Test at 21°C and at 0.2 amps for Cell #168

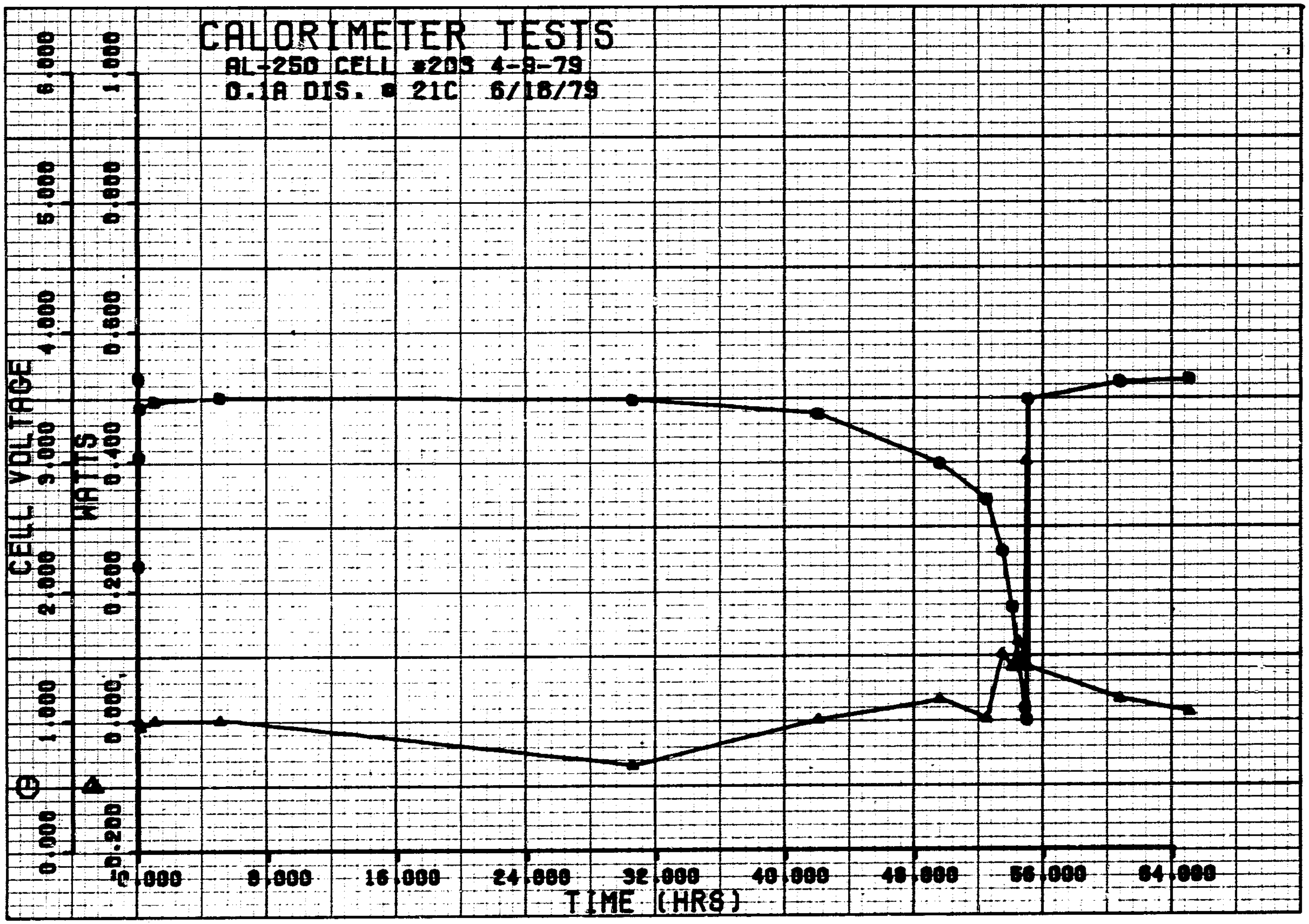

Figure A-12. Calorimeter Test at 21°C and at 0.1 amps for Cell #203

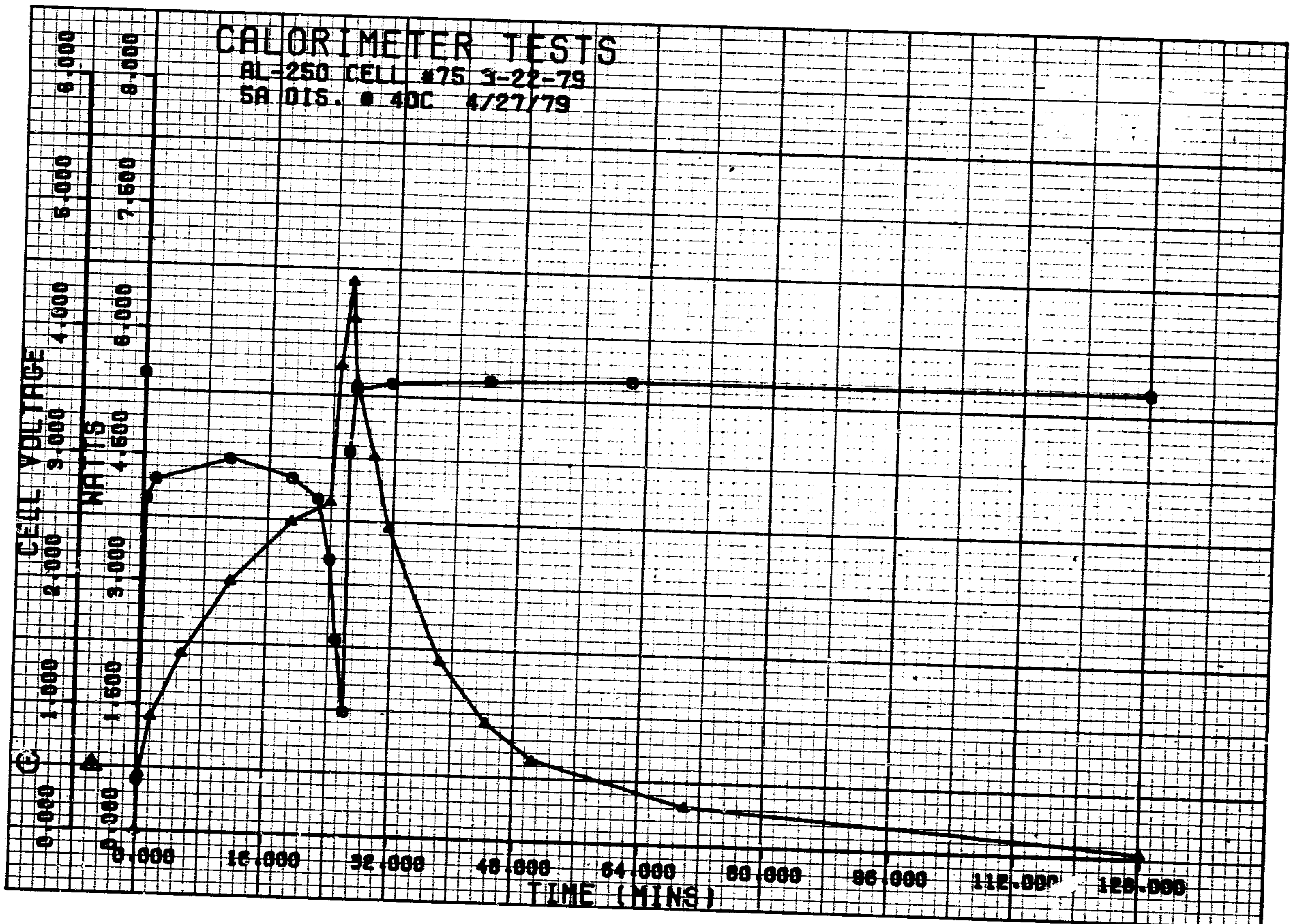

Figure A-13. Calorimeter Test at 40°C and at 5 amps for Cell #75

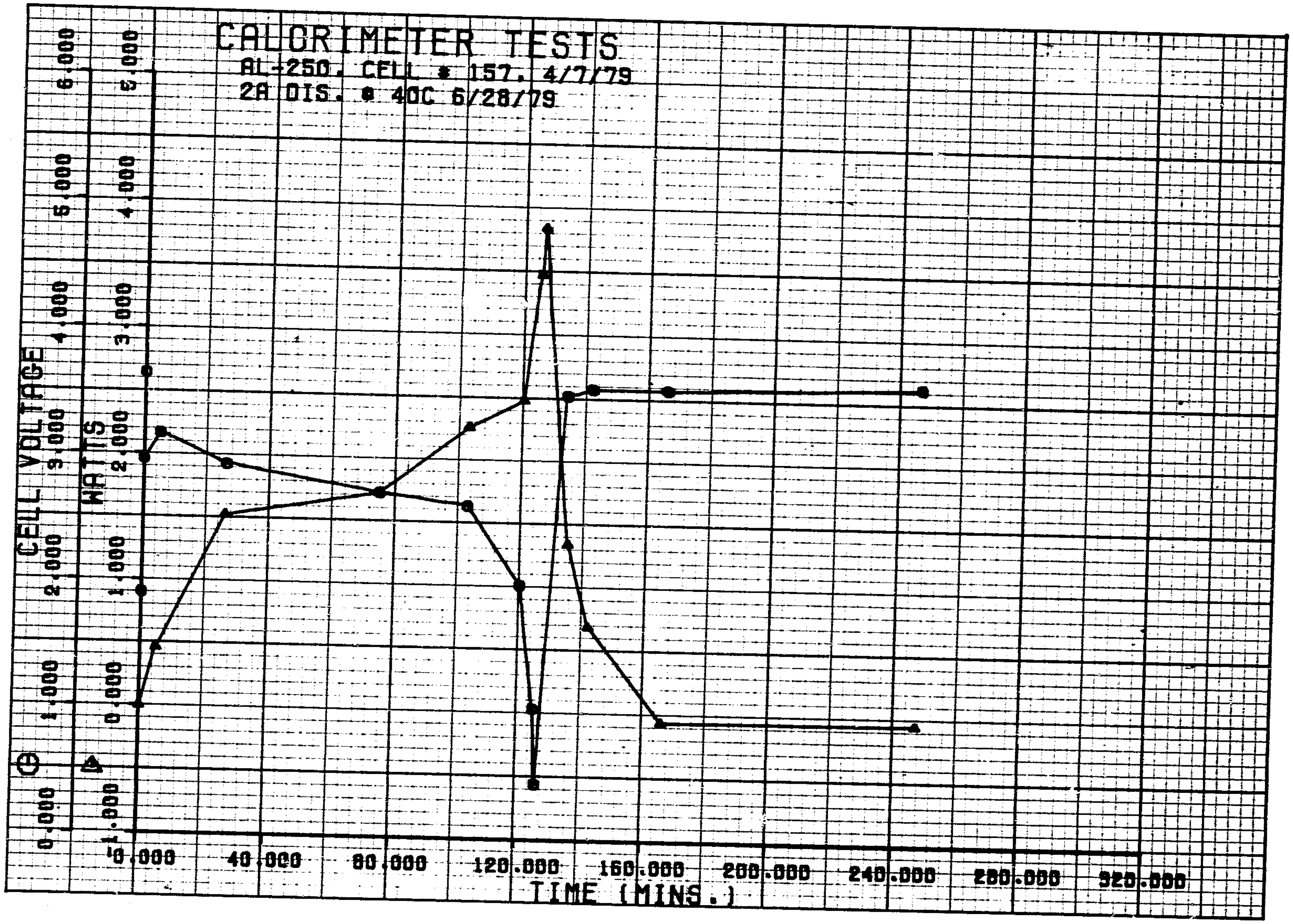

Figure A-14. Calorimeter Test at 40°C and at 2 amps for Cell #157

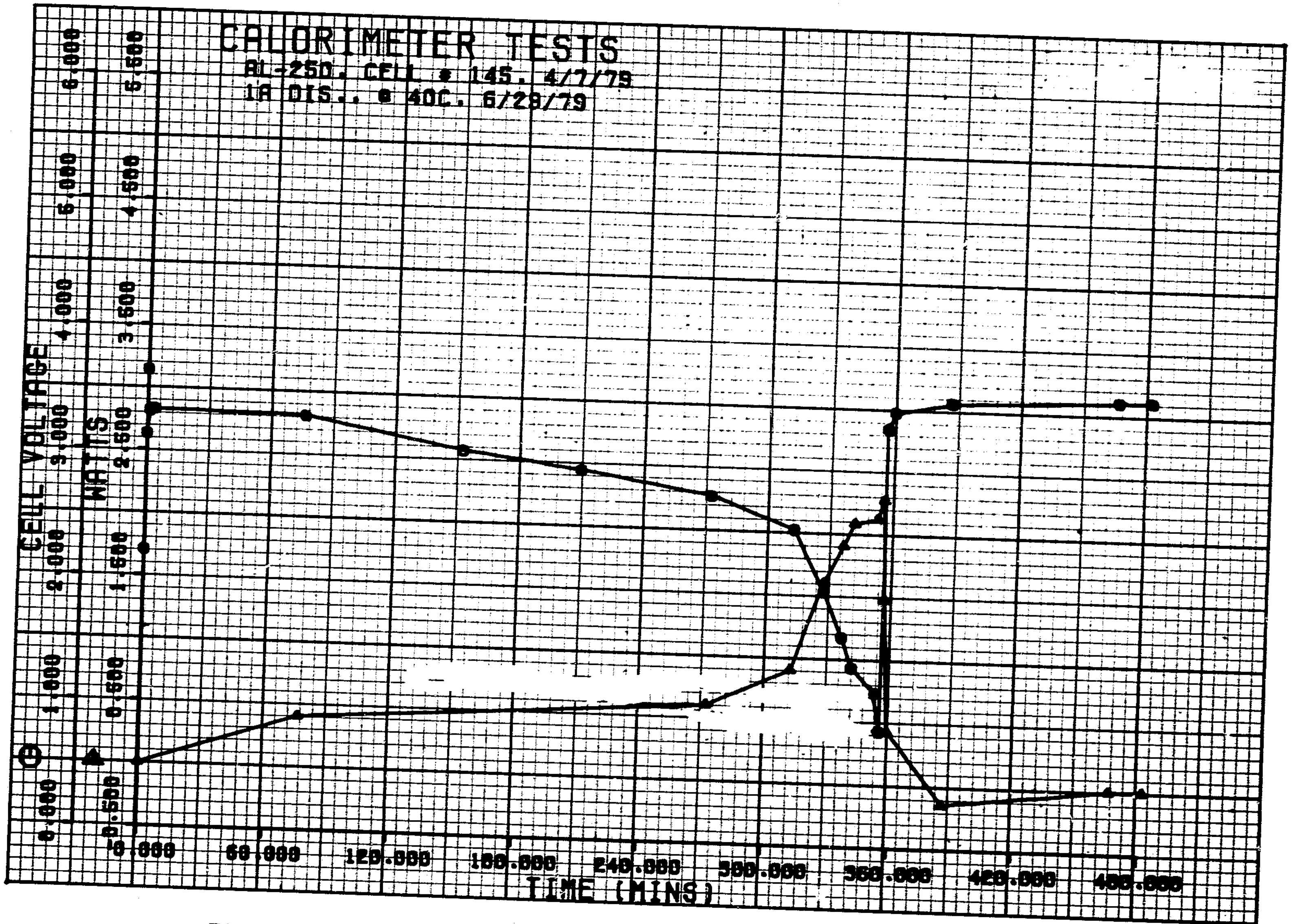

Figure A-15. Calorimeter Test at 40°C and at 1 amp for Cell #145

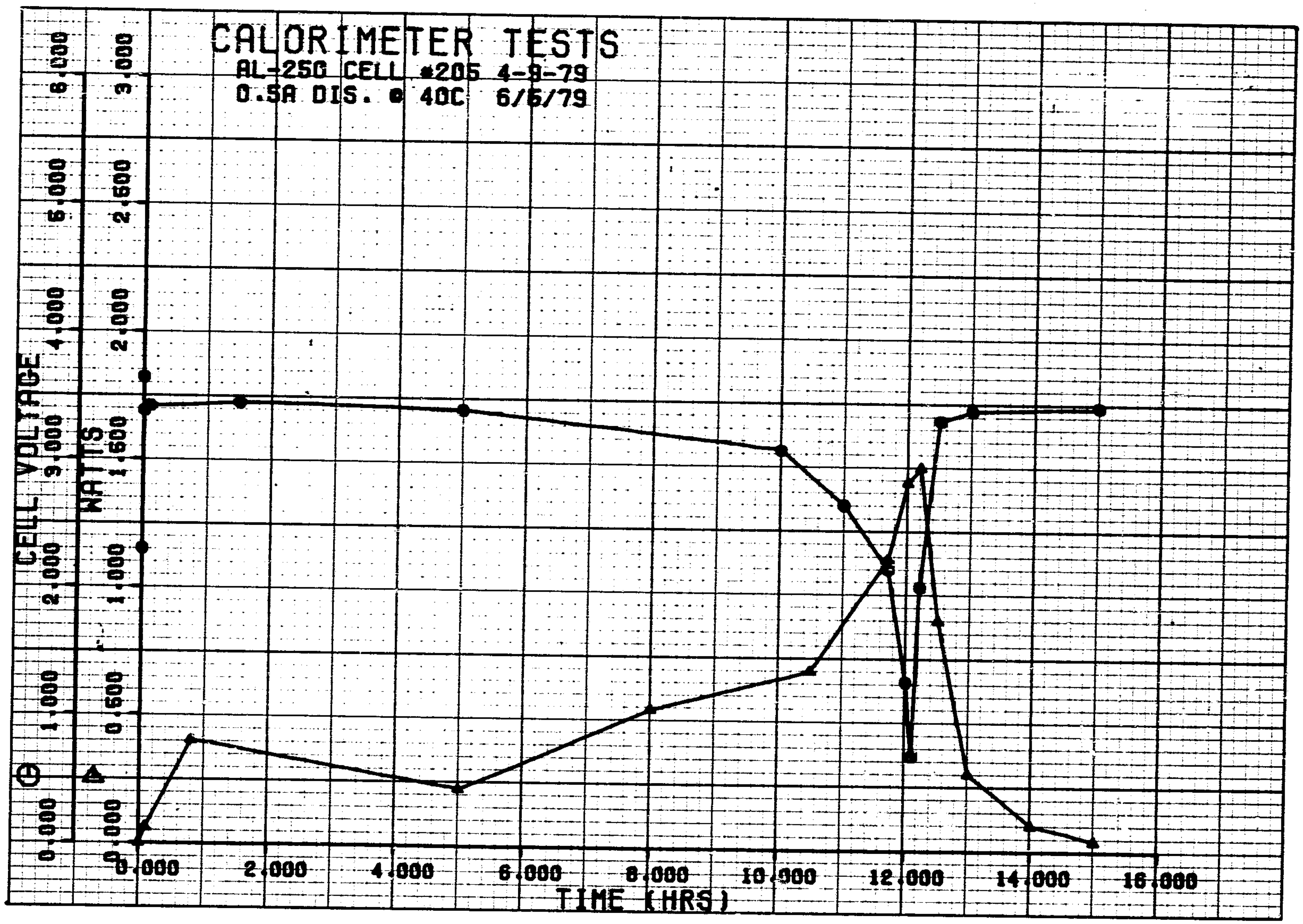

Figure A-16. Calorimeter Test at 40°C and at 0.5 amps for Cell #205

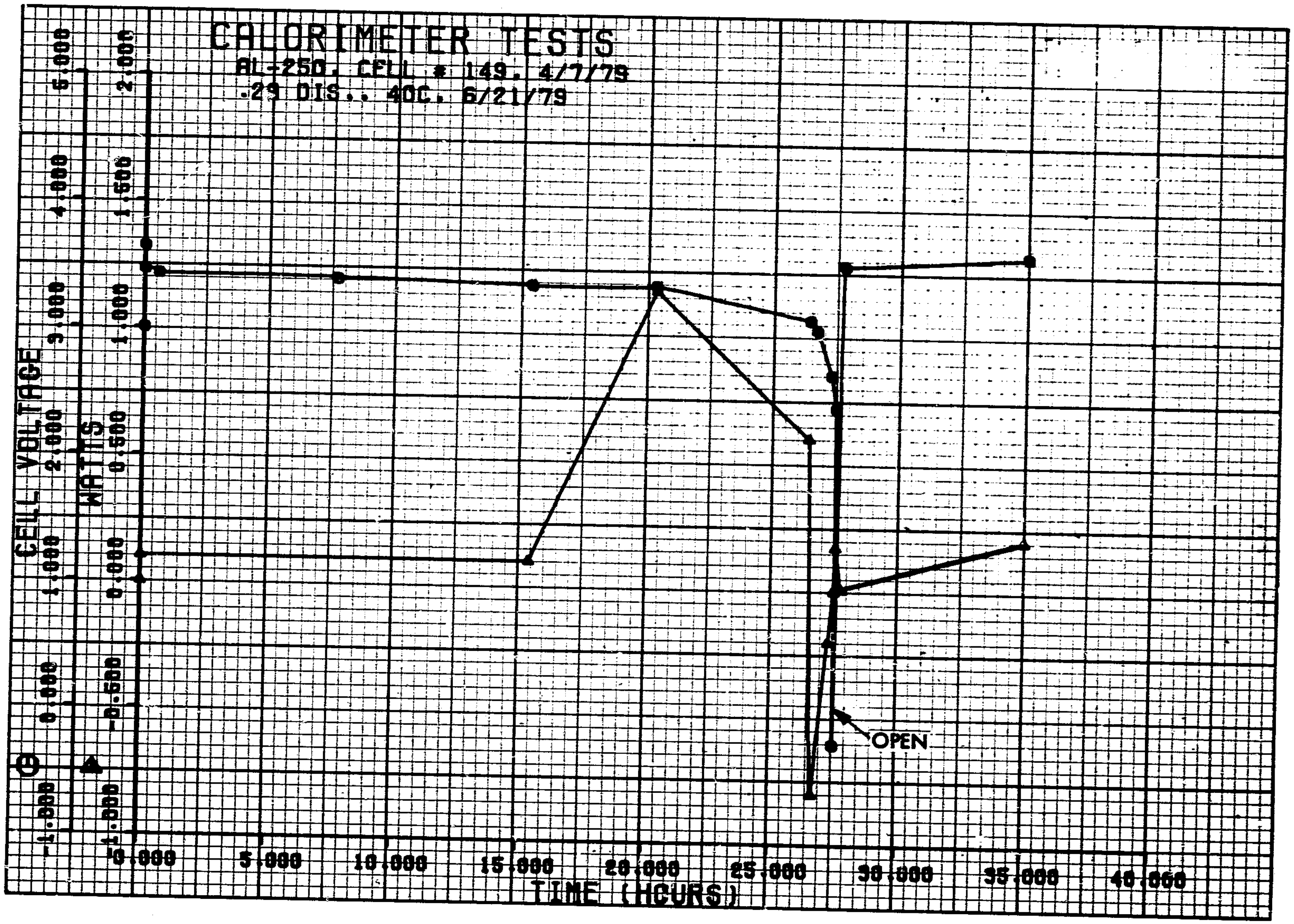

Figure A-17. Calorimeter Test at 40°C and at 0.2 amps for Cell #149

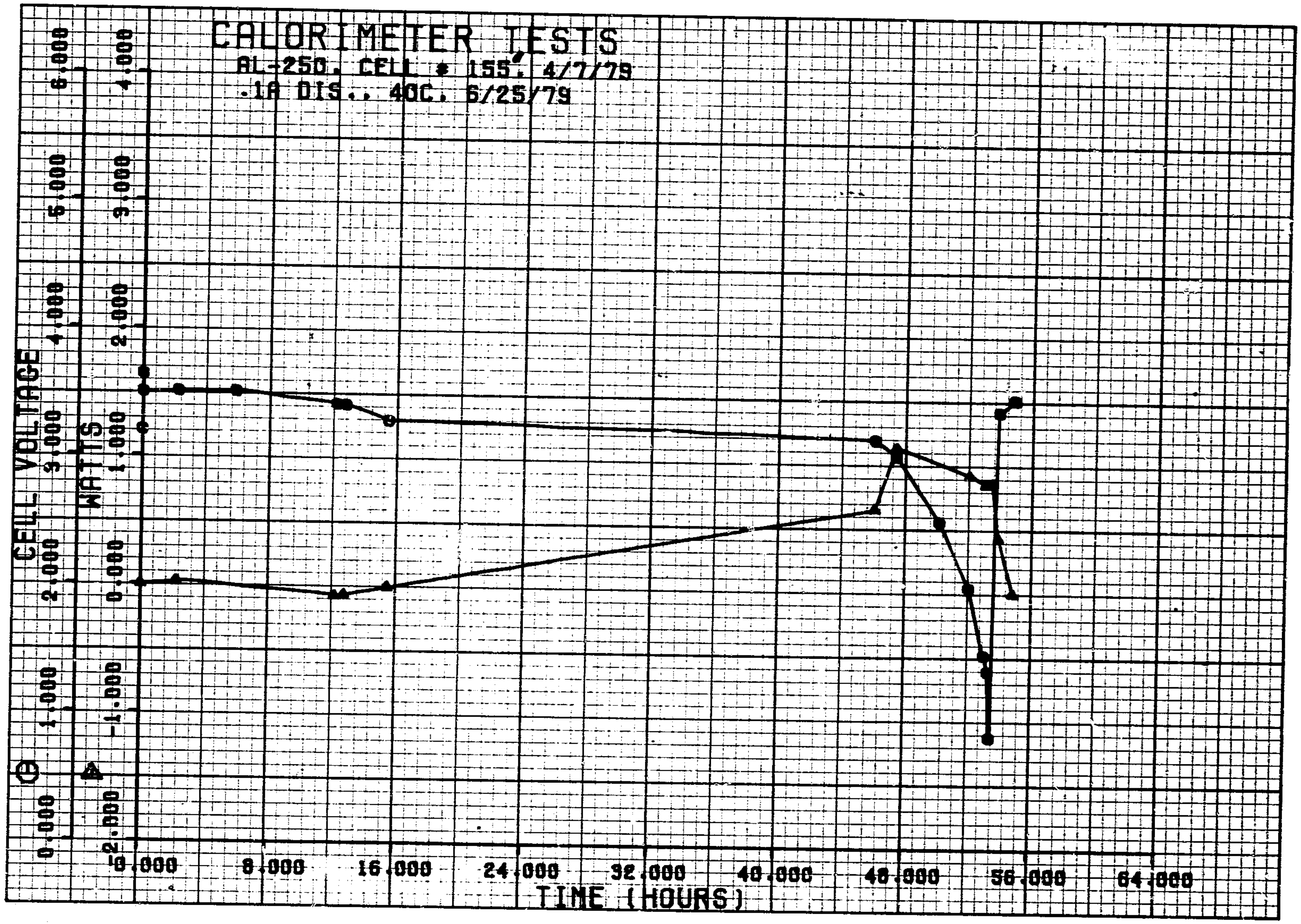

Figure A-18. Calorimeter Test at 40°C and at 0.1 amps for Cell #155

APPENDIX B

COMPUTER-DRAWN GRAPHS OF CONSTANT CURRENT DISCHARGE AND FORCED REVERSAL TESTS

(Tests were conducted at room temperature, 21°C.)

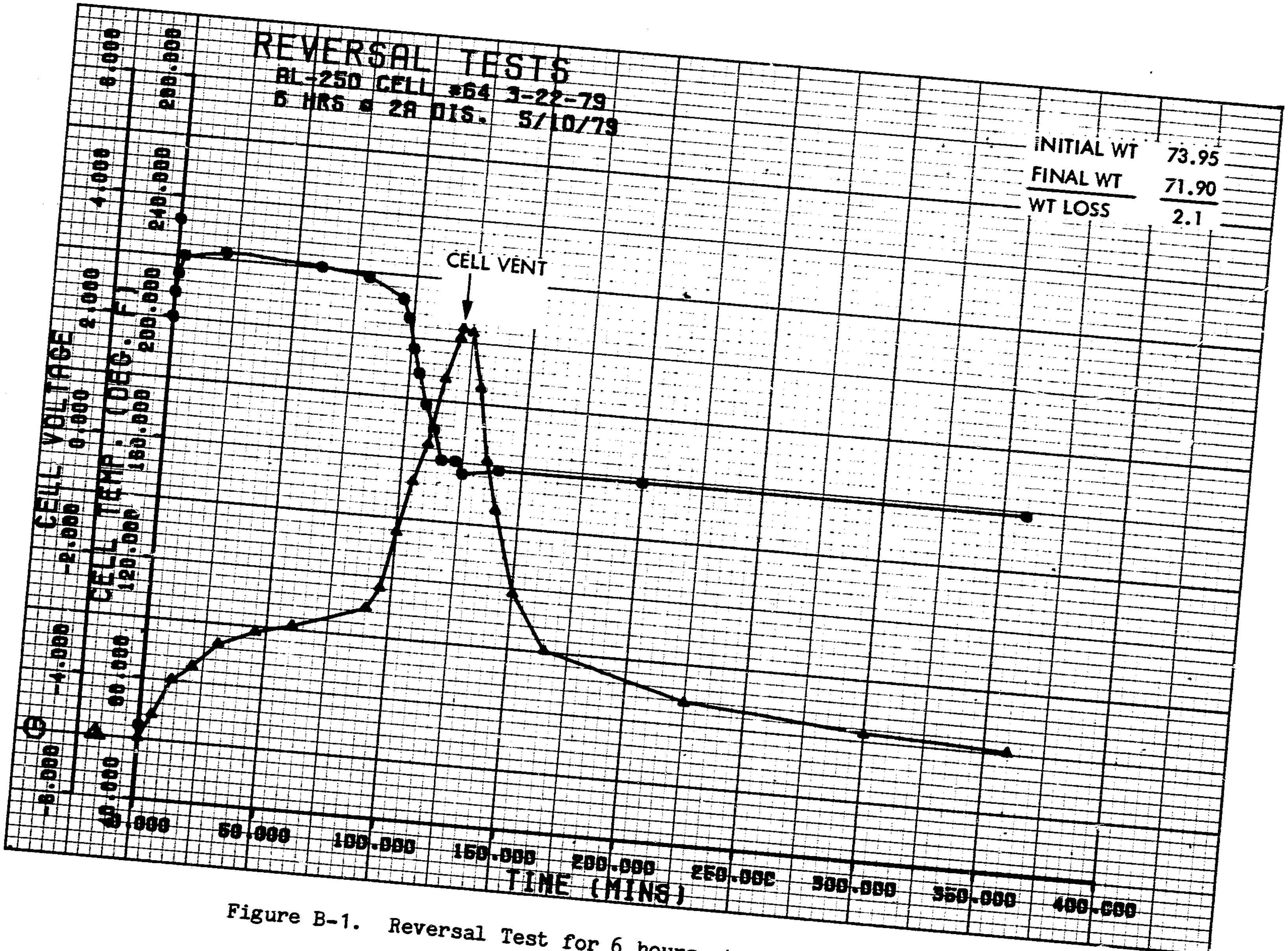

Figure B-1. Reversal Test for 6 hours at 2 amps for Cell #64

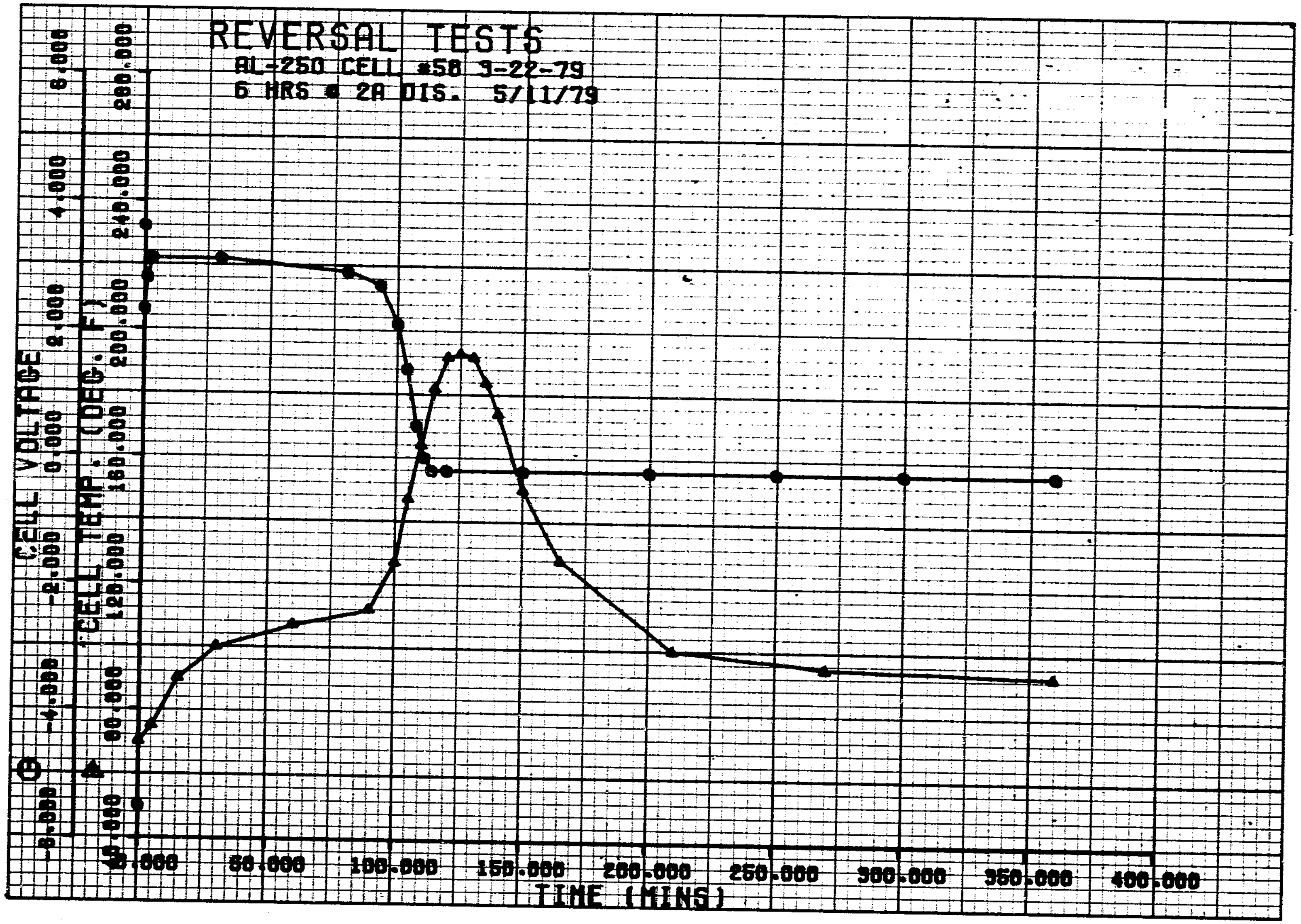

Figure B-2. Reversal Test for 6 hours at 2 amps for Cell #58

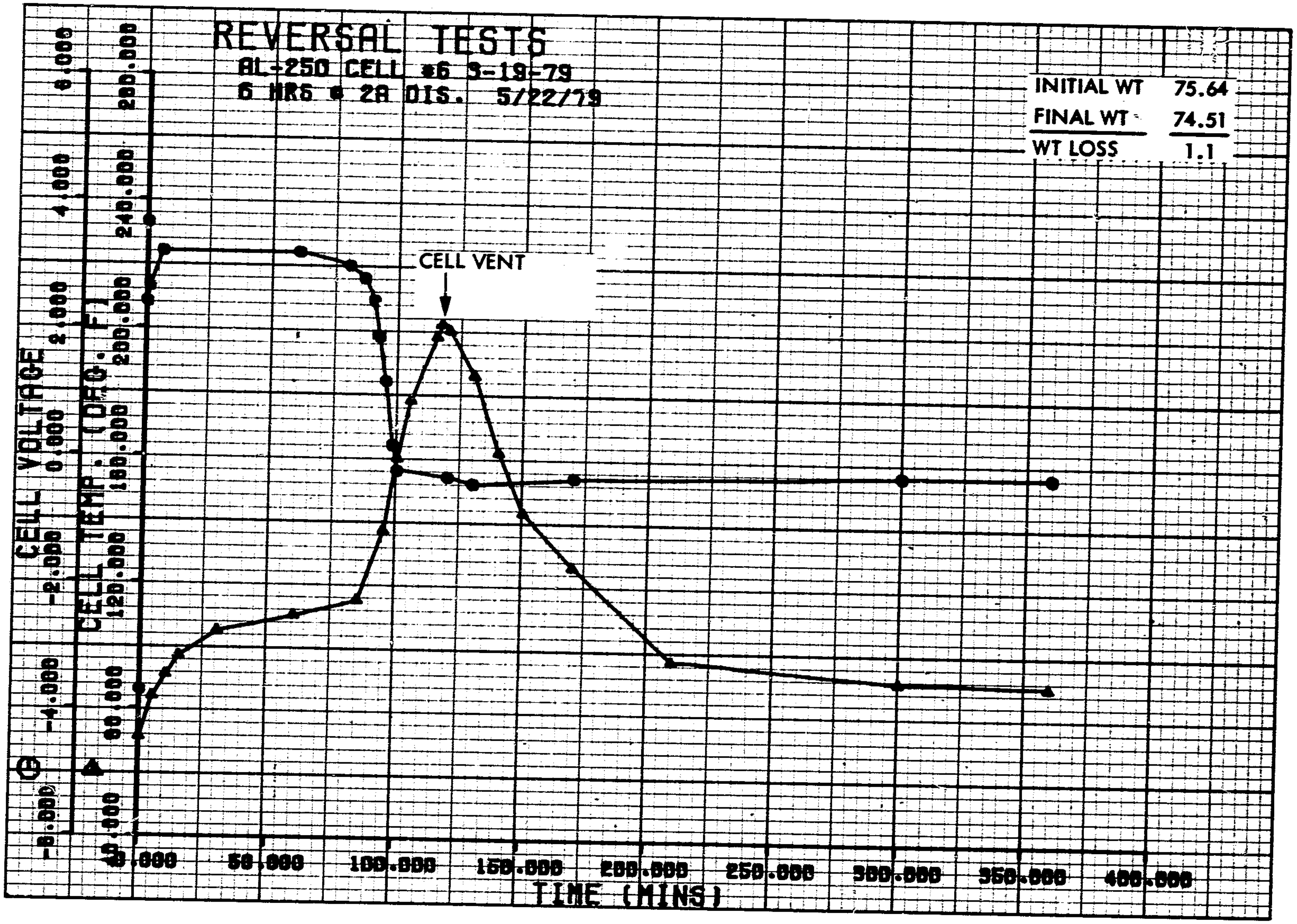

Figure B-3 Reversal Test for 6 hours at 2 amps for Cell #6

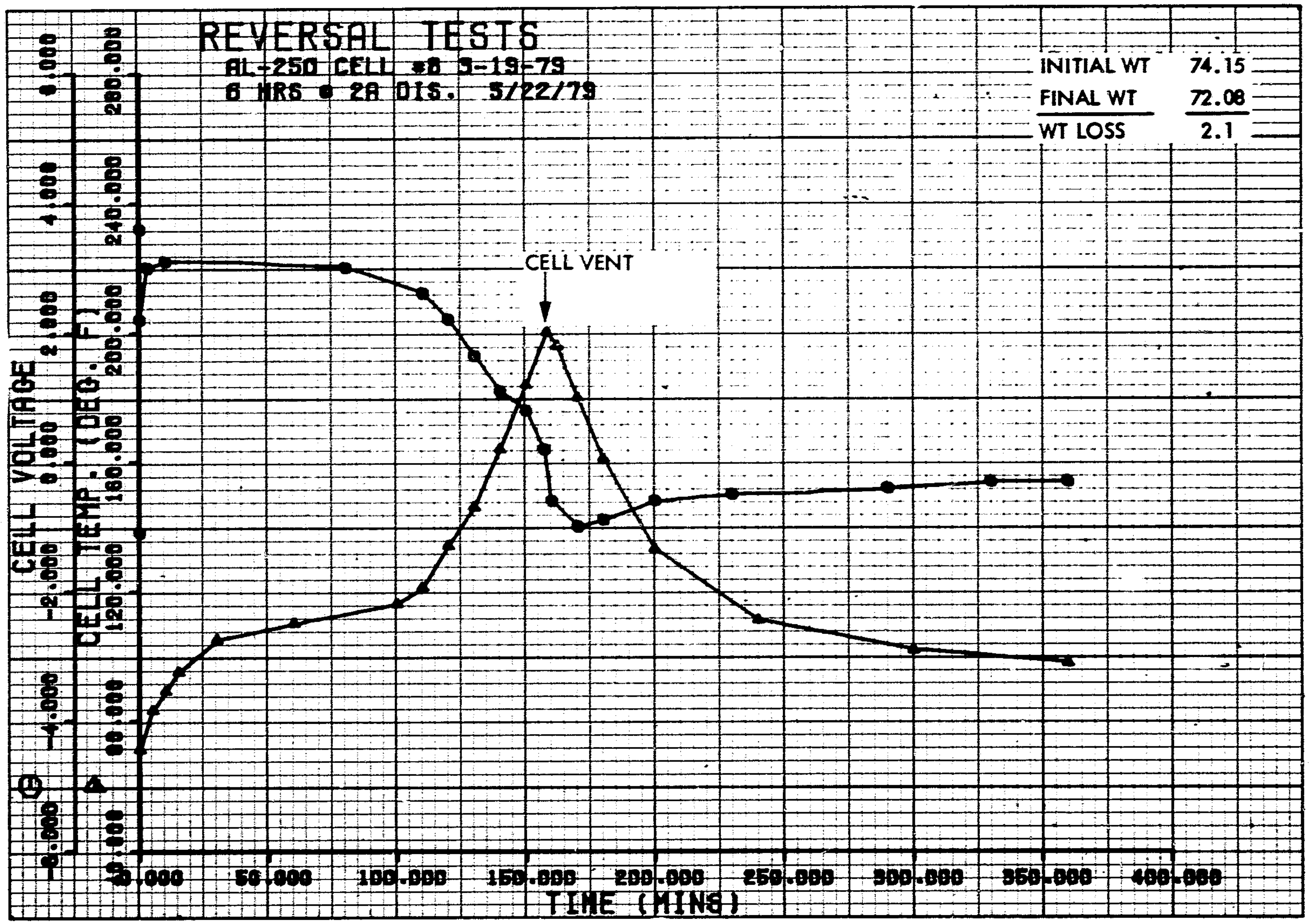

Figure B-4. Reversal Test for 6 hours at 2 amps for Cell #8

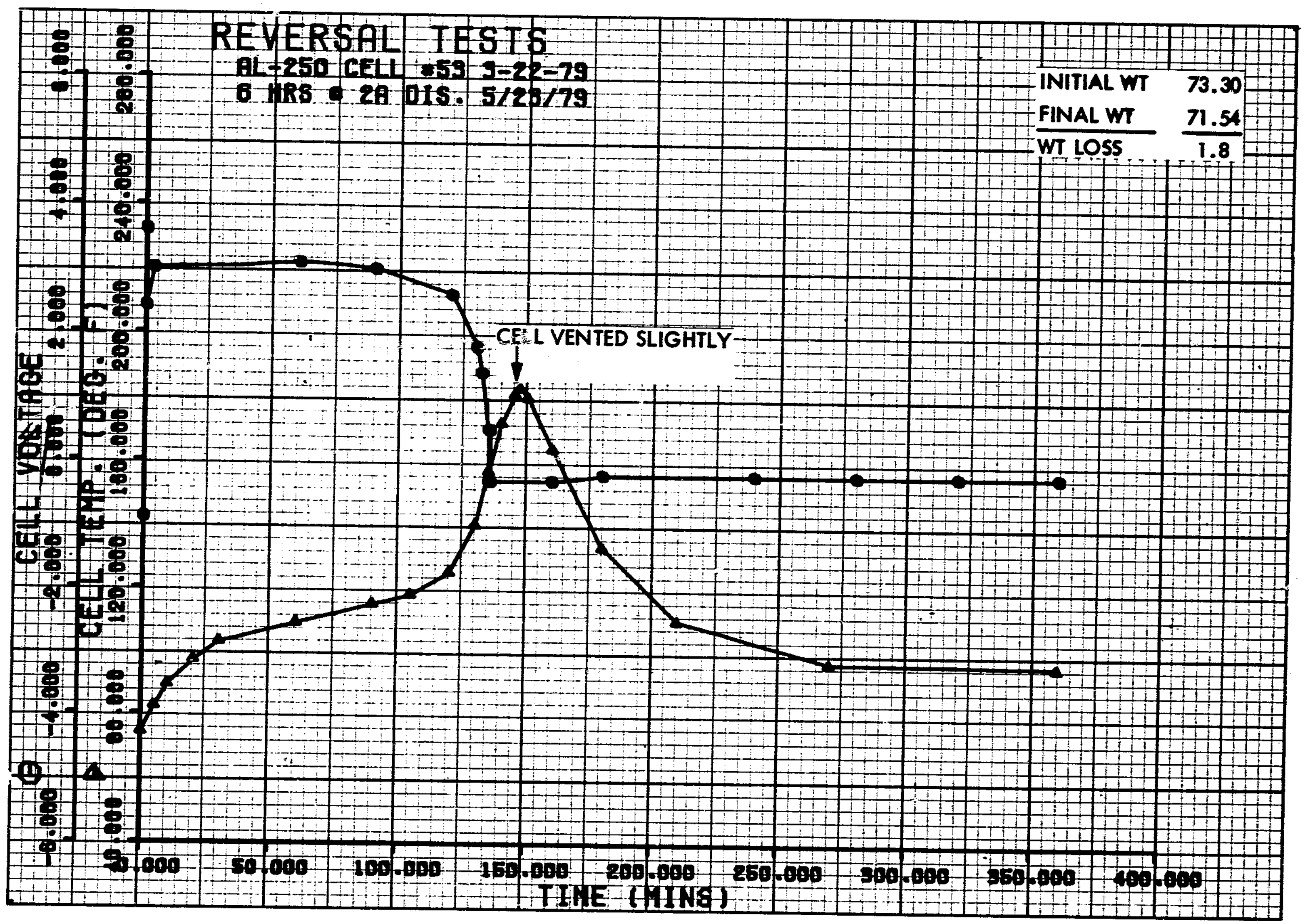

Figure B-5. Reversal Test for 6 hours at 2 amps for Cell #53

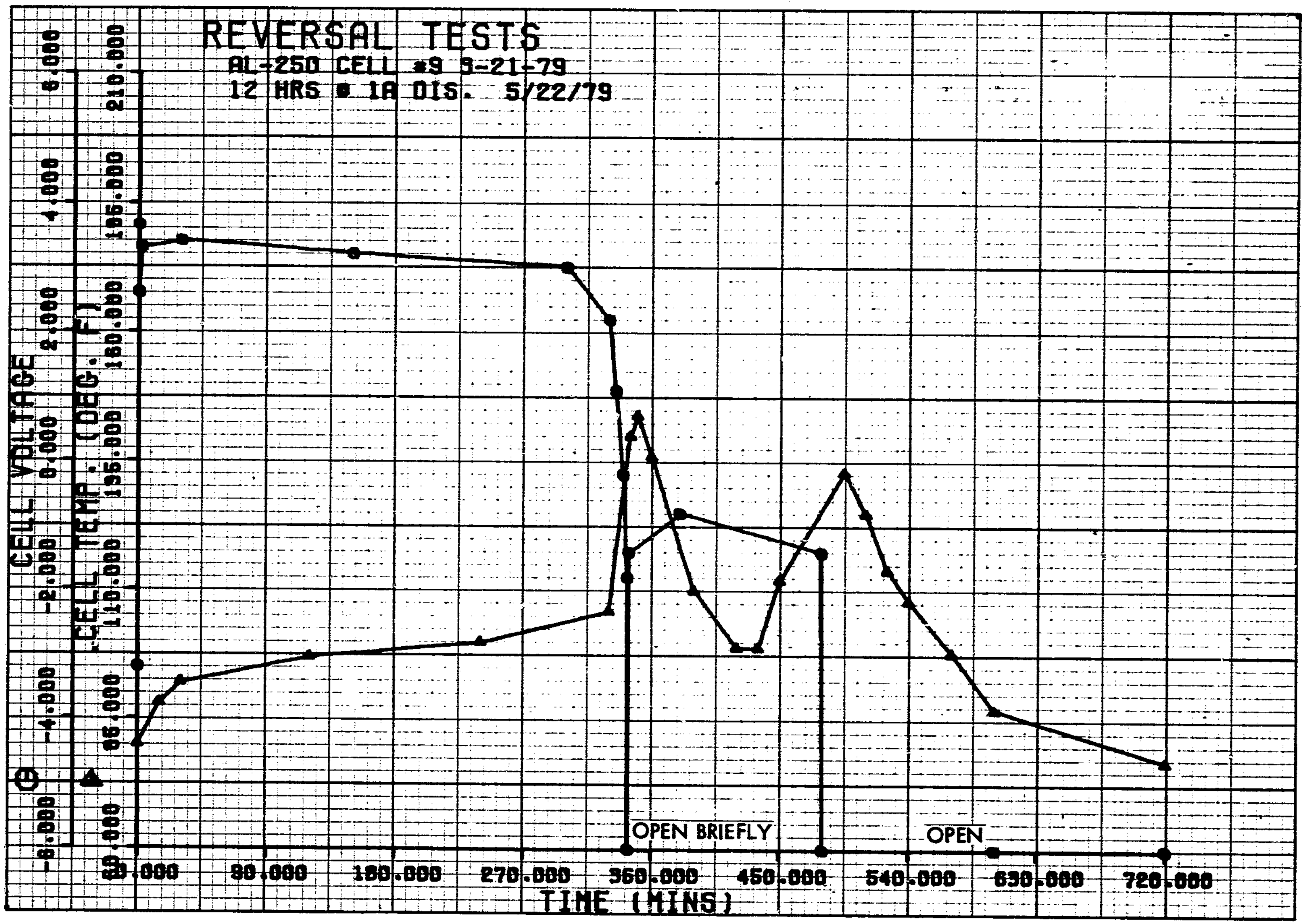

Figure B-6. Reversal Test for 12 hours at 1 amp for Cell #9

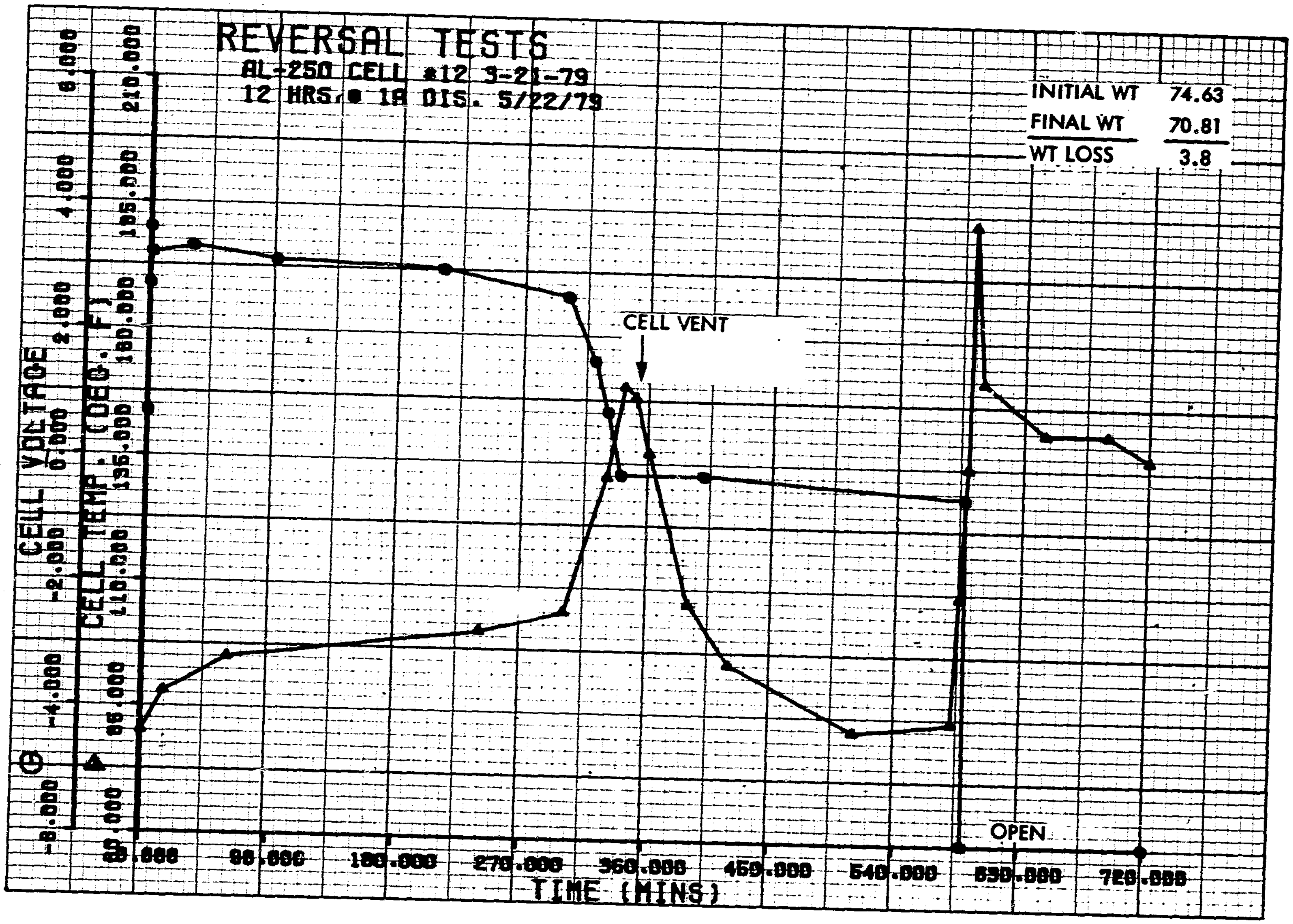

Figure B-7. Re ersal Test for 12 hours at 1 amp for Cell #12

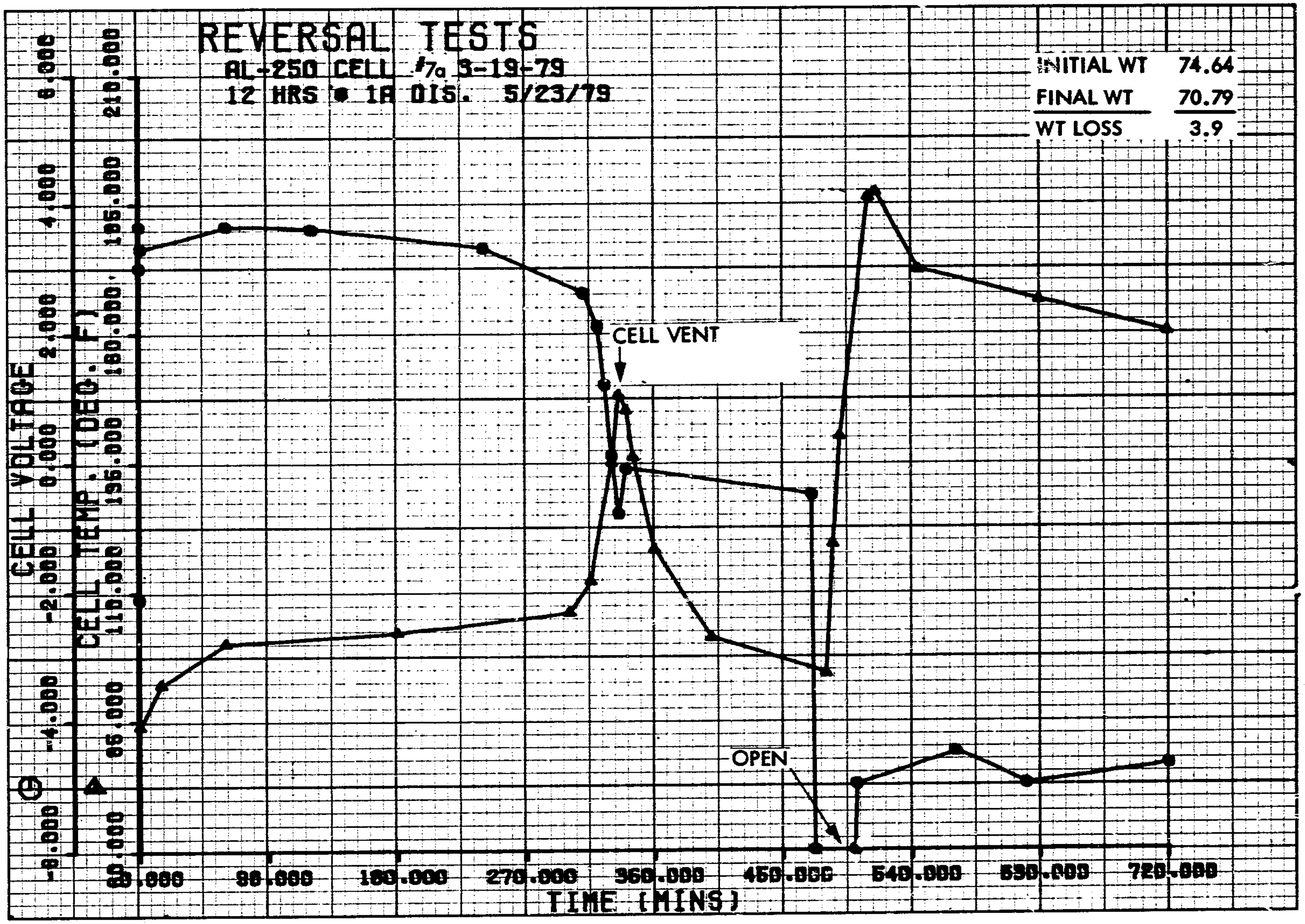

Figure B-8. Reversal Test for 12 hours at 1 amp for Cell #7a

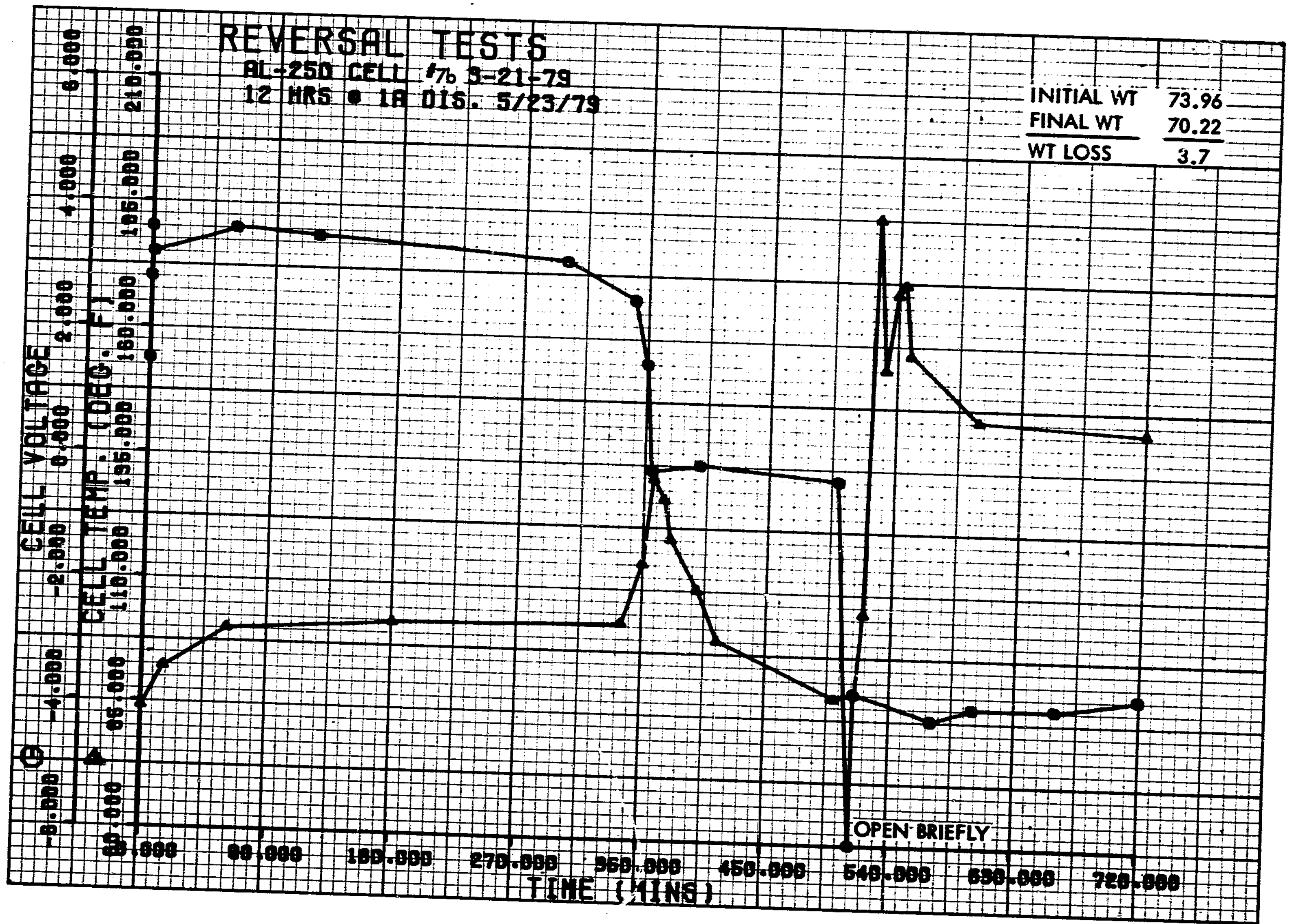

Figure B-9. Reversal Test for 12 hours at 1 amp for Cell #7b

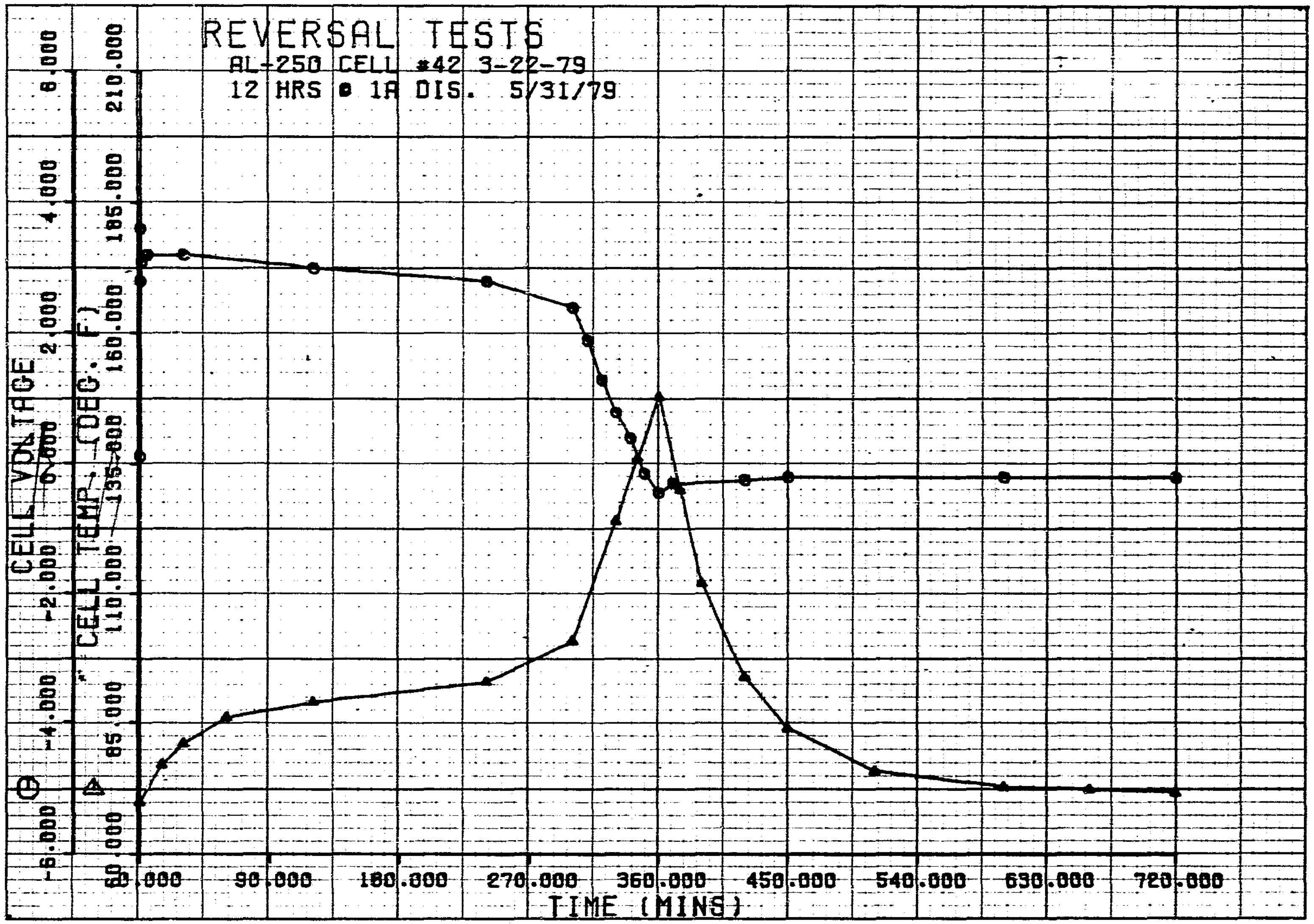

Figure B-10. Reversal Test for 12 hours at 1 amp for Cell #42

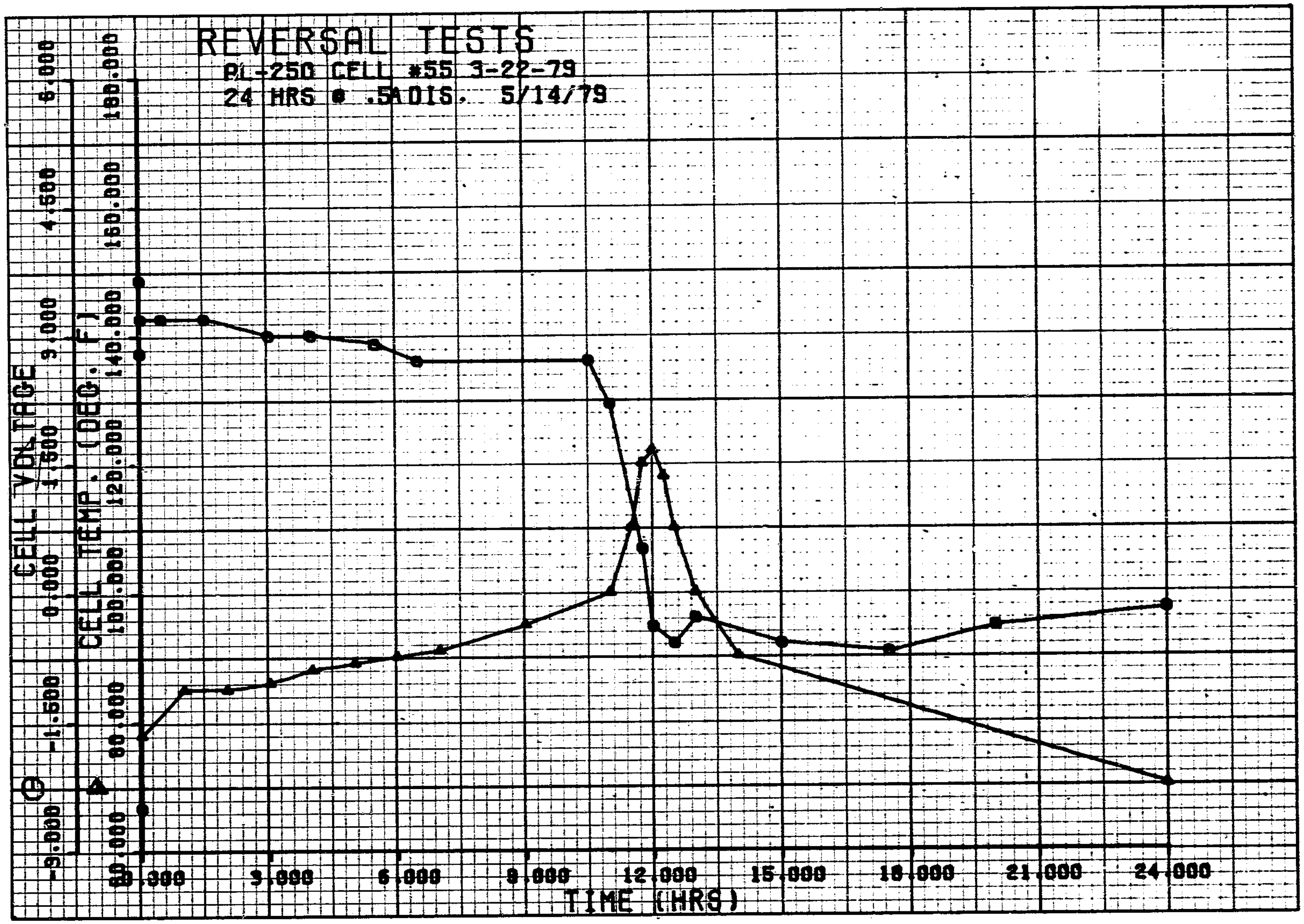

Figure B-11. Reversal Test for 24 hours at 0.5 amps for Cell #55

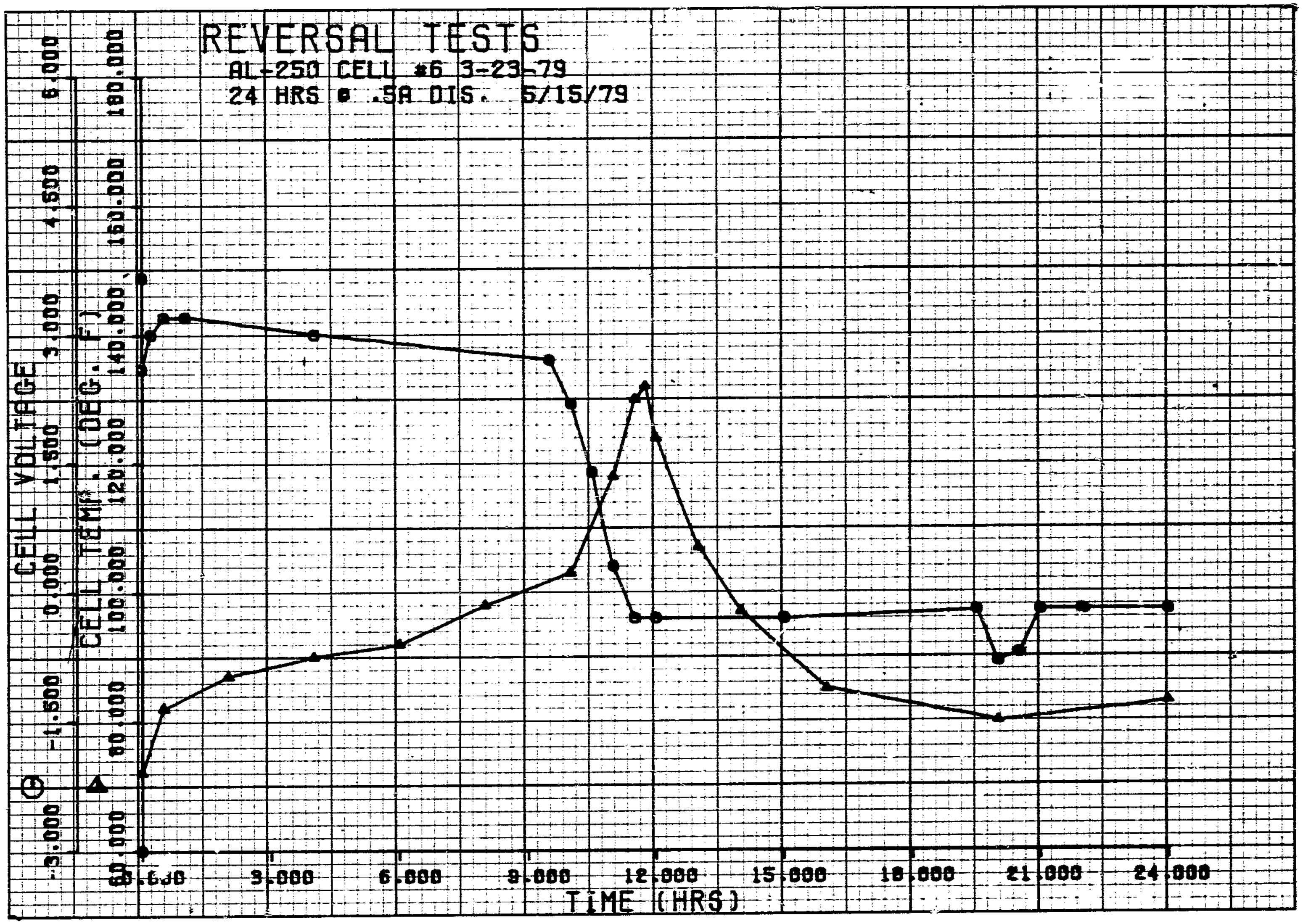

Figure B-12. Reversal Test for 24 hours at 0.5 amps for Cell #6

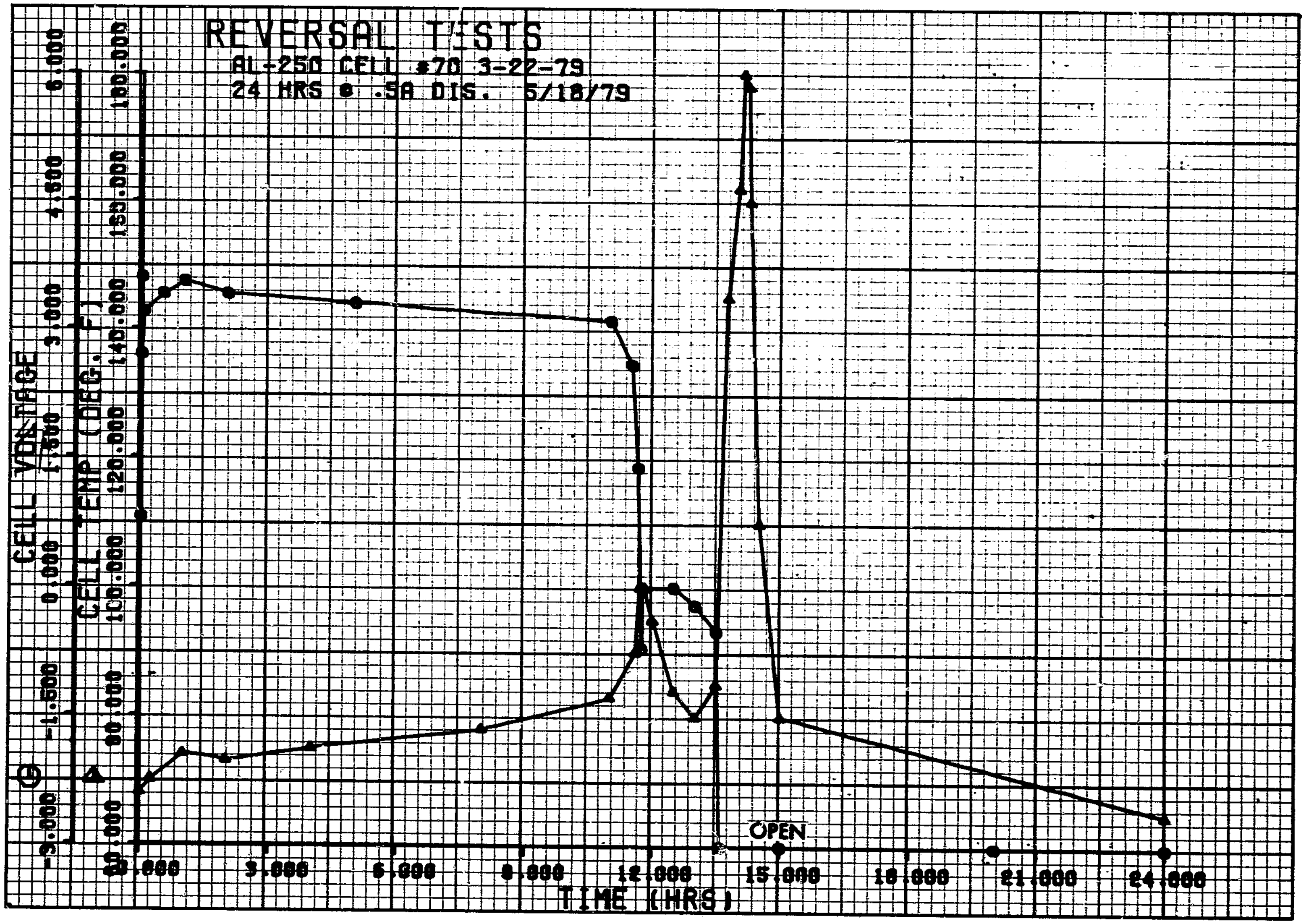

Figure B-13. Reversal Test for 24 hours at 0.5 amps for Cell #70

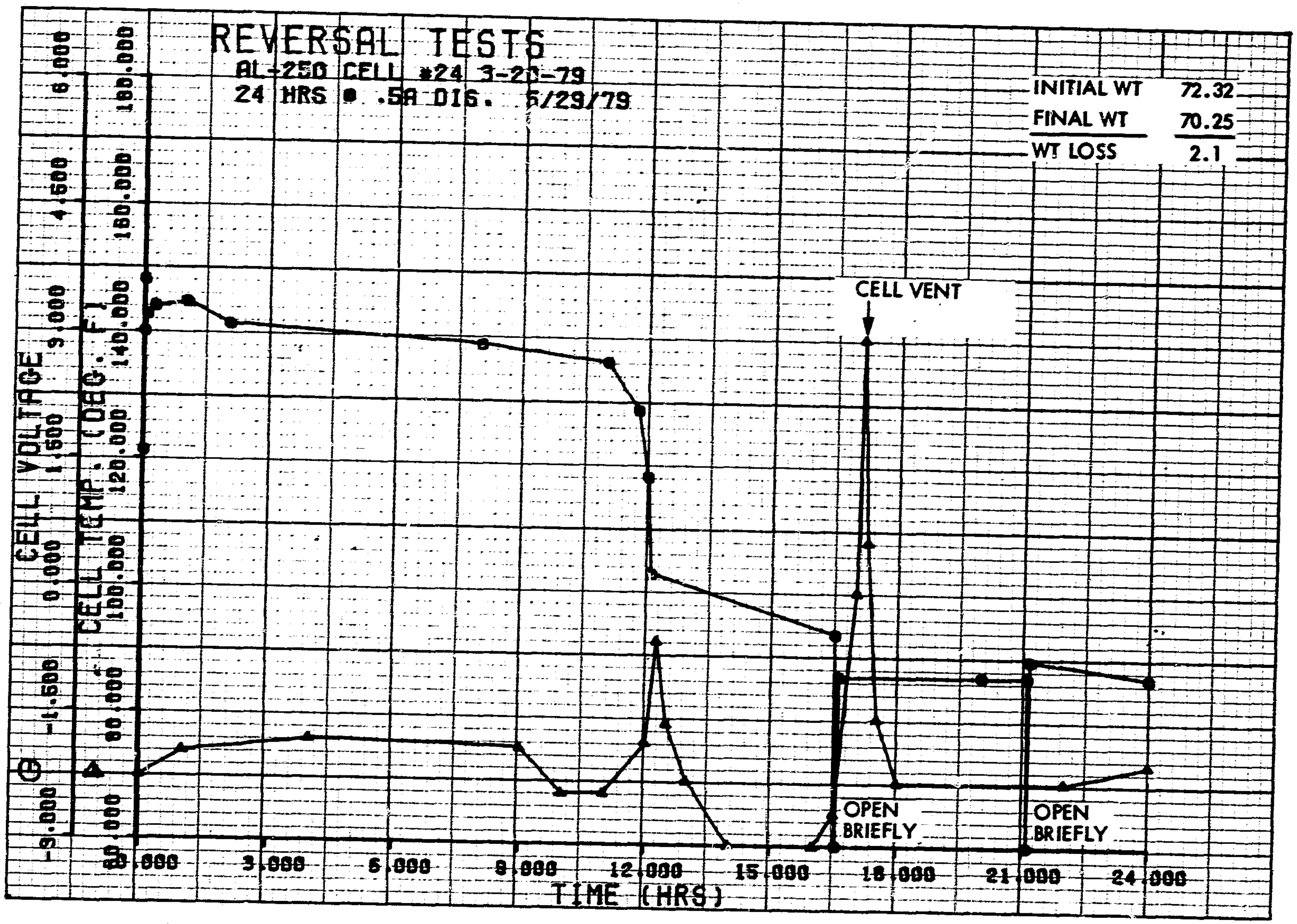

Figure B-14. Reversal Test for 24 hours at 0.5 amps for Cell #24

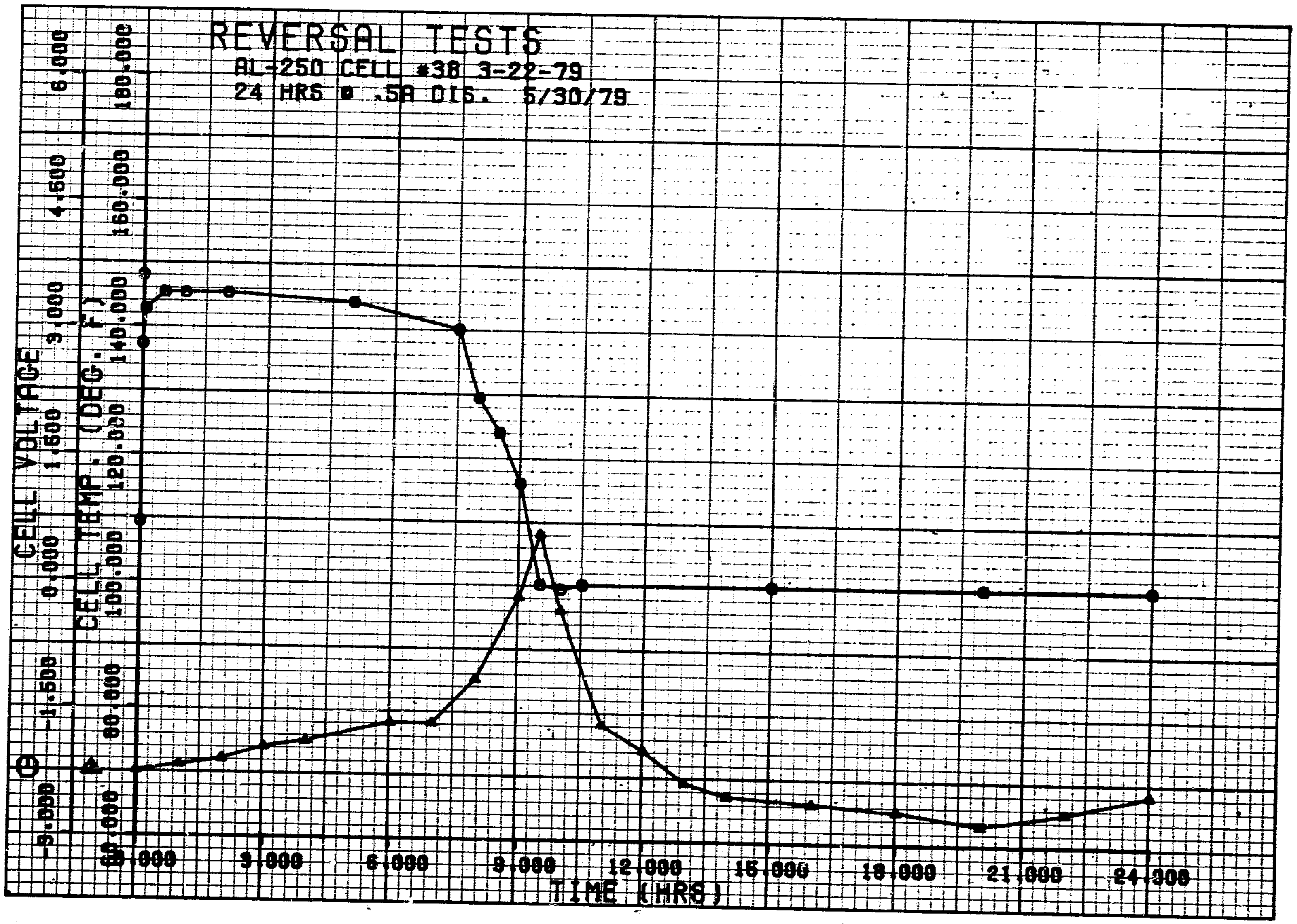

Figure B-15. Reversal Test for 24 hours at 0.5 amps for Cell #38

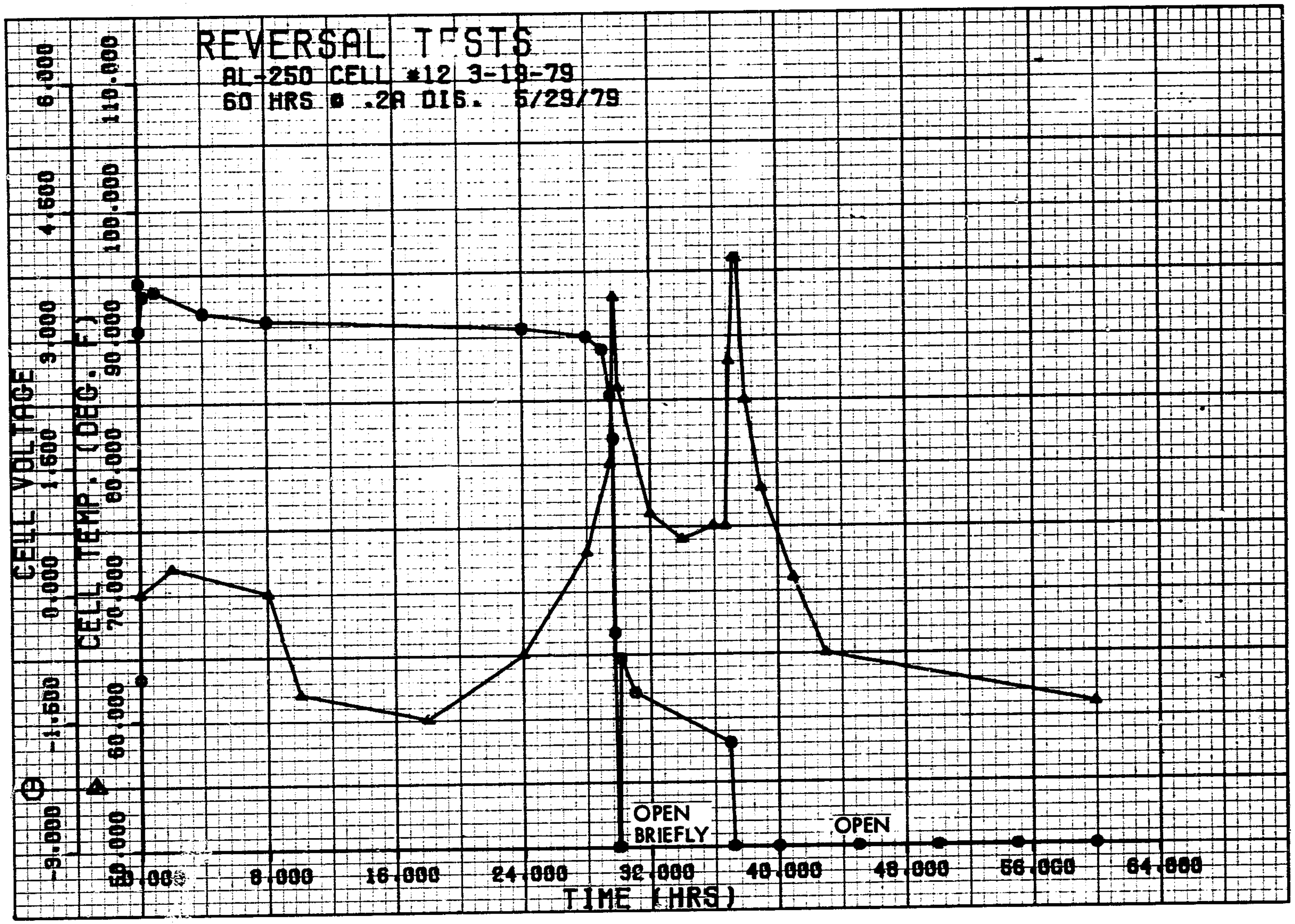

Figure B-16. Reversal Test for 60 hours at 0.2 amps for Cell #12

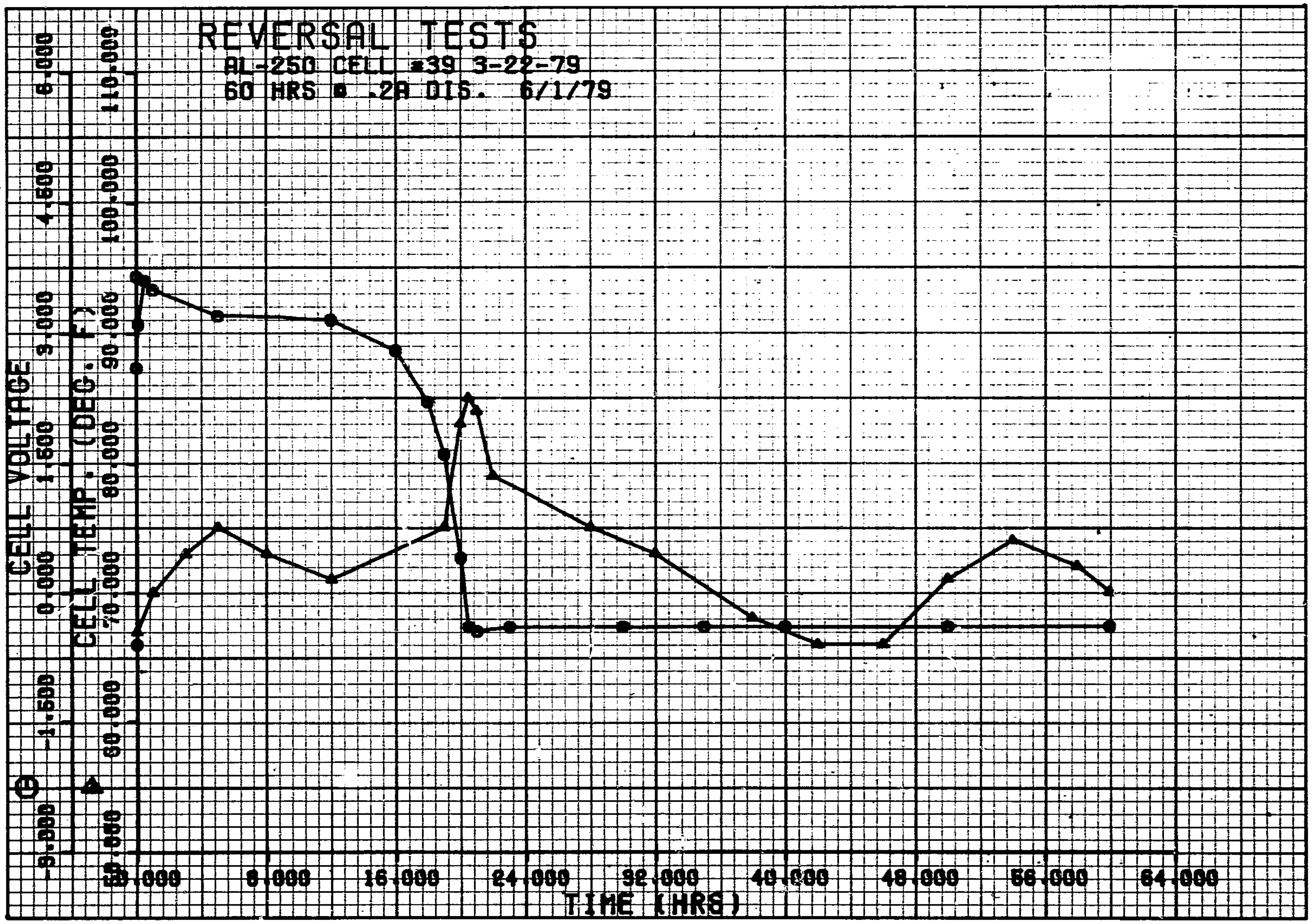

Figure B-17. Reversal Test for 60 hours at 0.2 amps for Cell #39

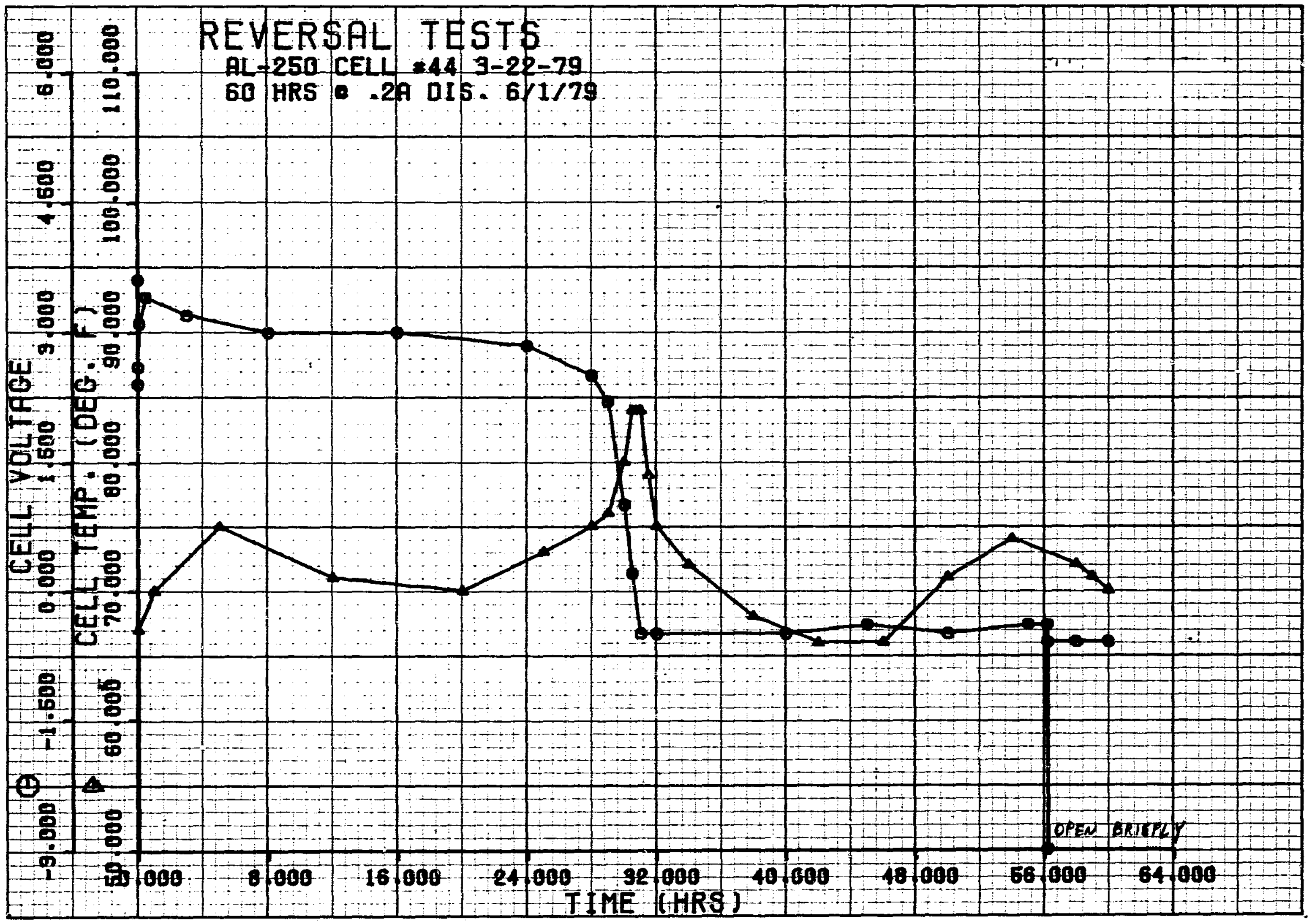

Figure B-18. Reversal Test for 60 hours at 0.2 amps for Cell #44

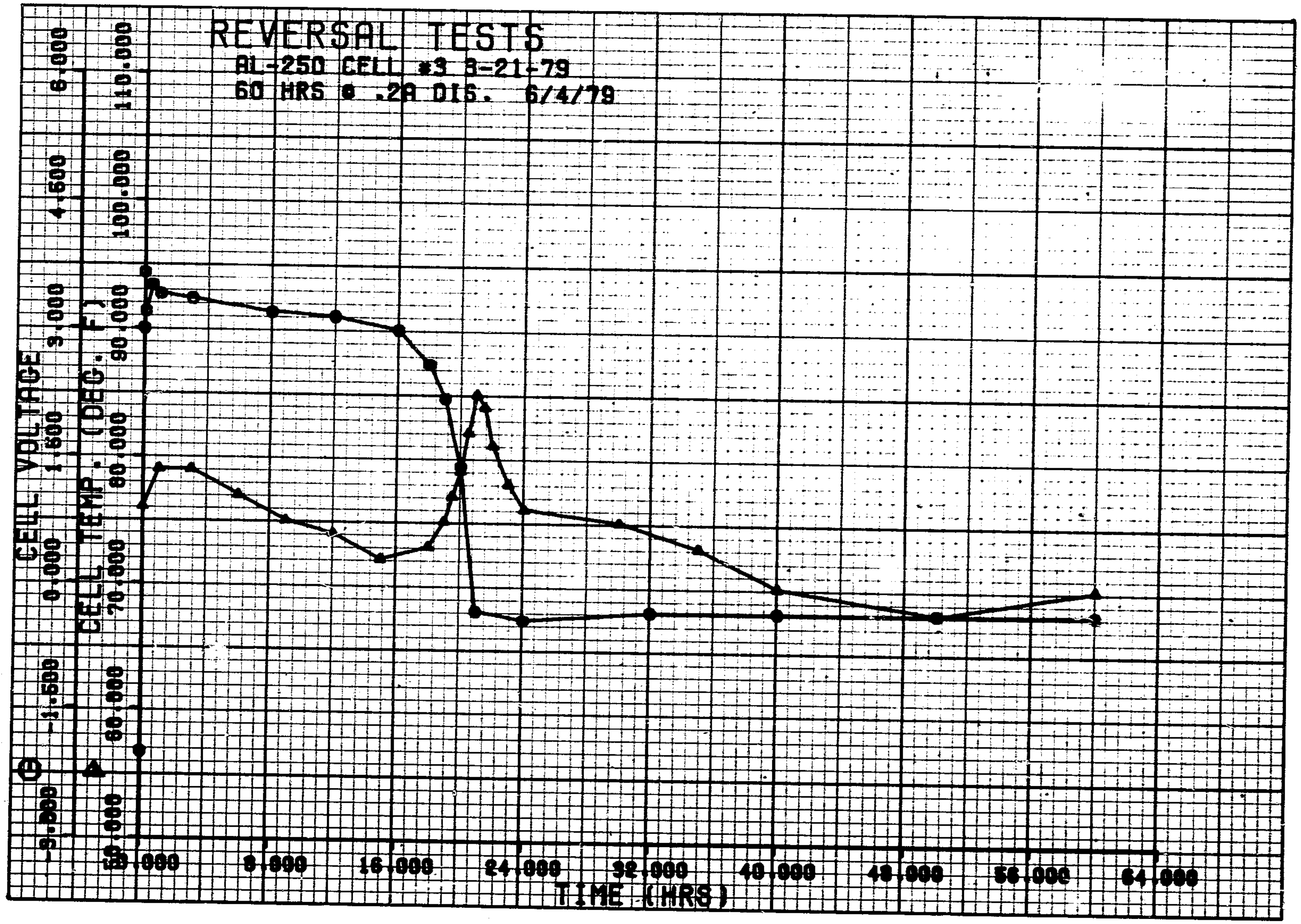

Figure B-19. Reversal Test for 60 hours at 0.2 amps for Cell #3

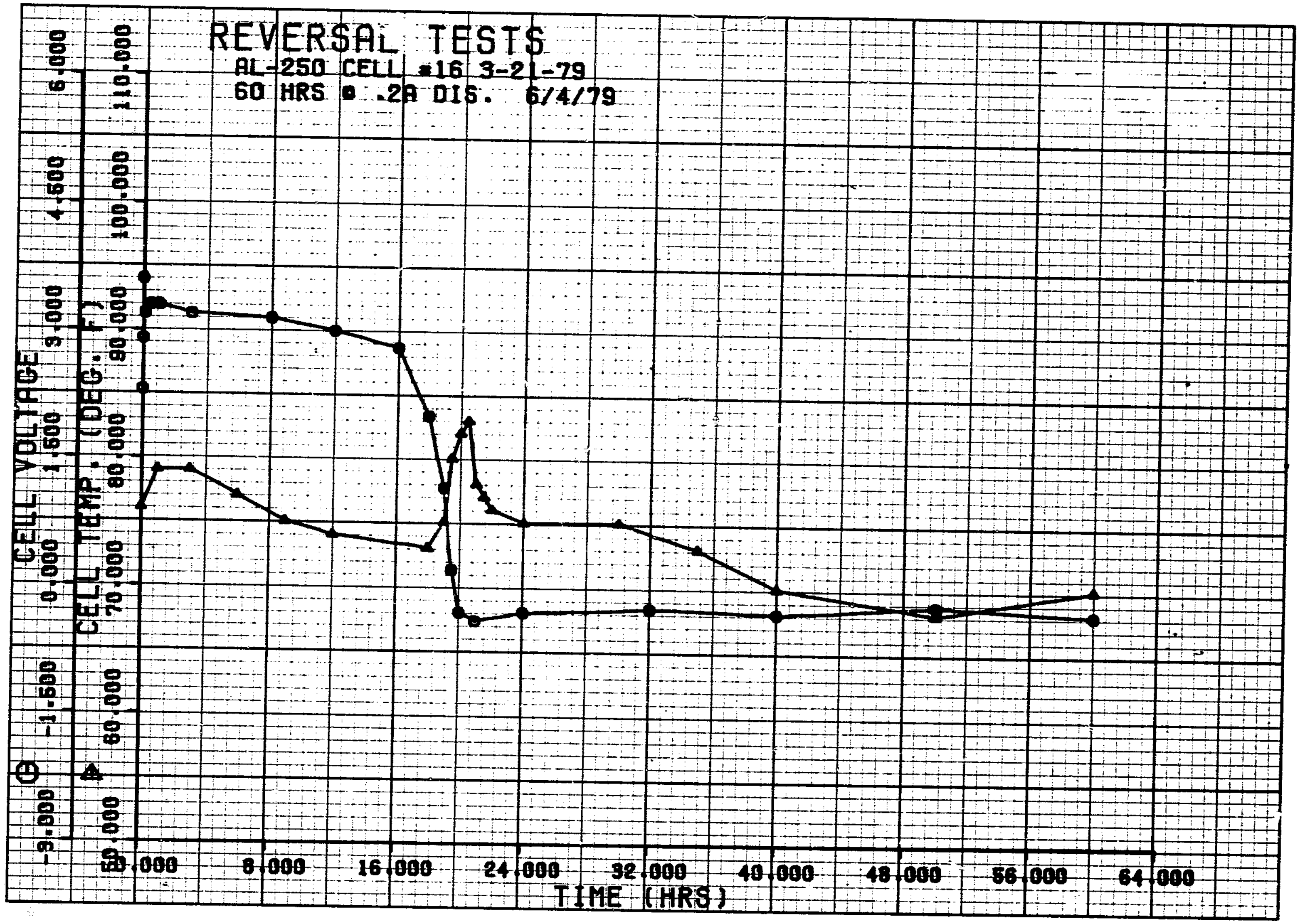

Figure B-20. Reversal Test for 60 hours at 0.2 amps for Cell #16

APPENDIX C

COMPUTER-DRAWN GRAPHS OF HIGH-RATE DISCHARGE TESTS

(Load is given in ohmns; tests were conducted at room temperature, 21^{o}C.)

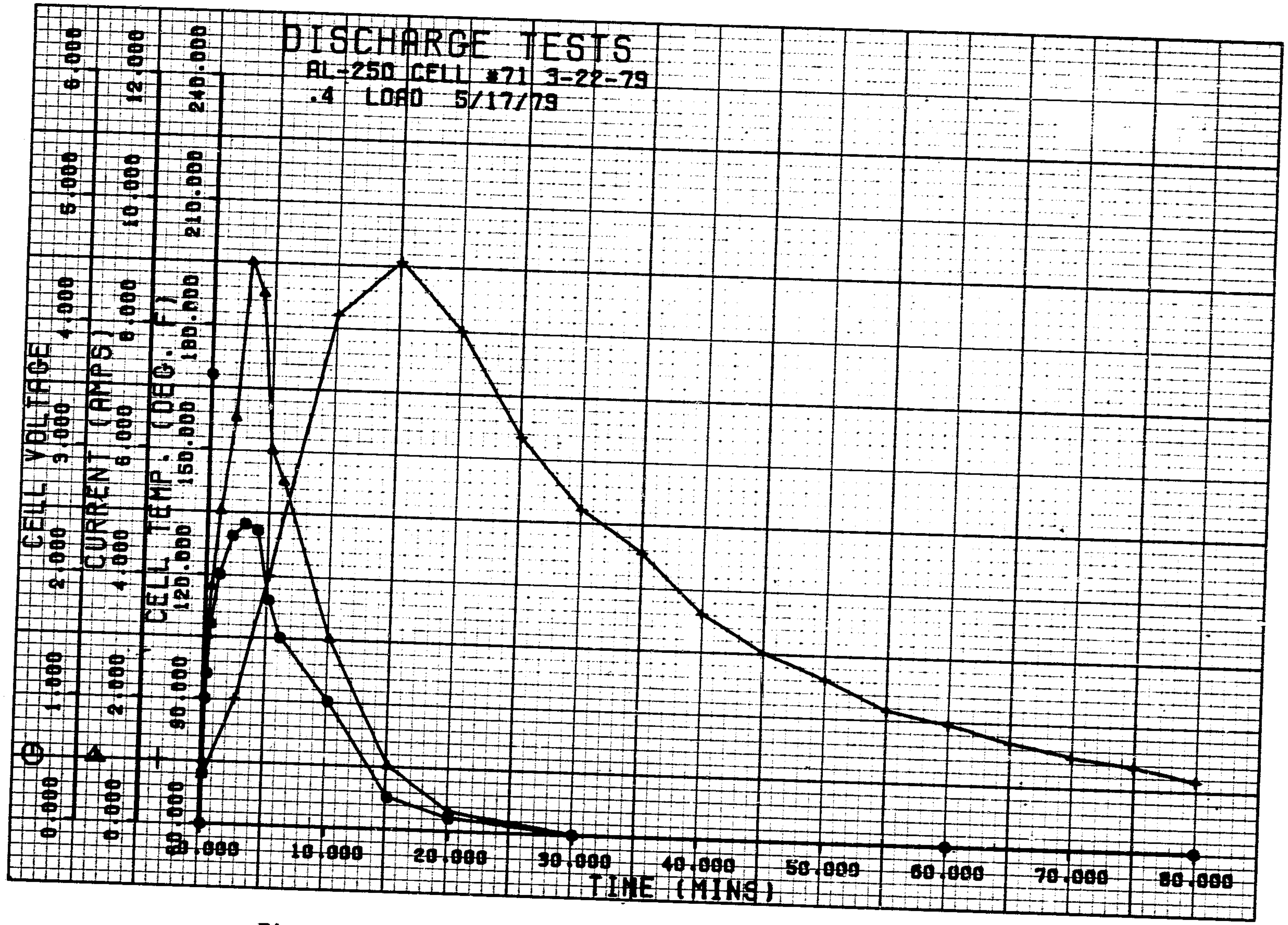

Figure C-1. Discharge Test with 0.4-ohm load for Cell #71

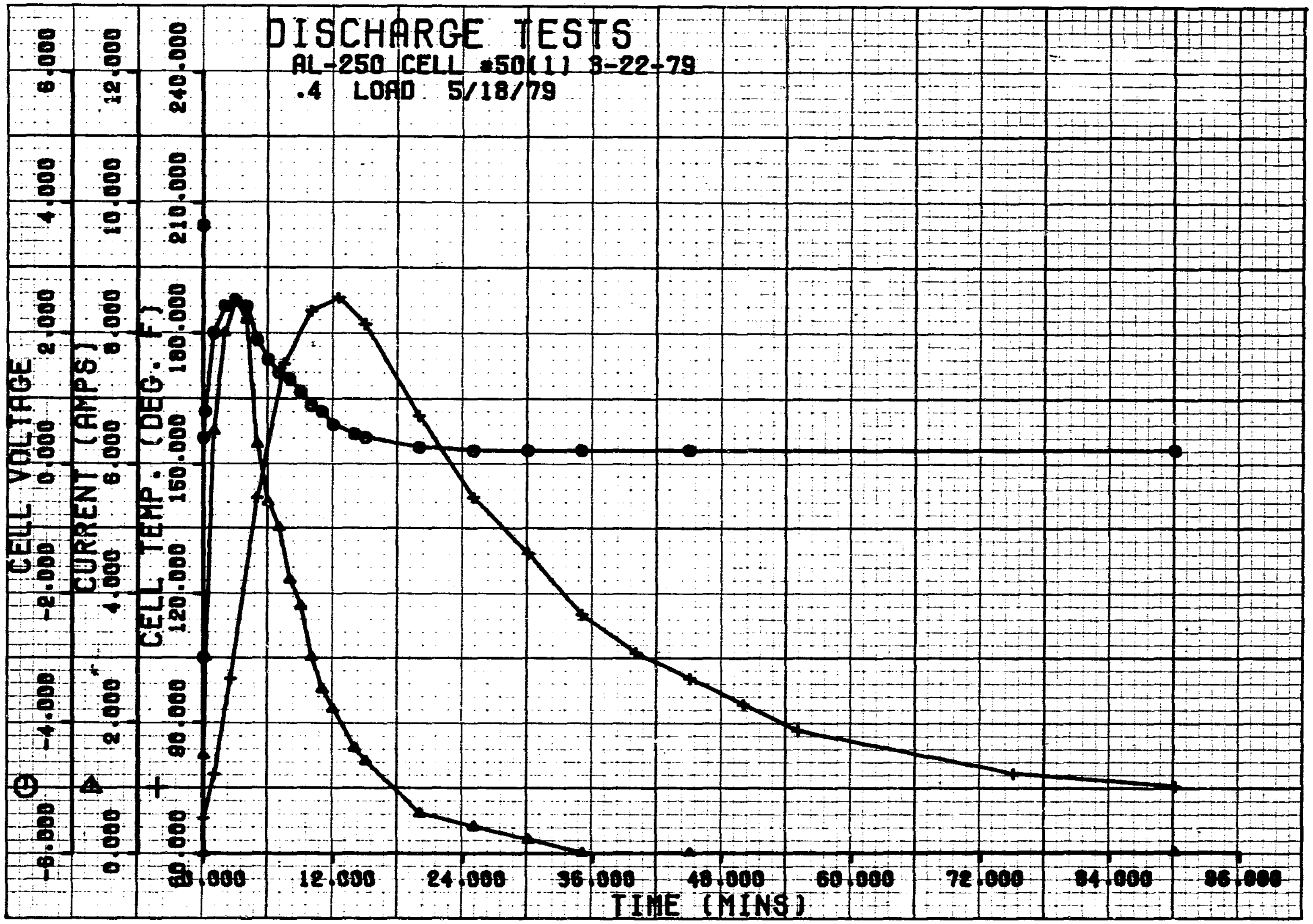

Figure C-2. Discharge Test with 0.4-ohm load for Cell #50

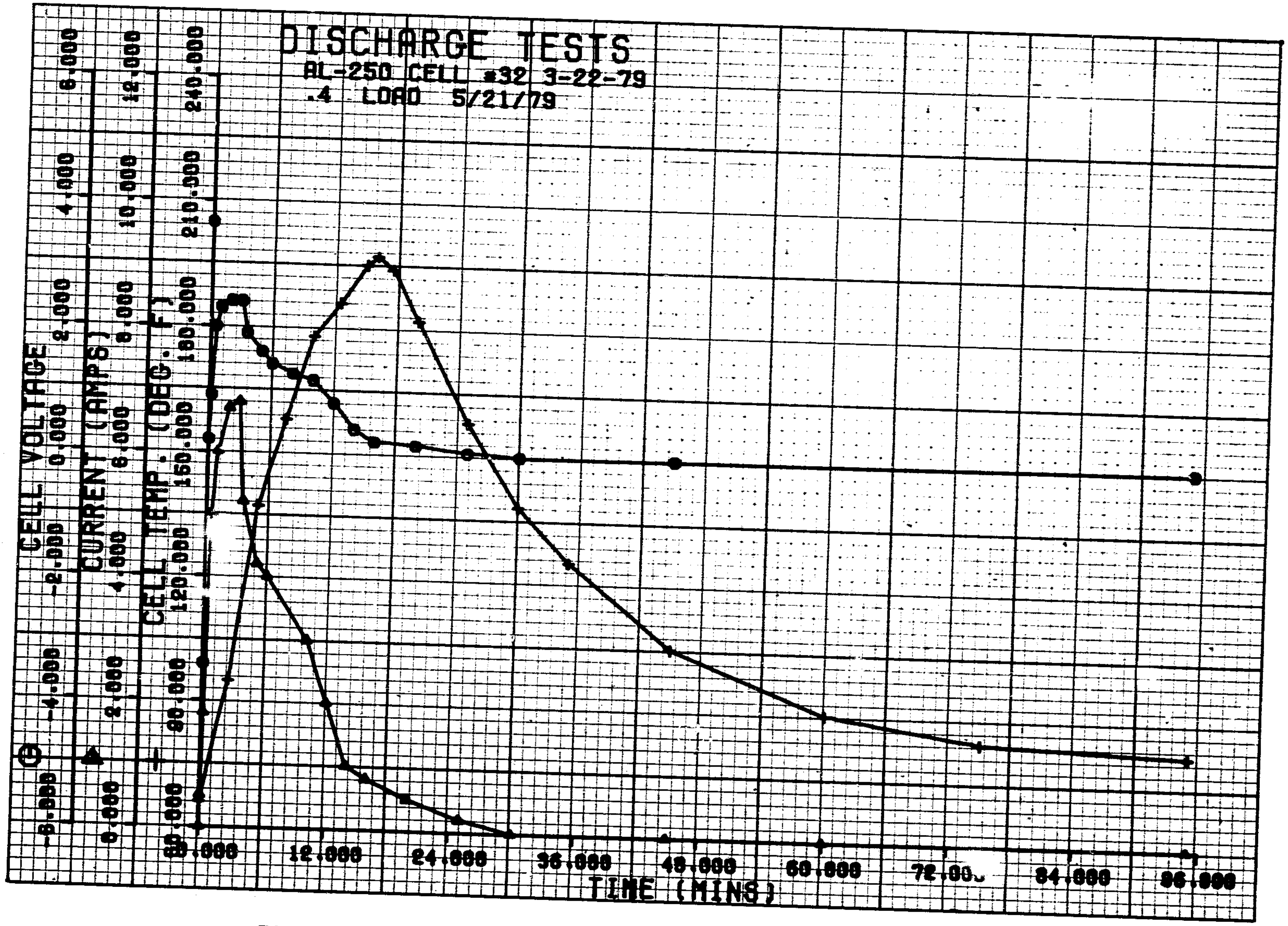

Figure C-3. Discharge Test with 0.4-ohm load for Cell #32

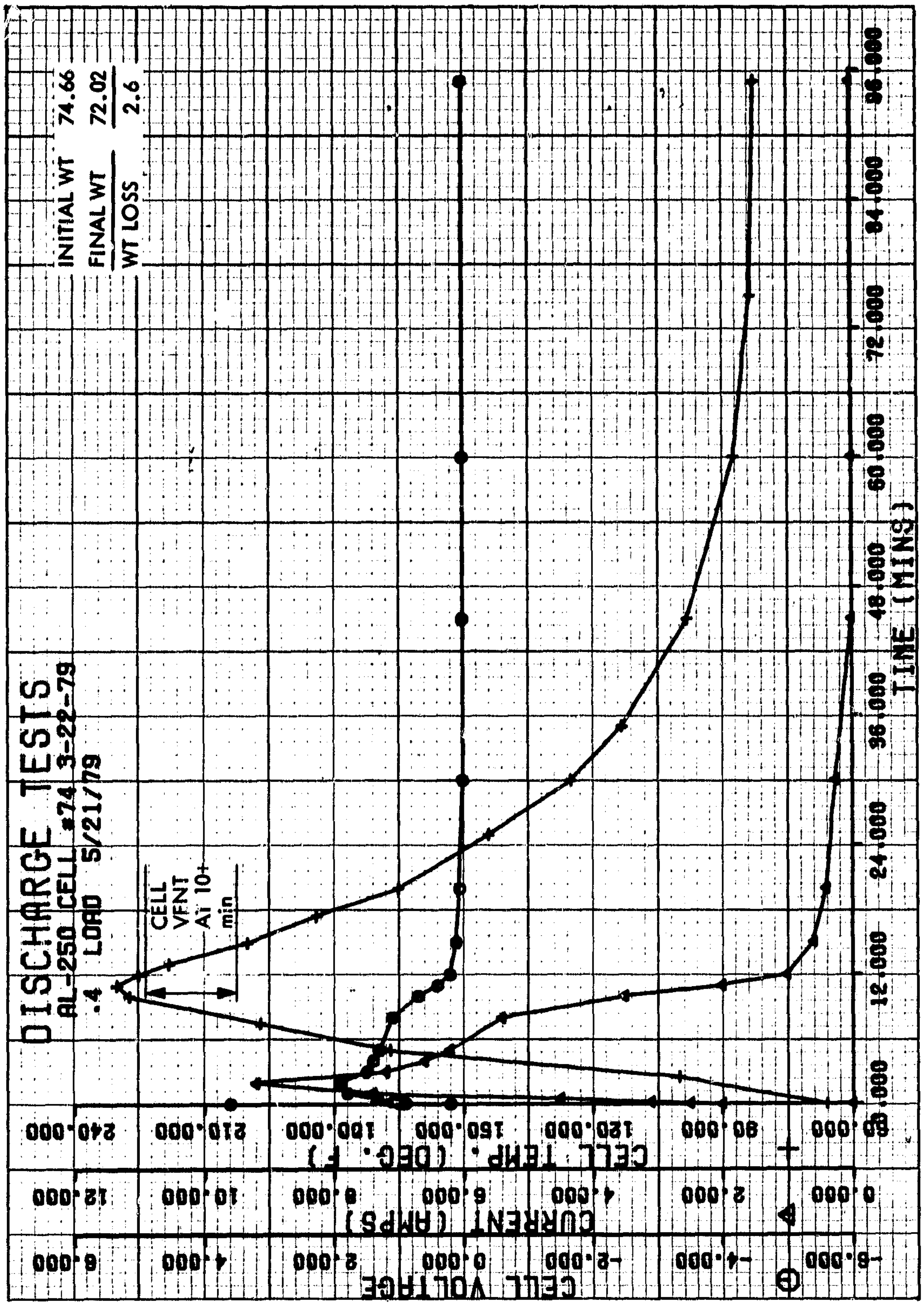

Figure C-4. Discharge Test with 0.4-ohm load for Cell #74

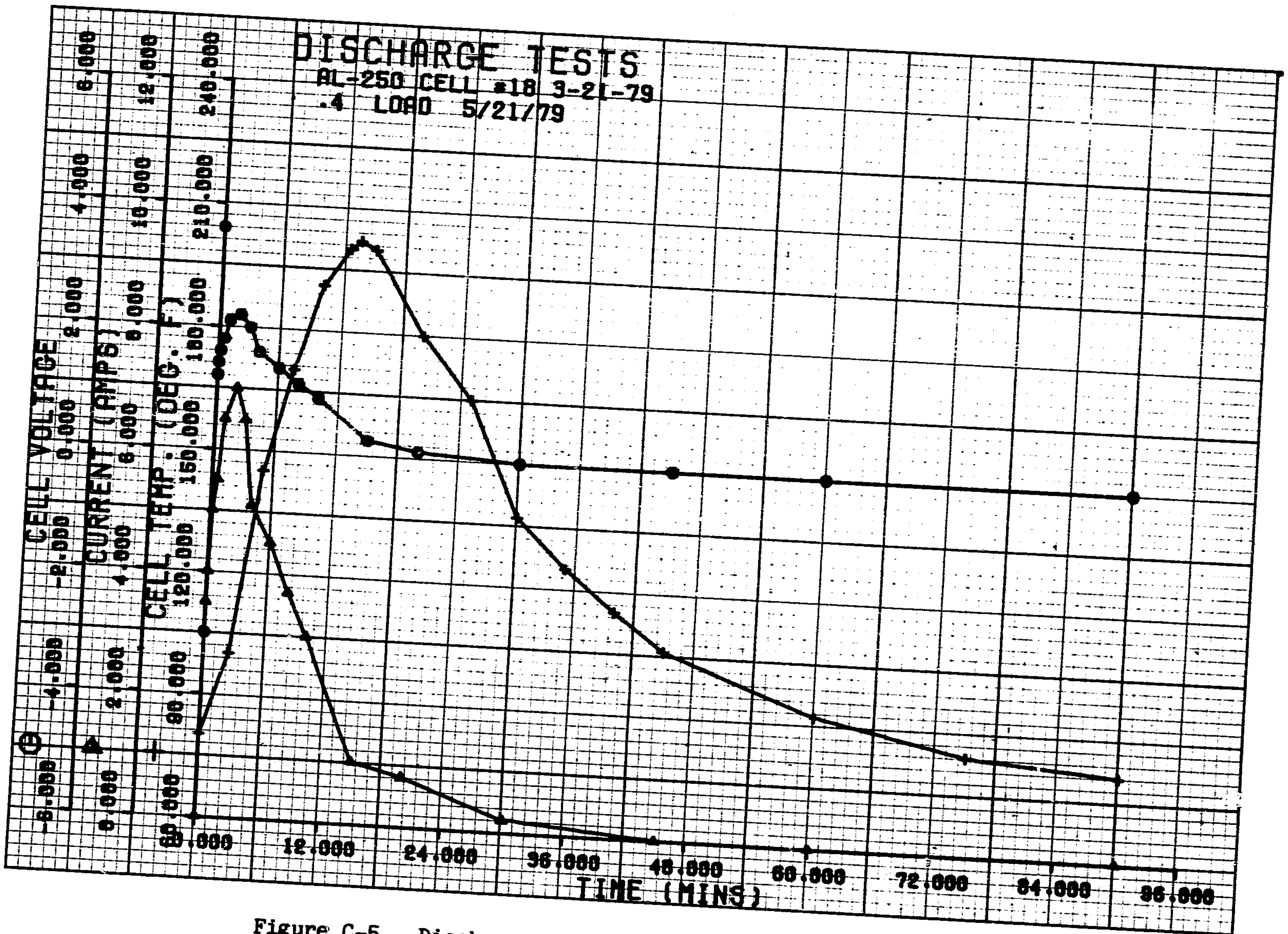

Figure C-5. Discharge Test with 0.4-ohm load for Cell #18

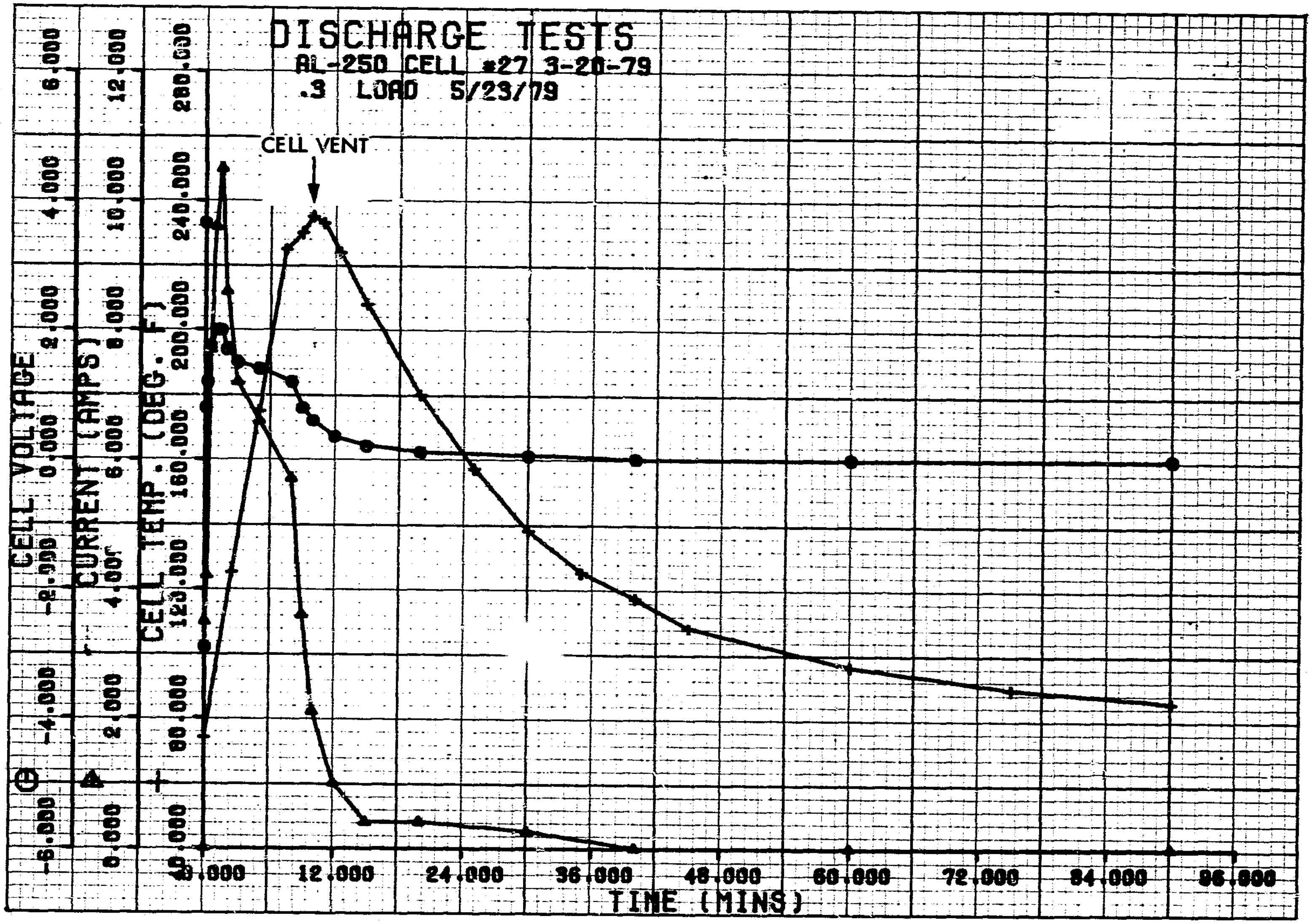

Figure C-6. Discharge Test with 0.3-ohm load for Cell #27

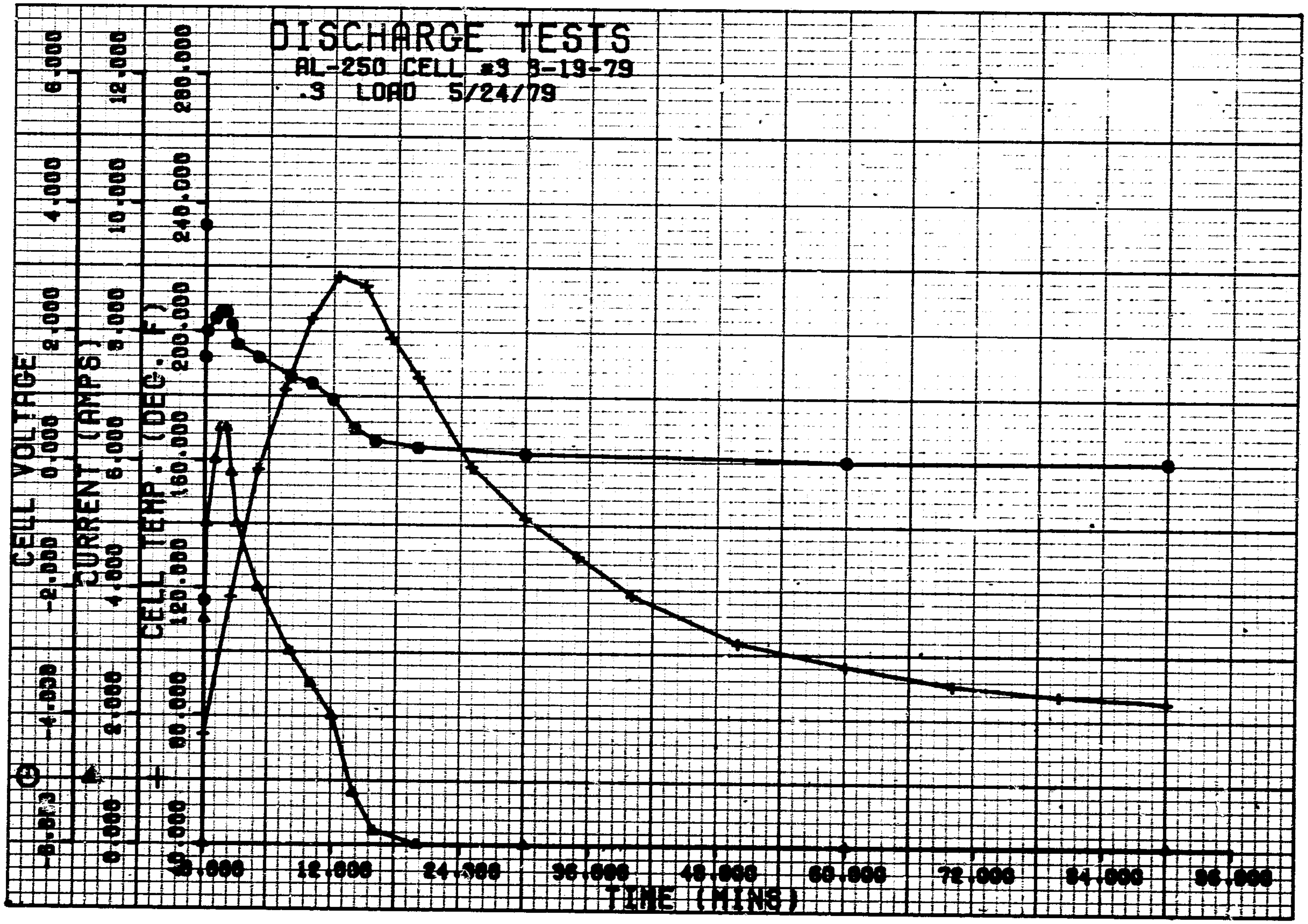

Figure C-7. Discharge Test with 0.3-ohm load for Cell #3

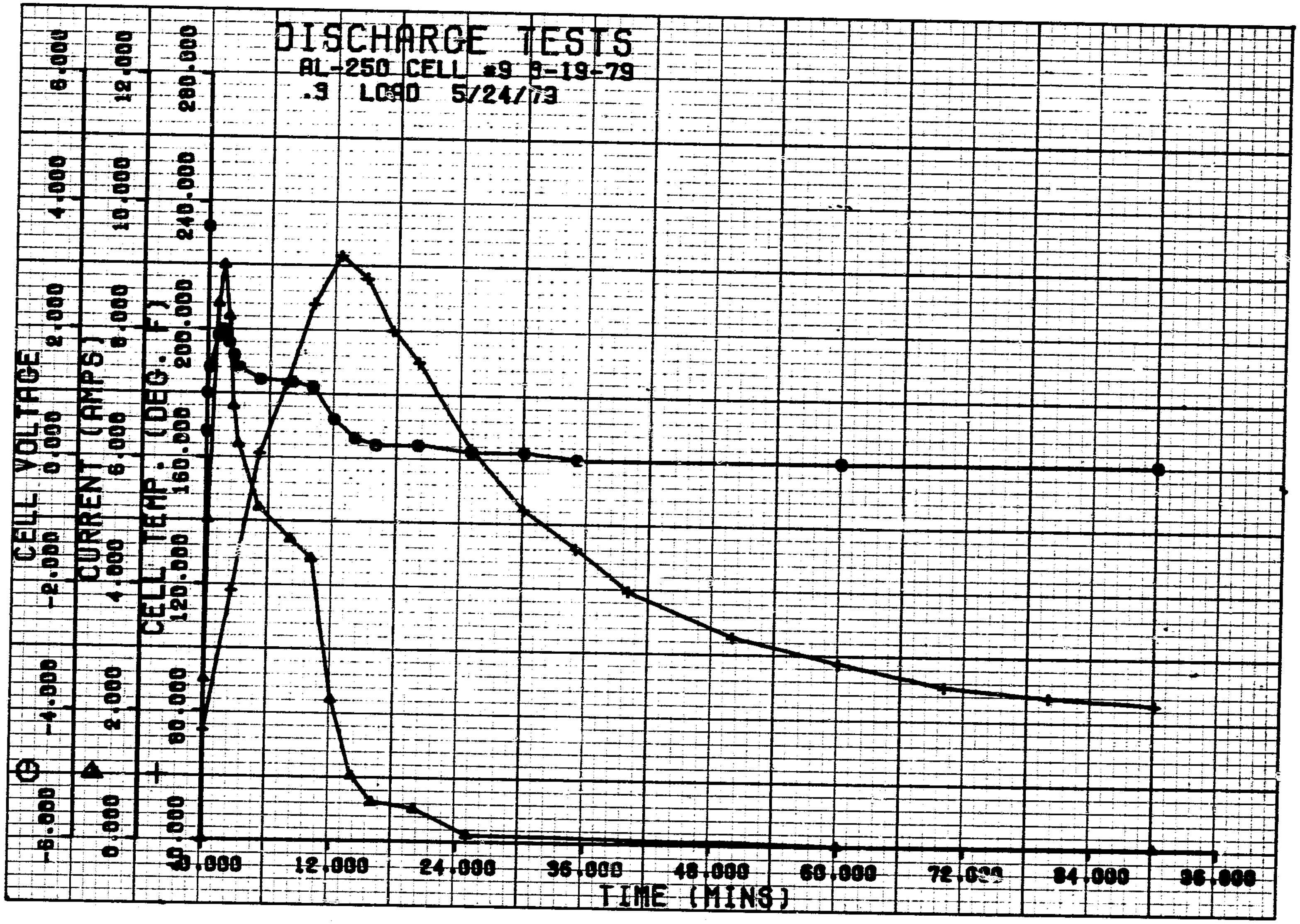

Figure C-8. Discharge Test with 0.3-ohm load for Cell #9

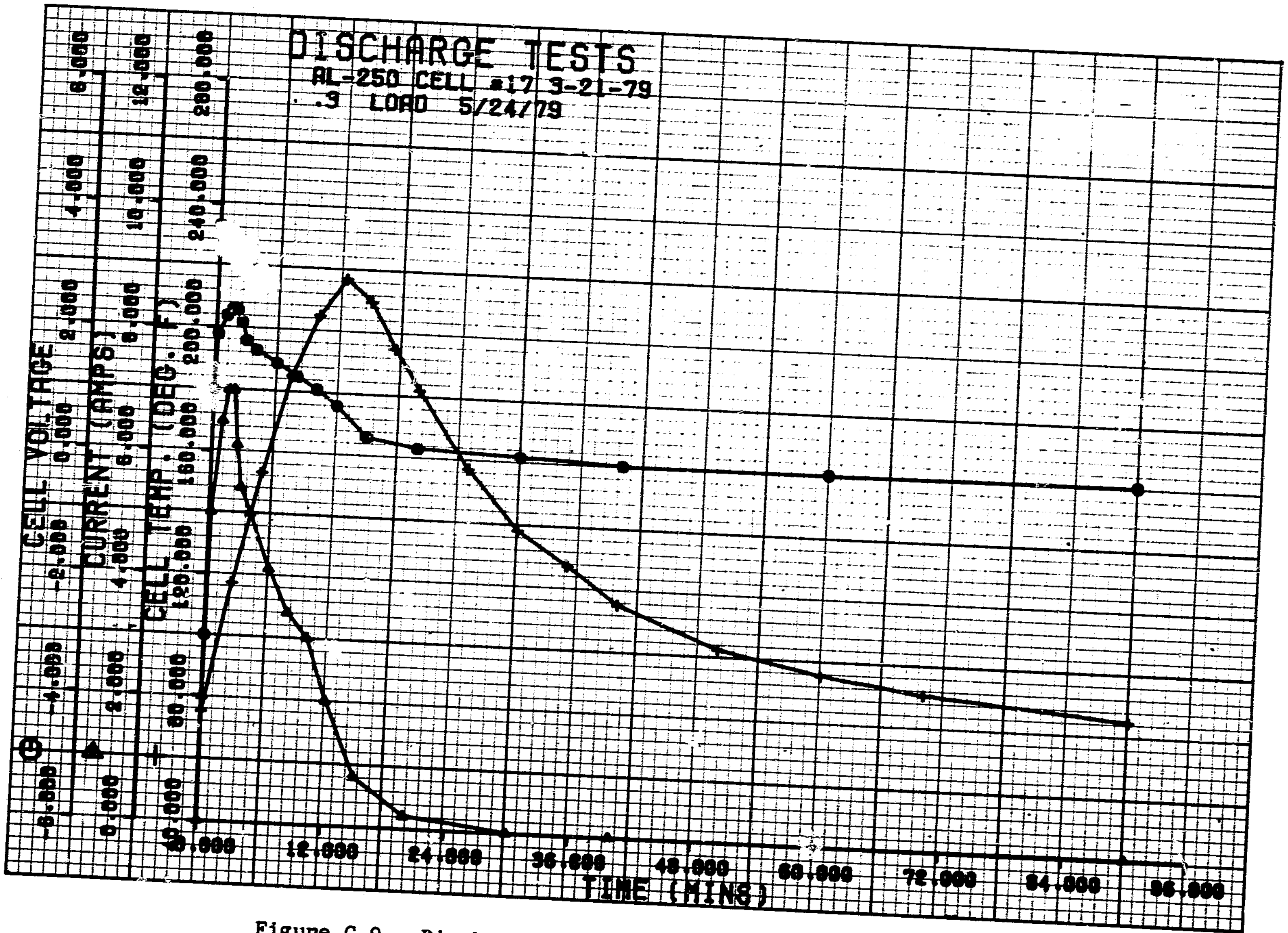

Figure C-9. Discharge Test with 0.3-ohm load for Cell #17

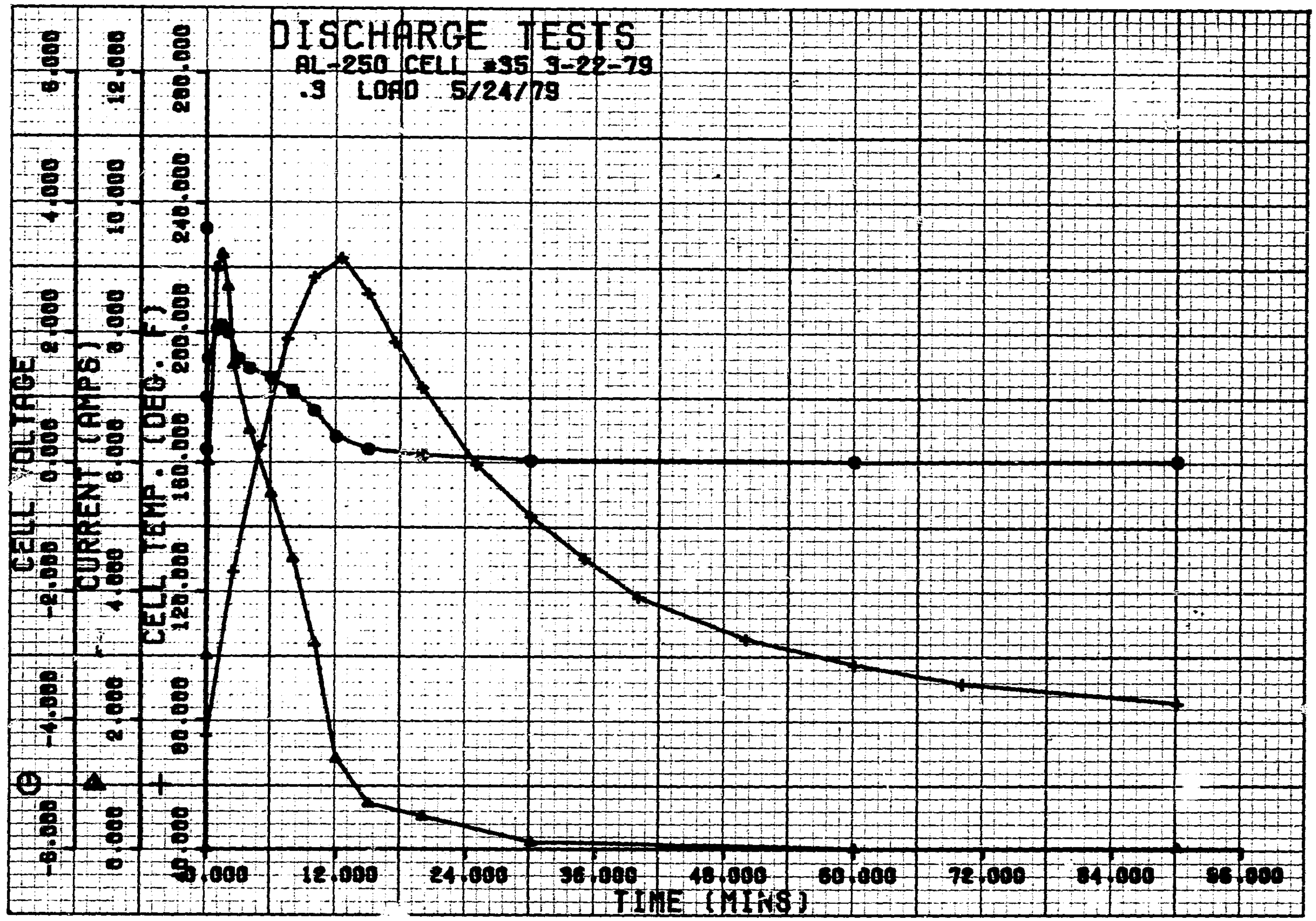

Figure C-10. Discharge Test with 0.3-ohm load for Cell #35

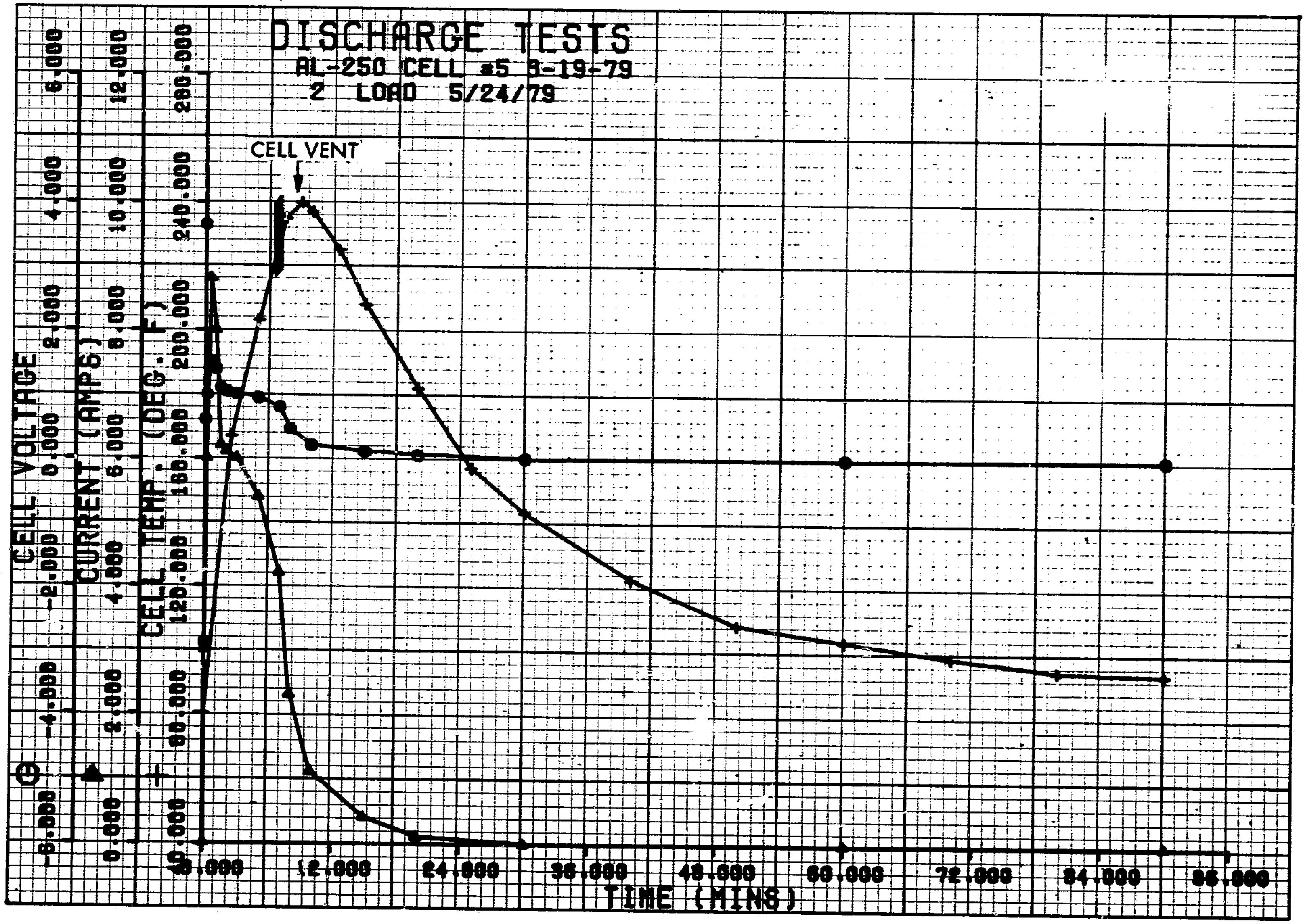

Figure C-11. Discharge Test with 0.2-ohm load for Cell #5

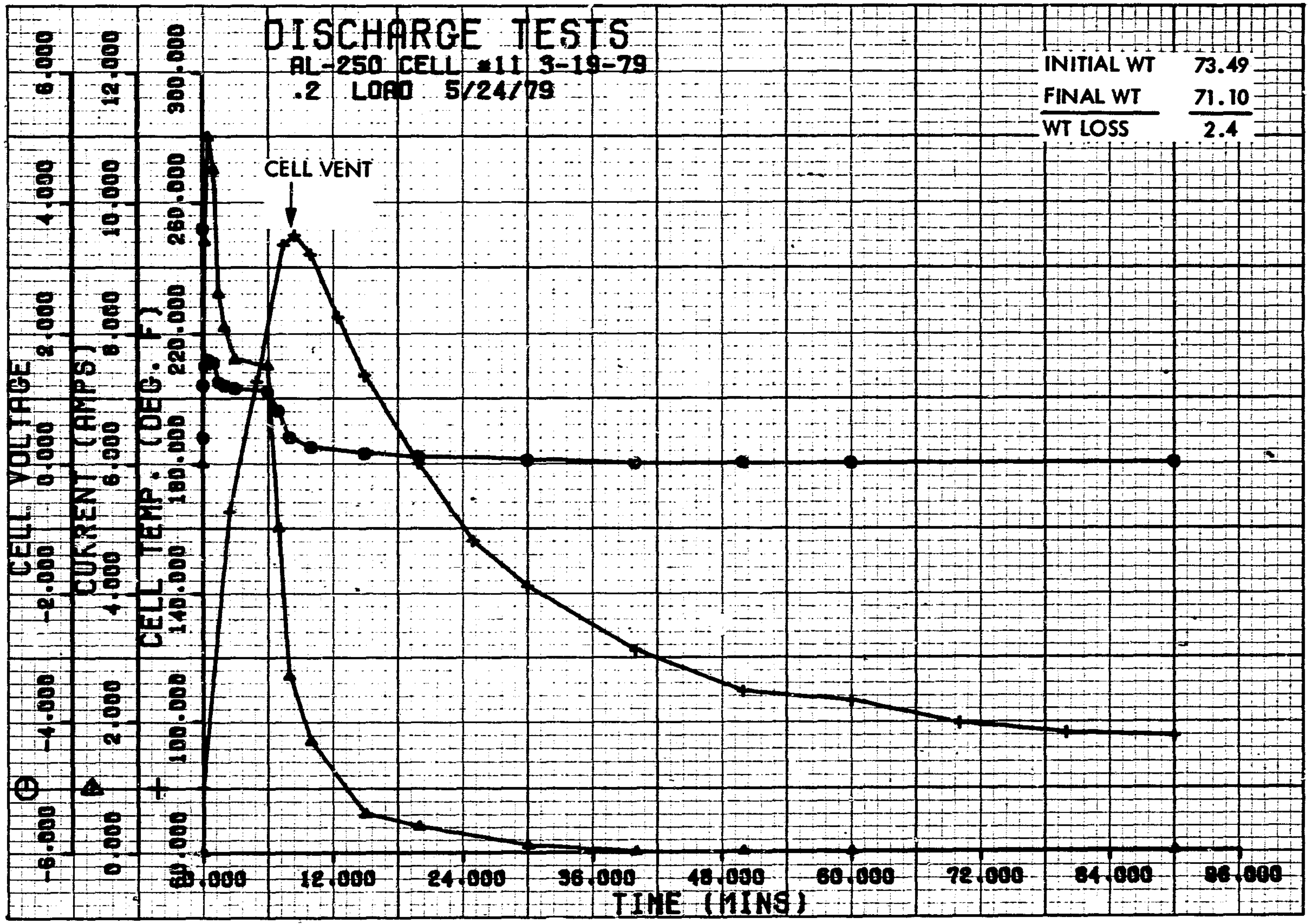

Figure C-12. Discharge Test with 0.2-ohm load for Cell #11

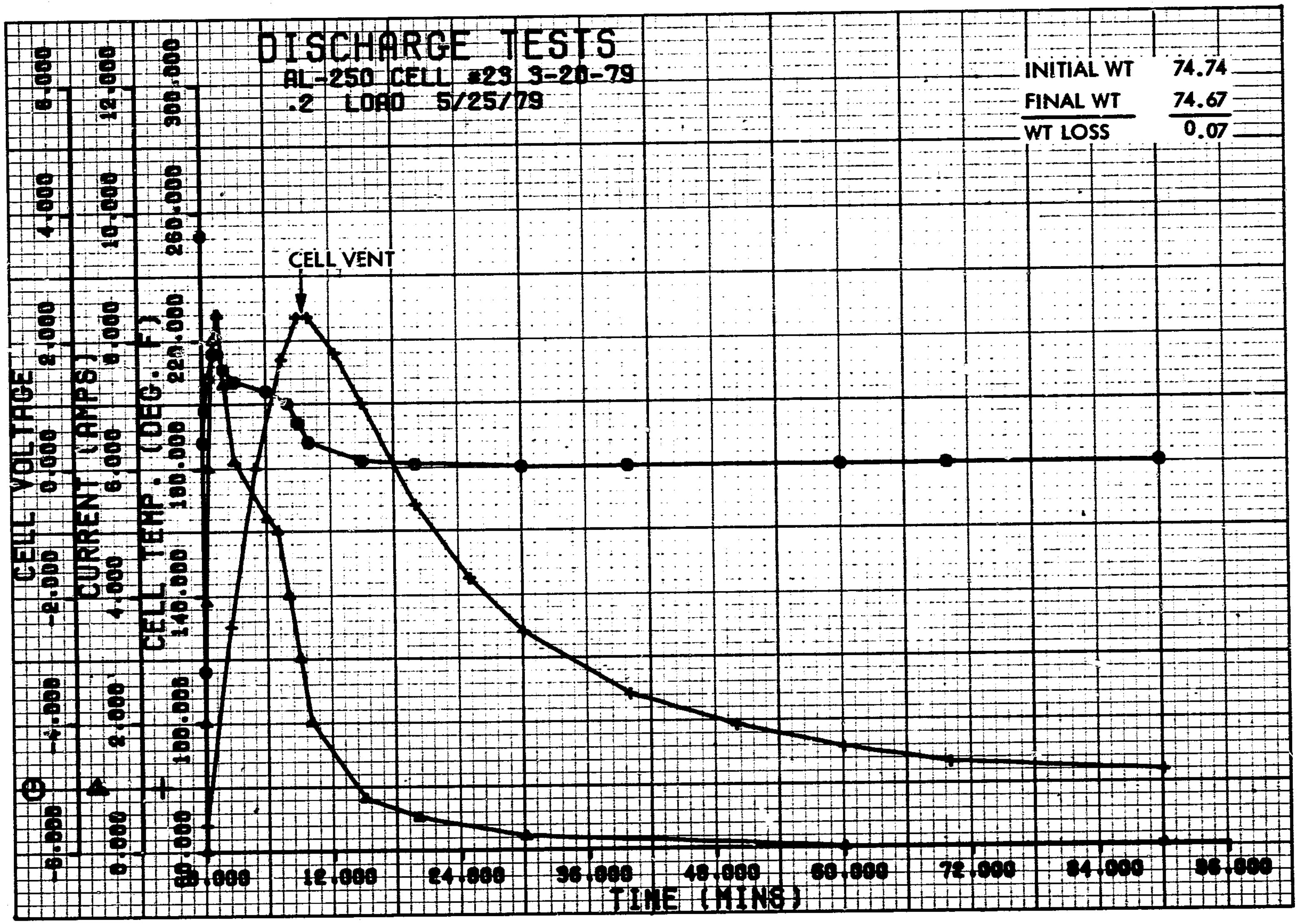

Figure C-13. Discharge Test with 0.2-ohm load for Cell #23

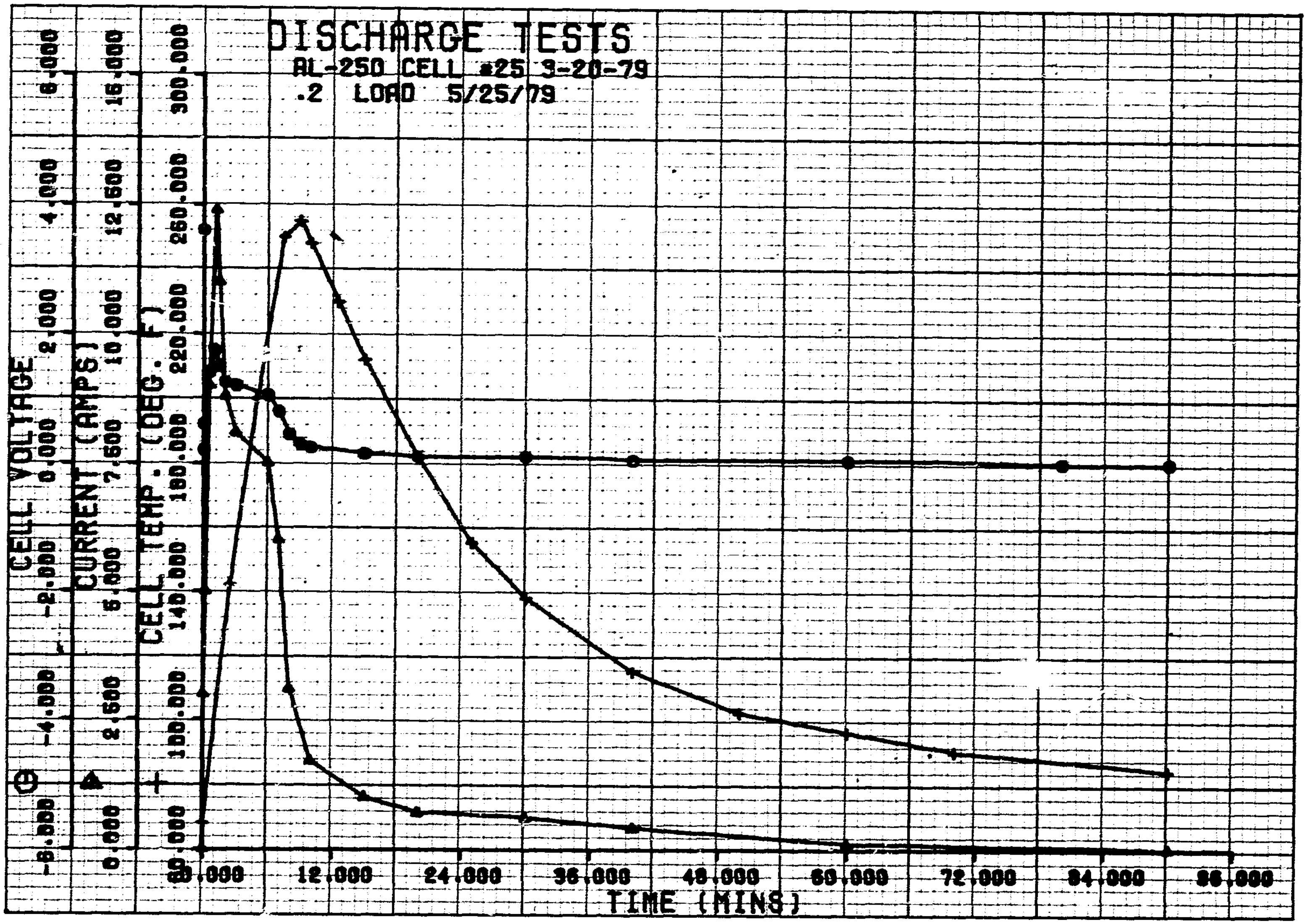

Figure C-14. Discharge Test with 0.2-ohm load for Cell #25

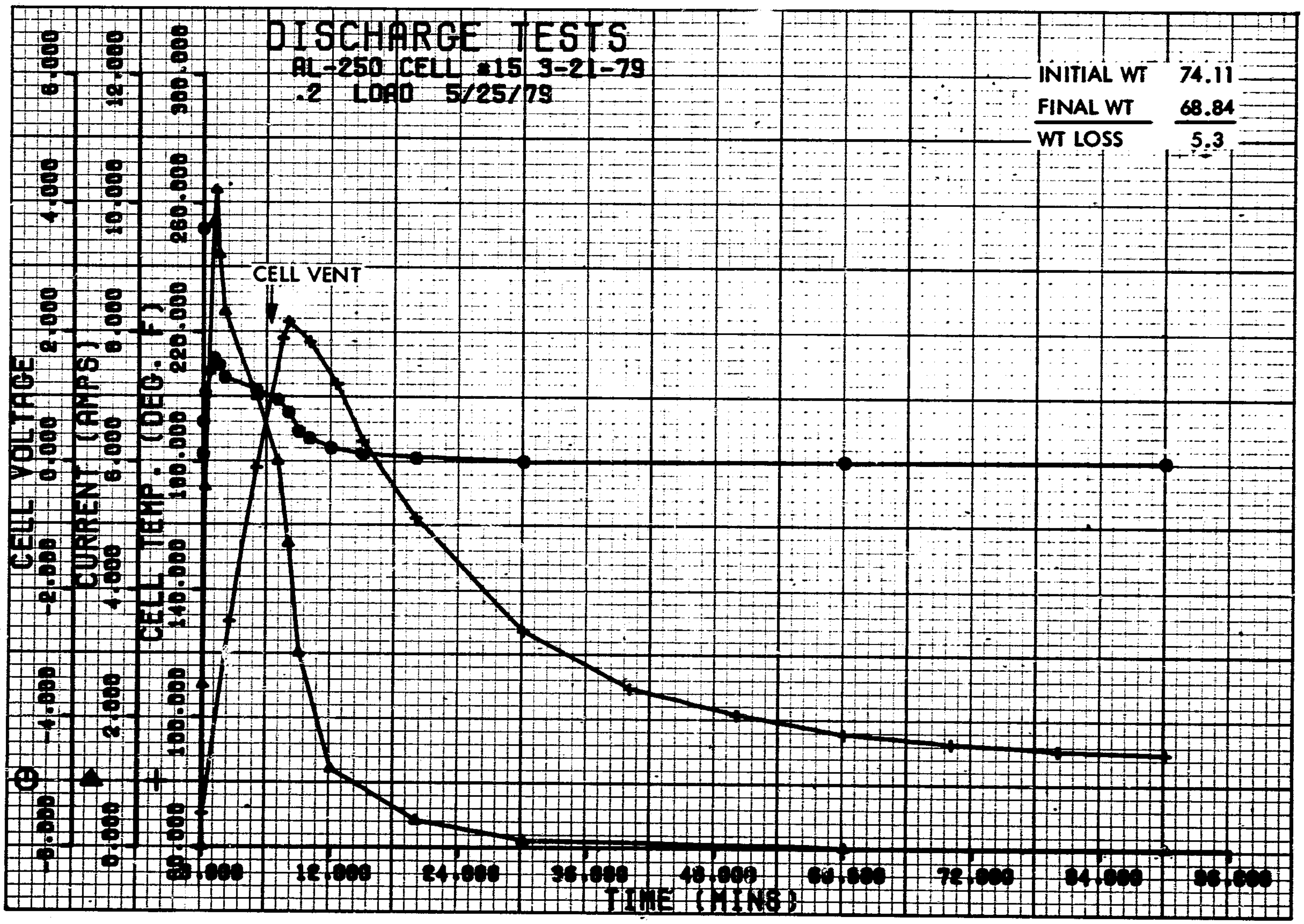

Figure C-15. Discharge Test with 0.2-ohm load for Cell #15

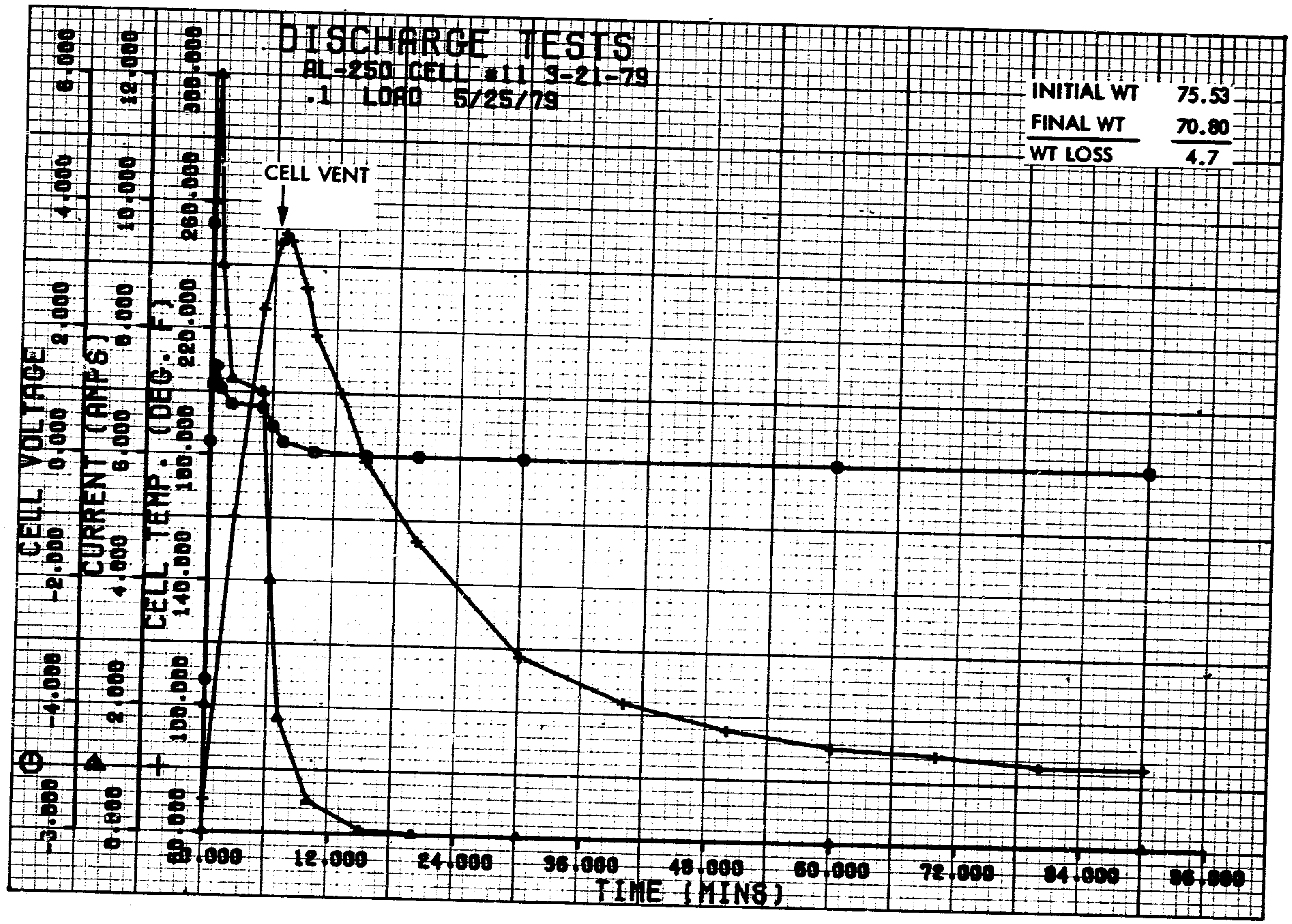

Figure C-16. Discharge Test with 0.1-ohm load for Cell #11

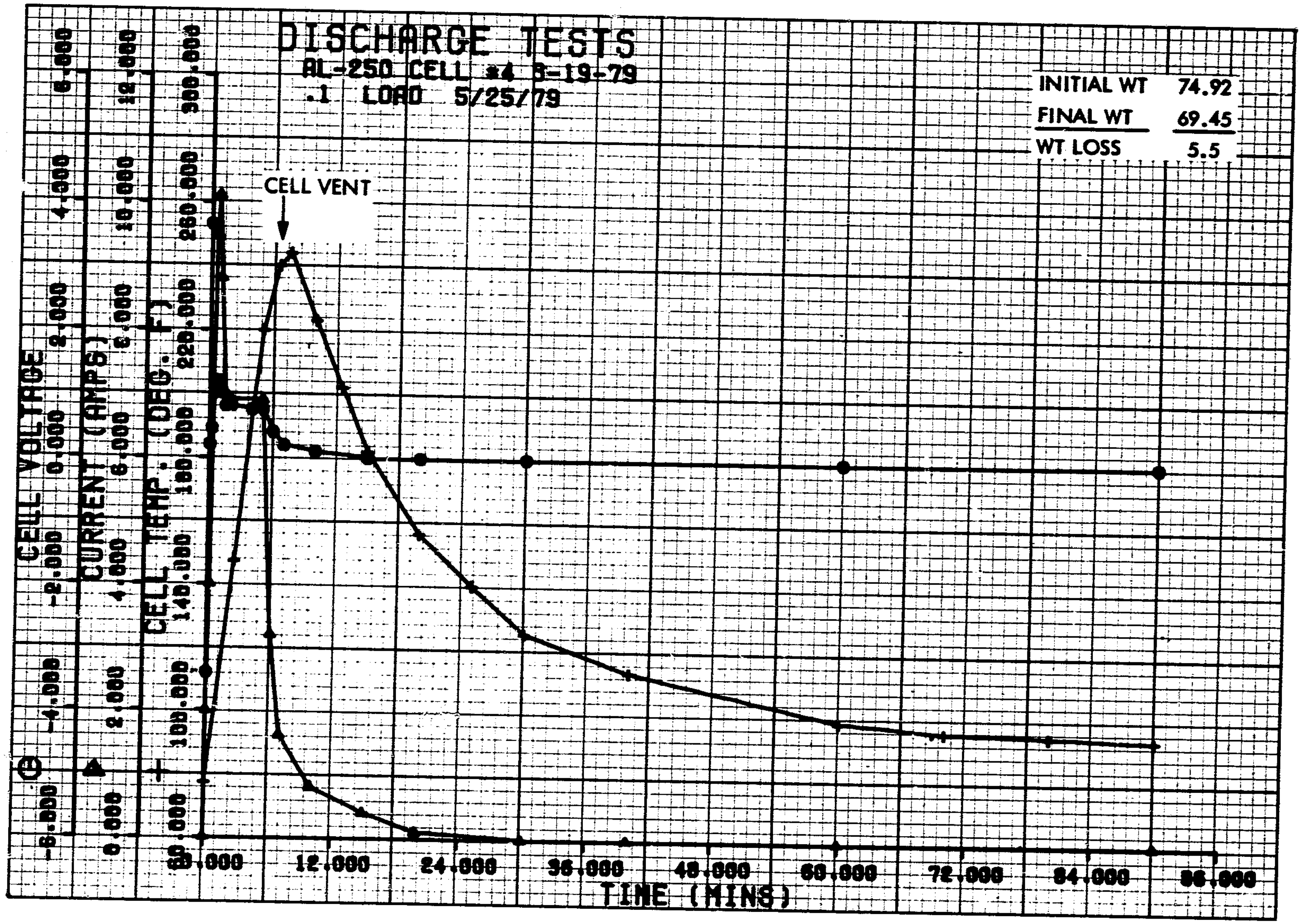

Figure C-17. Discharge Test with 0.1-ohm load for Cell #4

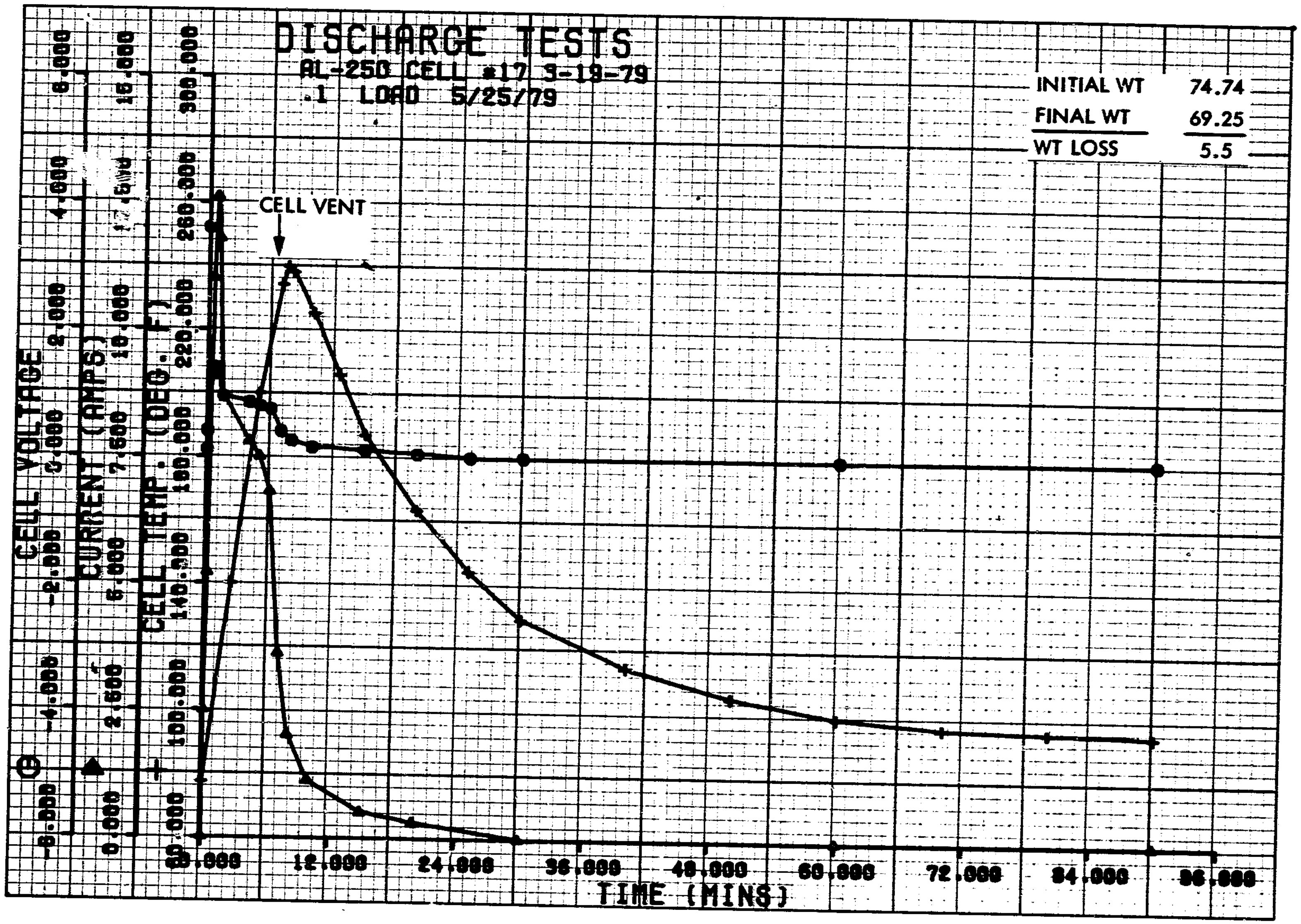

Figure C-18. Discharge Test with 0.1-ohm load for Cell #17

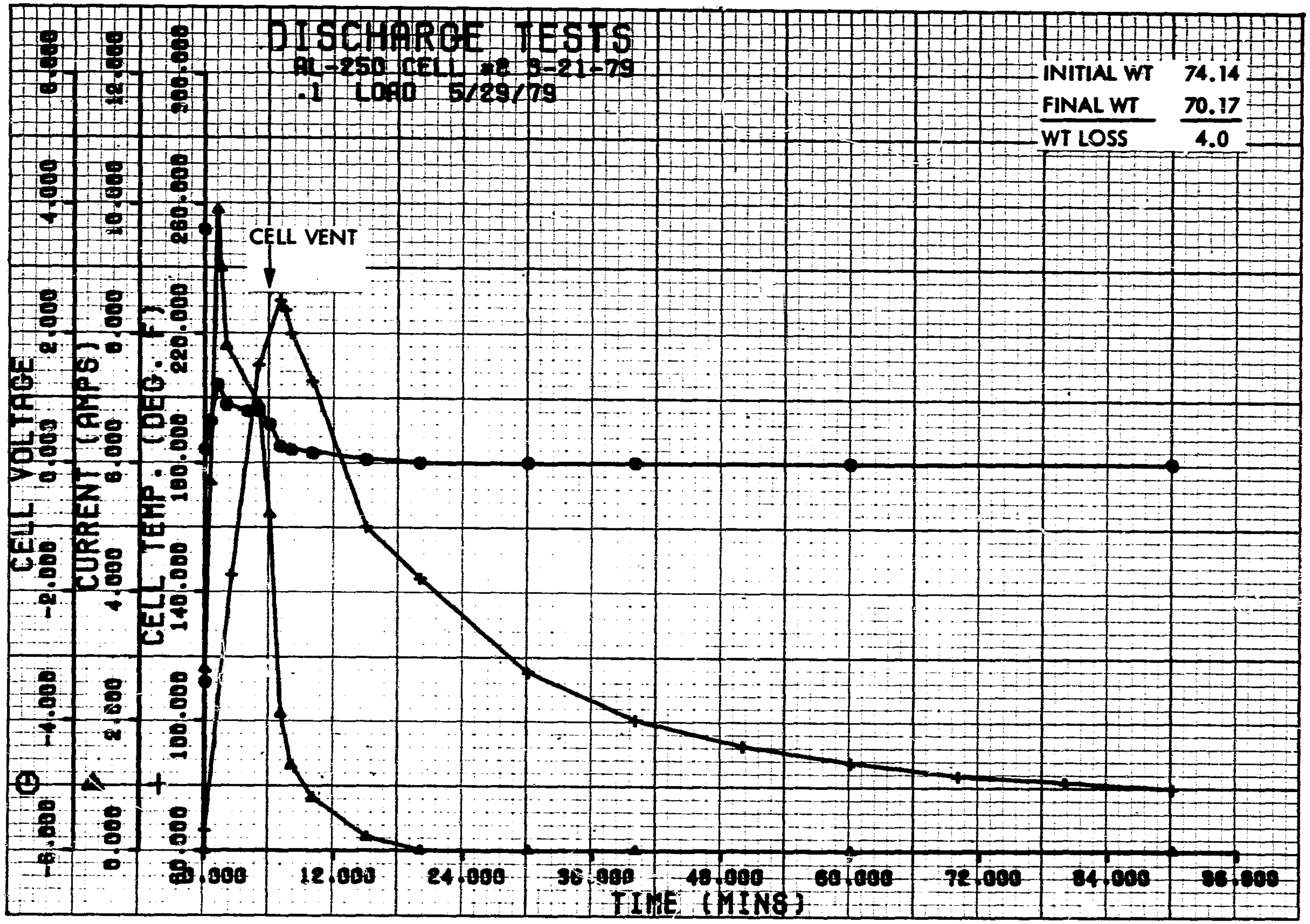

Figure C-19. Discharge Test with 0.1-ohm load for Cell #8

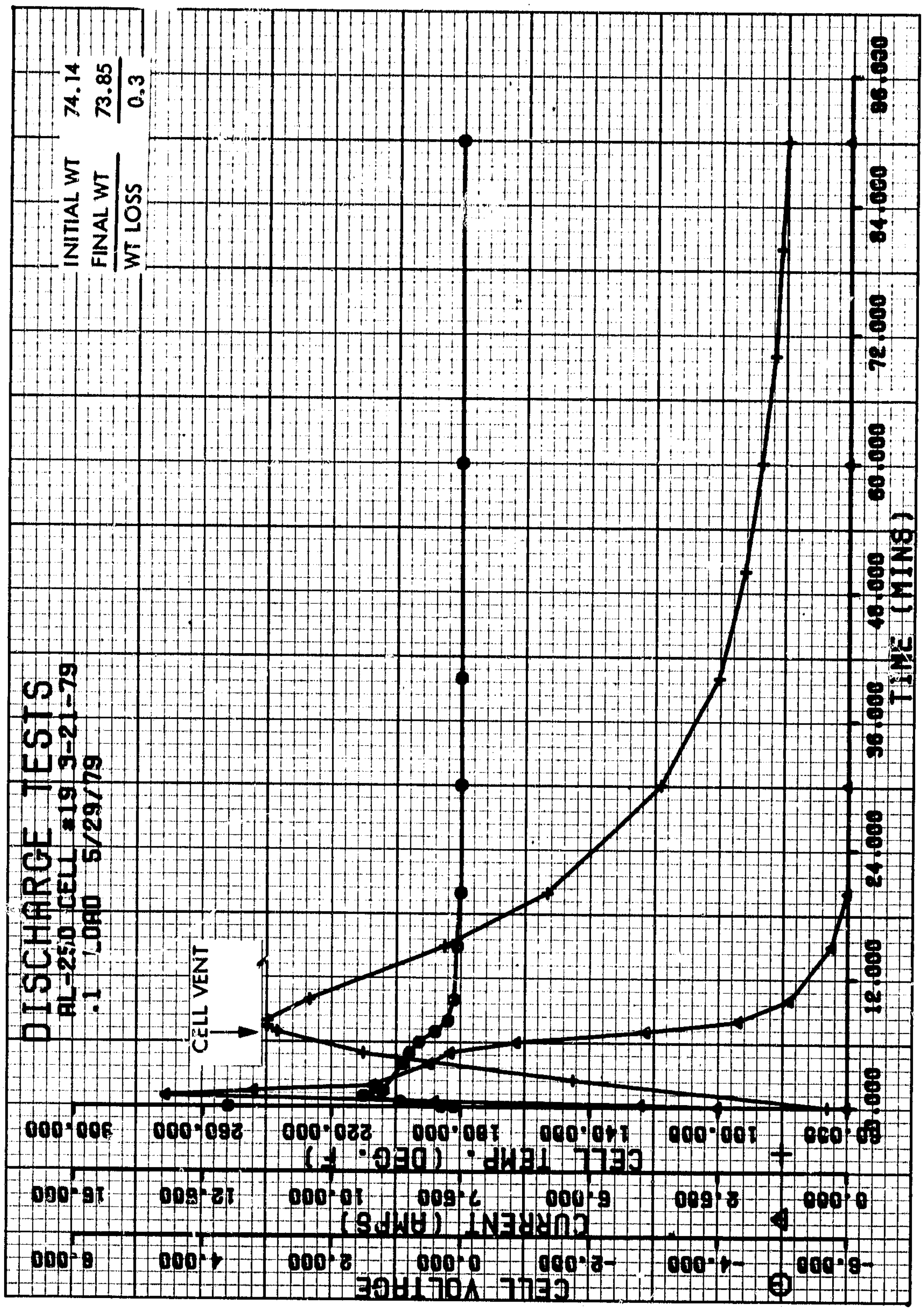

Figure C-20. Discharge Test with 0.1-ohm load for Cell #19